

Klaus Fiedler

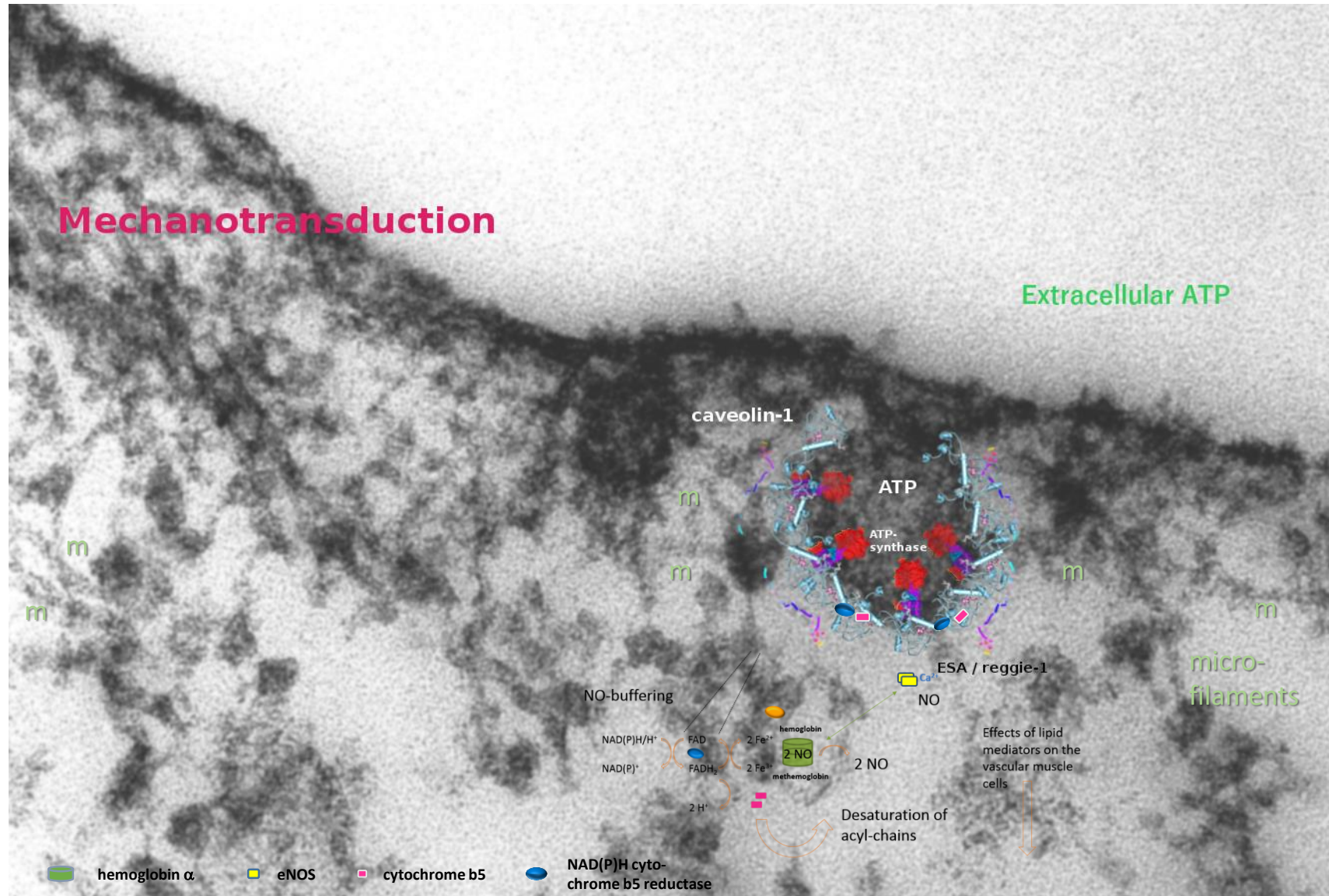
**Caveolae: Endothelial model, «budding» assay
and proposed physiological function**

Transcytosis in vascular endothelia

p24–TMED proteins: Are these lectins?

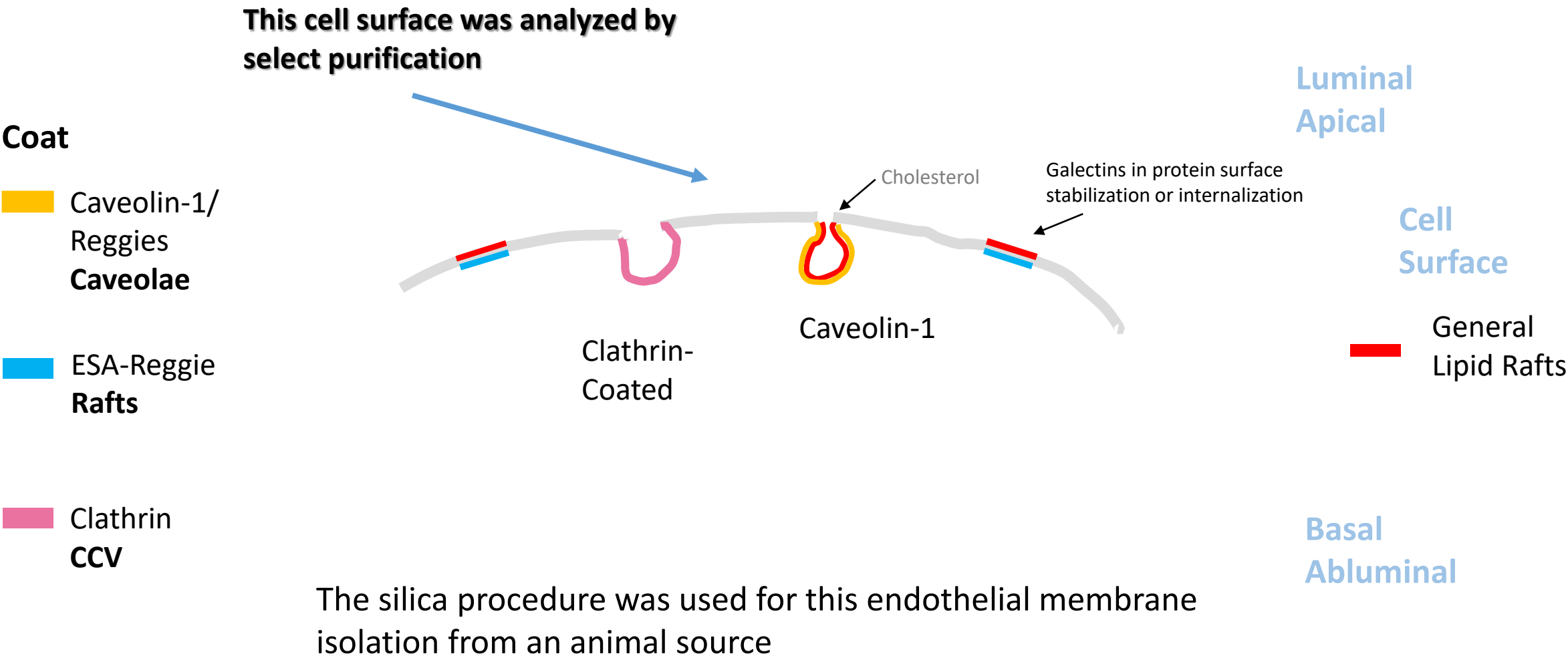
Endothelial Caveolae: Model

Microfilaments (m), cells were not pre-extracted (see Schliwa et al. 1981); includes recent results of Straub et al. (2012)



Fiedler and collaborators, 1998-2002

The Cell Surface of Endothelia



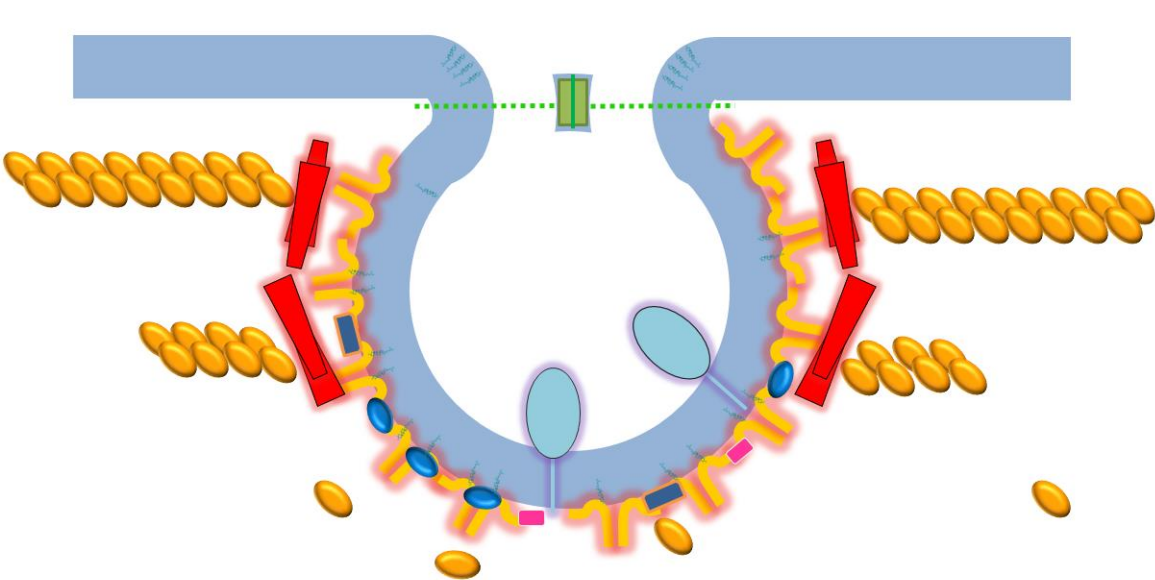
Immunoisolations from Rat Lung: Quantitative Results

Ponceau S, Coomassie-Blue and Silver Stain

Caveola

The subunit composition of ATP-synthase has not been exactly determined




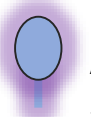



Immunoisolations were carried through with caveolae released by sonication or “vesicle untethering”



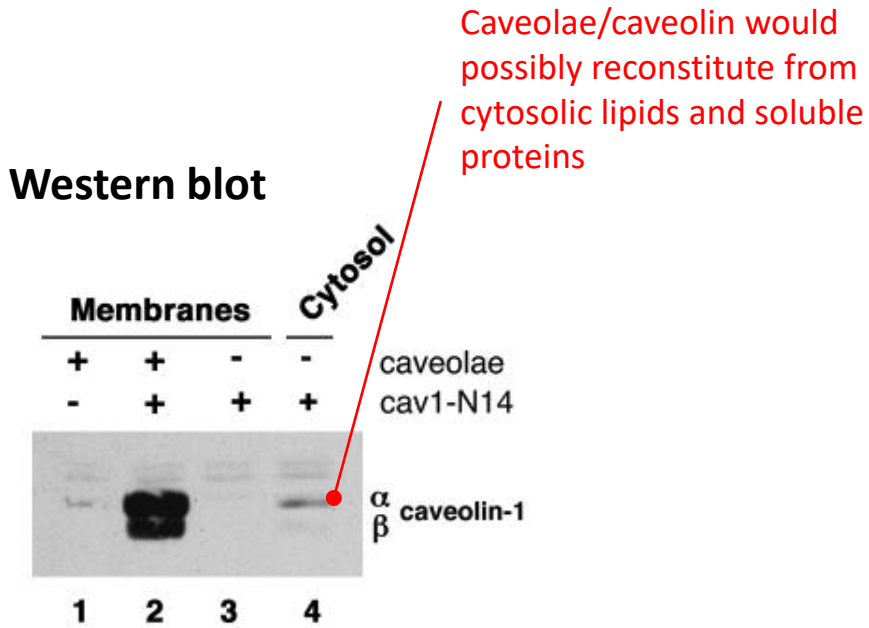
EM: PV-1
Various Procedures Cholesterol

Cholesterol likely binds to caveolin-1 super-stoichiometrically

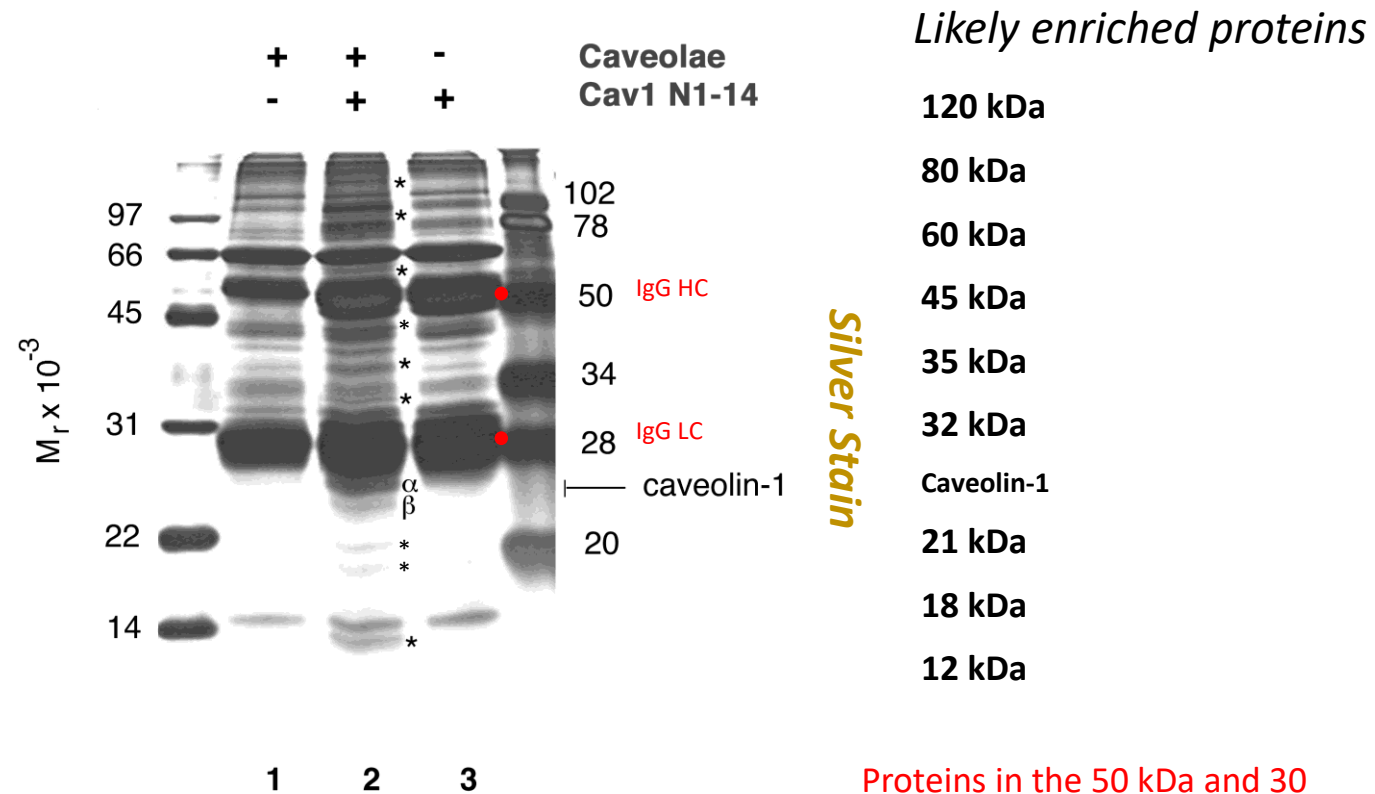
Half-maximal raft binding of Anx 5 at 1 μM Ca^{2+} ; half-maximal binding at $\sim 150 \mu\text{M}$ Ca^{2+} to PS-containing vesicles

 β, γ Actin  Caveolin-1
Includes some caveolin-2  Reggie-1  ATP-Synthase β  NAD(P)H cytochrome b5 reductase  Cytochrome b5  Annexin A5

The Immunoisolation of Caveolae was Achieved with Cytosol Incubation Mimicking a Budding Reaction and Immunobeads



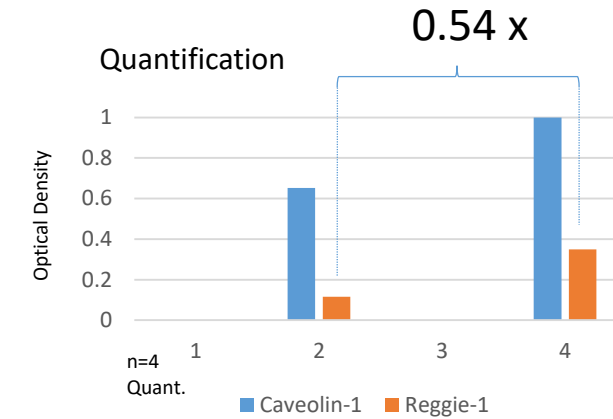
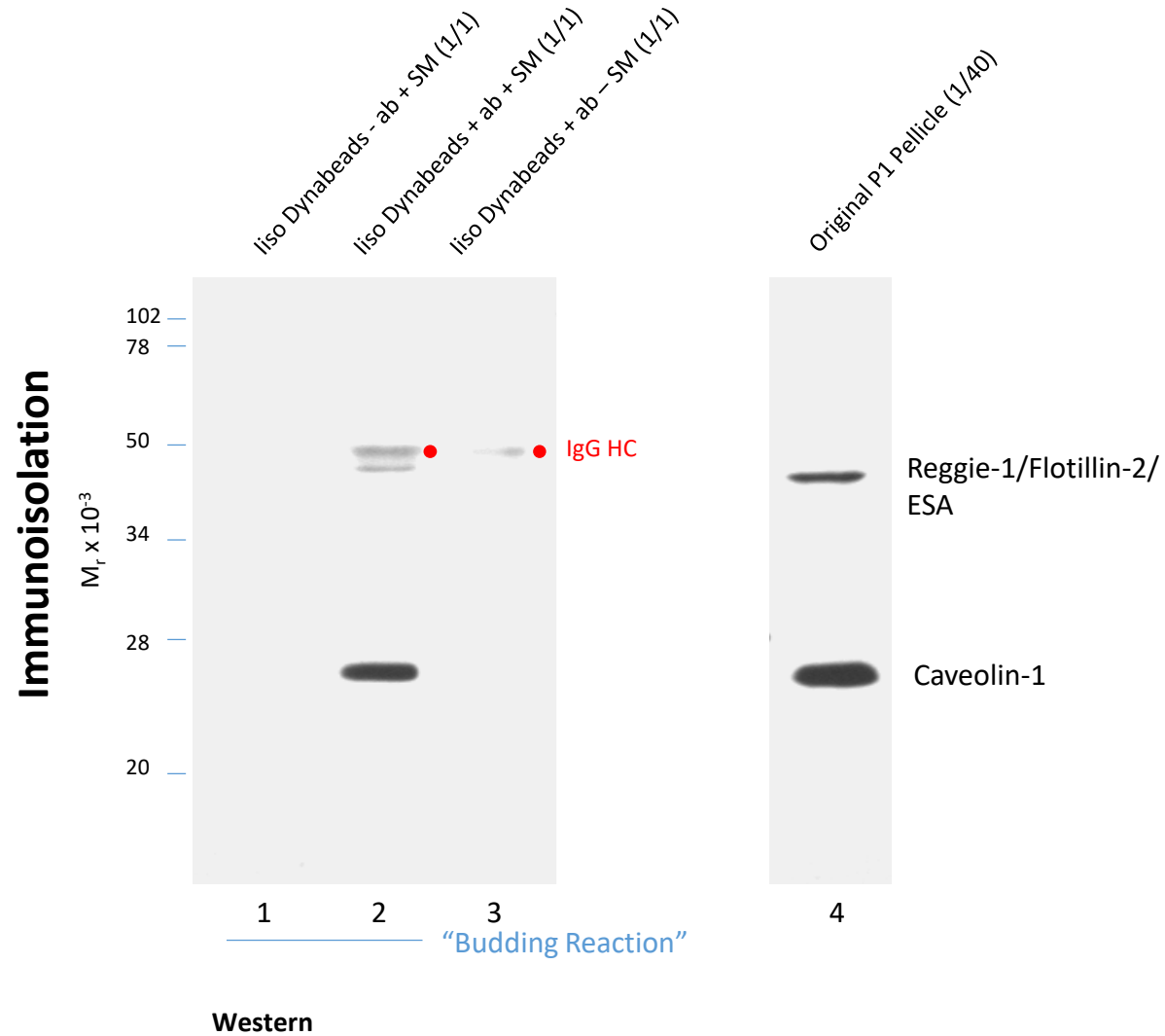
Membranes on isolated silica beads/cytosol and cytosol alone
were incubated in a budding reaction
(see next slide)



The cytosolic and membrane proteins were not identified

Proteins in the 50 kDa and 30 kDa range could not be delineated due to co-migration of IgG subunits

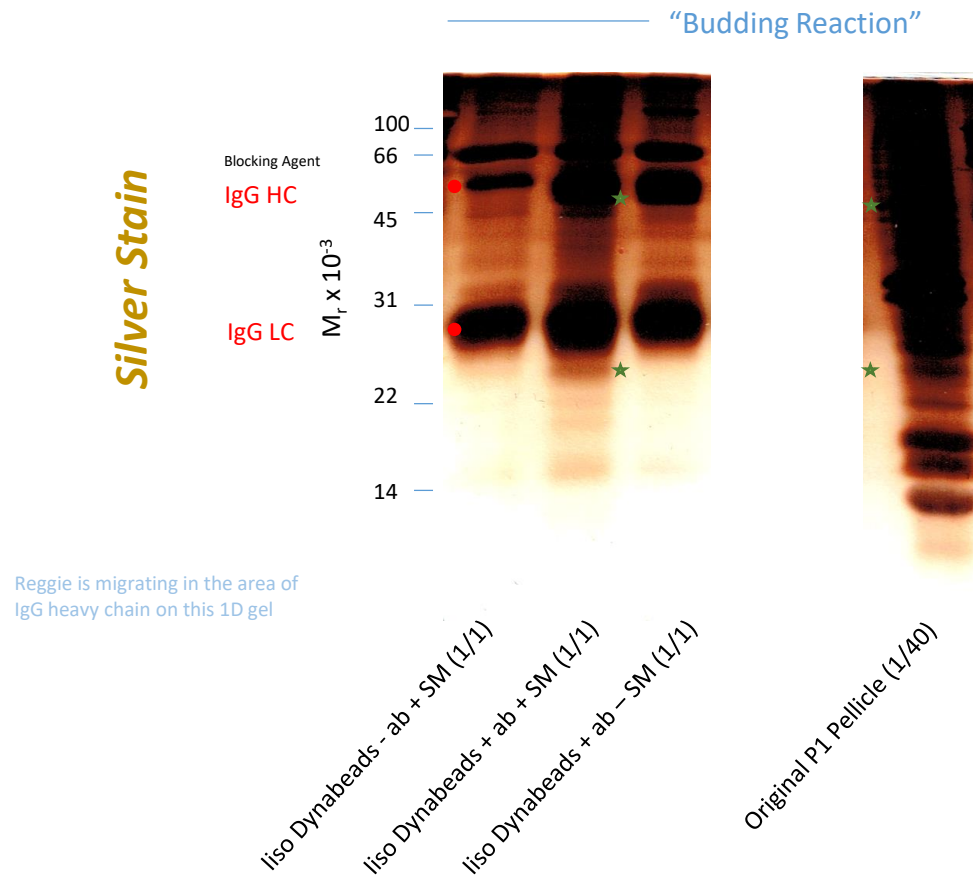
The Immunoisolation of Released Caveolar Membranes Demonstrated the Abundance of ESA/Reggie-1



*The reggie-1/ESA that was co-isolated was enriched 0.54-fold relative to **P1** membranes, in the following experiments enrichment was quantified relative to floated membranes which corresponded also to the input of membranes (SM) here!*

The Immunoisolation of Released Caveolar Membranes Demonstrated the Abundance of ESA/Reggie-1

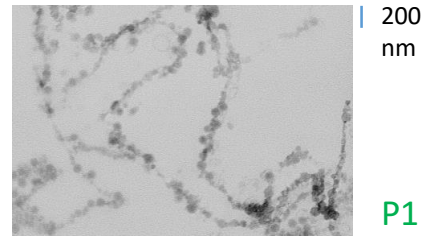
A quantity of the previous experiment (same gel) was resolved on SDS-PAGE and silver-stained



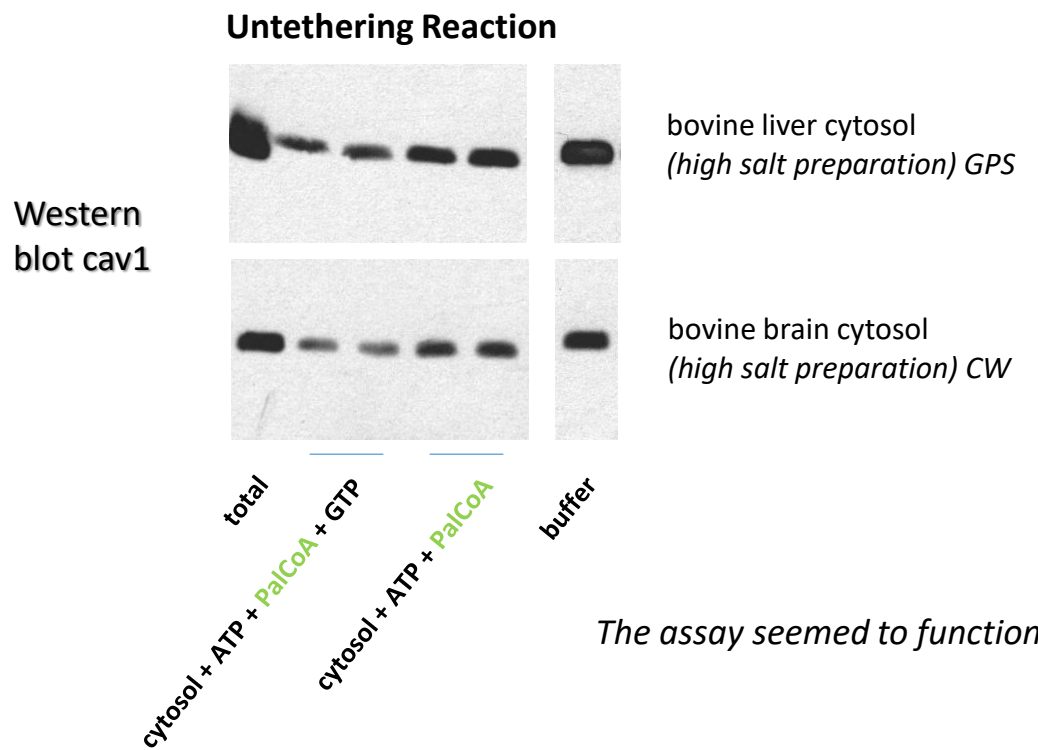
Reggie is migrating in the area of IgG heavy chain on this 1D gel

Reggie-1/Flotillin-2/
ESA

Caveolin-1

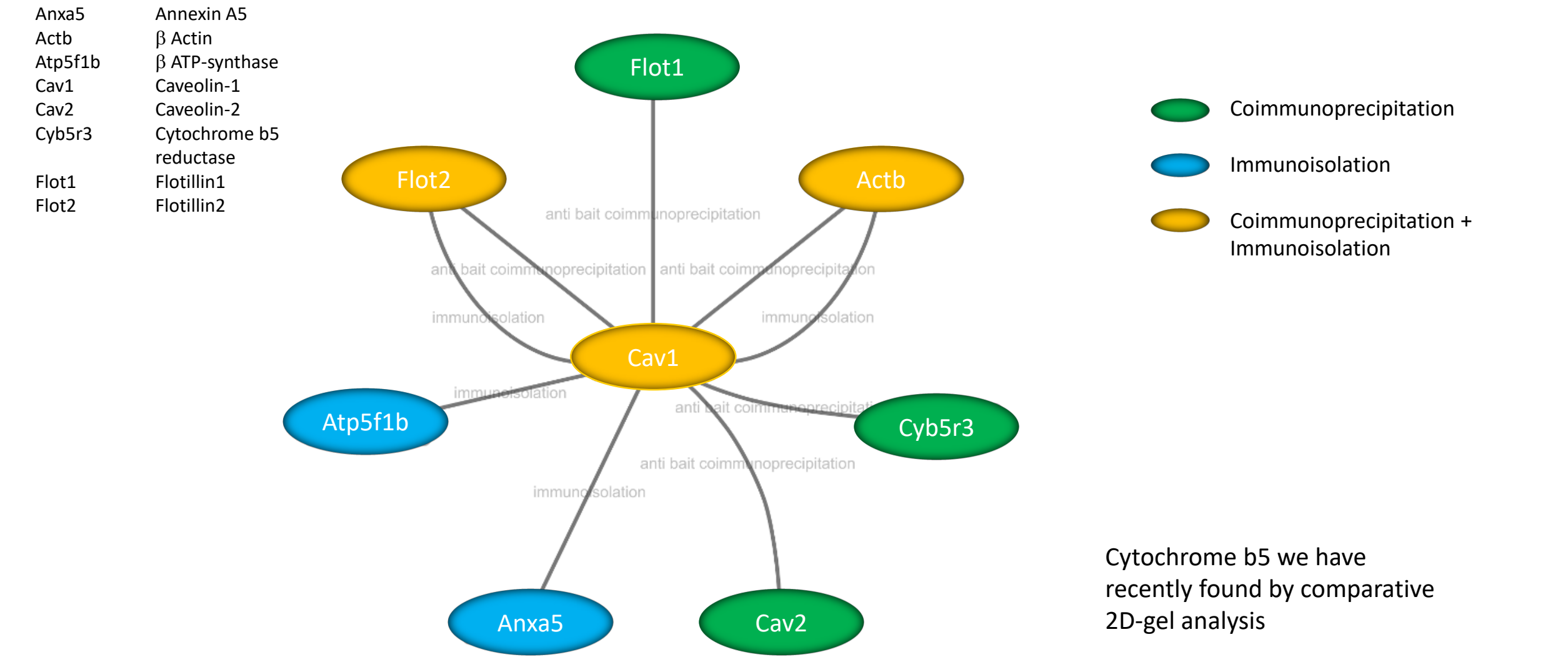


Lung membranes (Silica perfusion)
Fixed in 3% glutaraldehyde, 50 mM Na⁺-cacodylate pH 7.2, 1 mM MgCl₂, 1 mM CaCl₂, 90 mM KCl



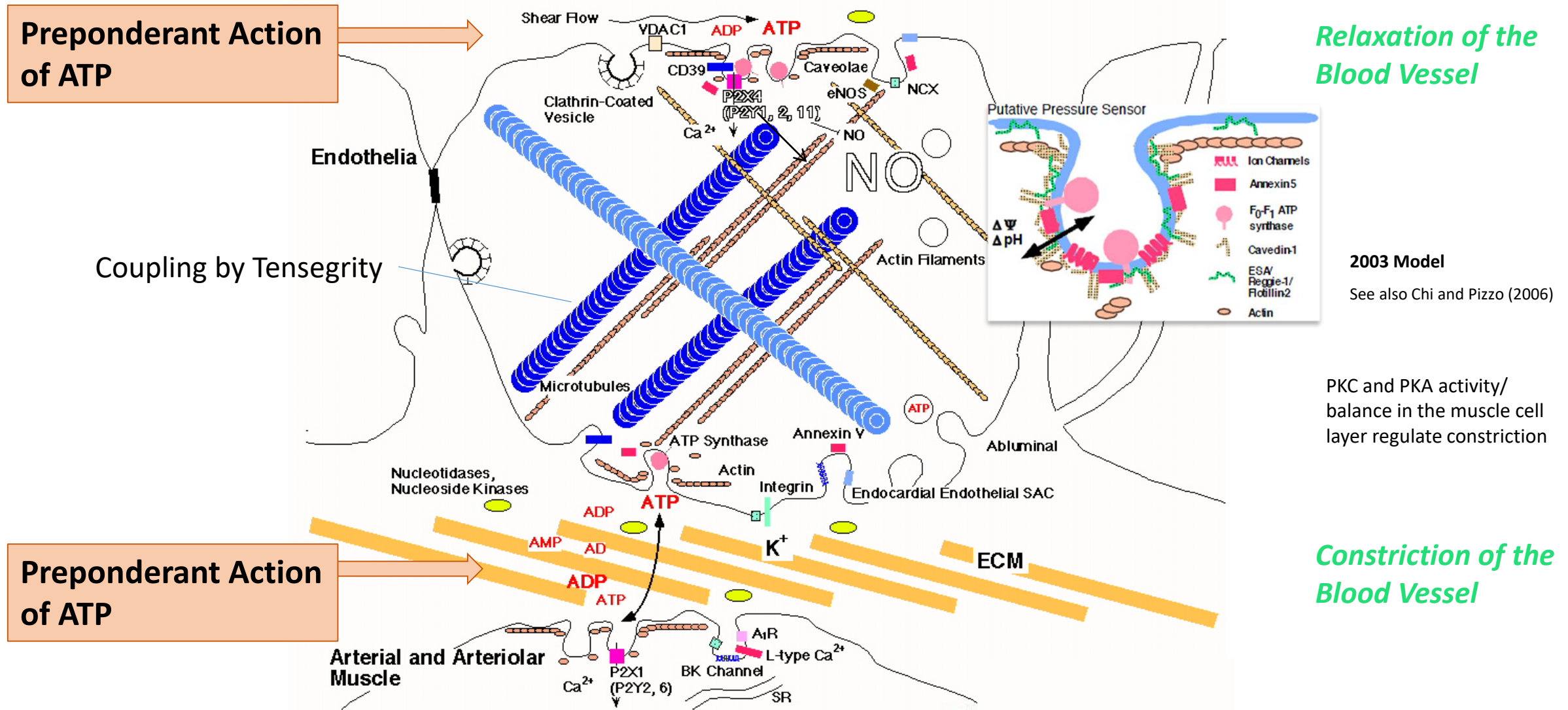
The assay seemed to function...

Interactome That we Found in Caveolae from an Animal Source



- Coimmunoprecipitation
- Immunoisolation
- Coimmunoprecipitation + Immunoisolation

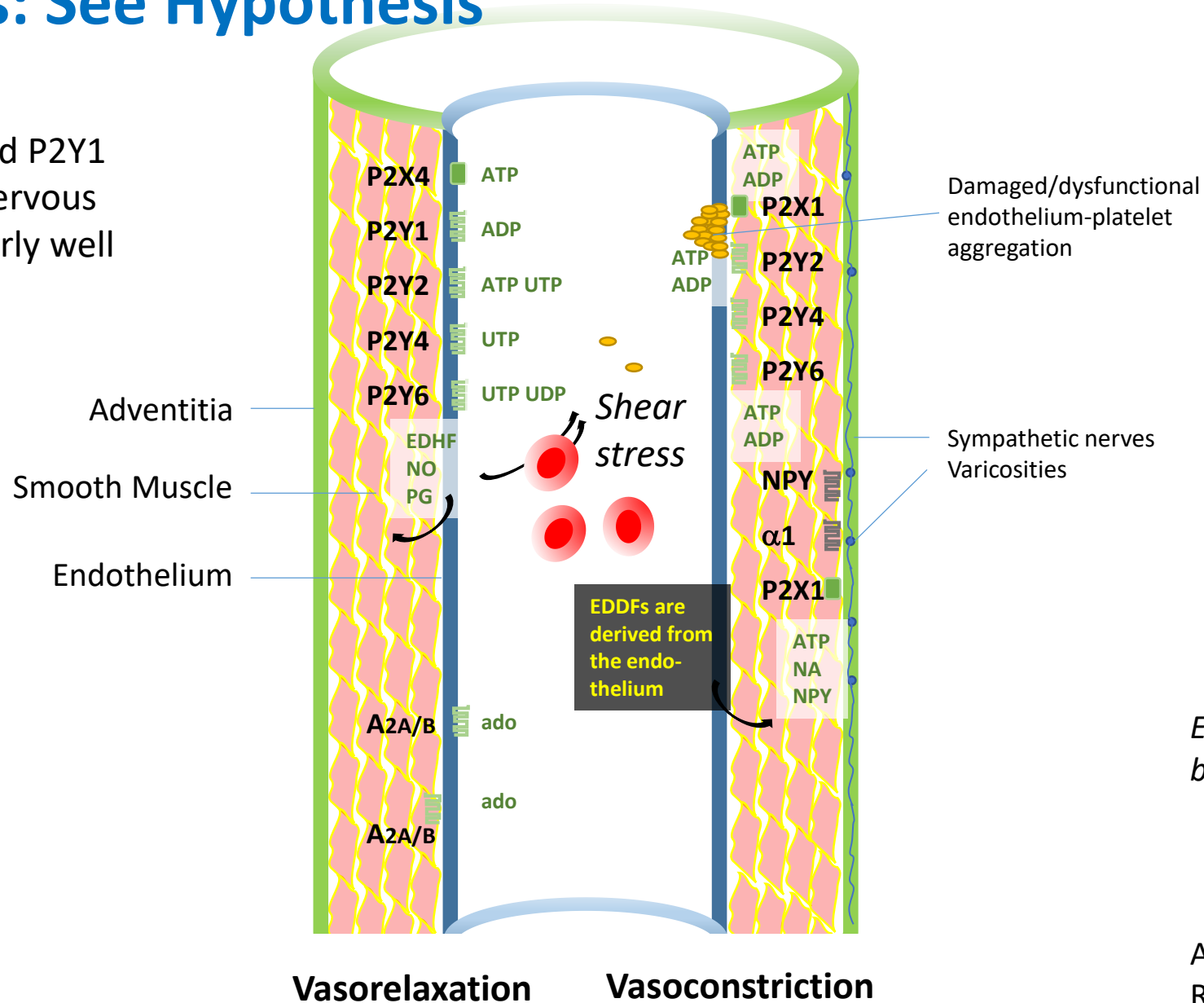
A Molecular Hypothesis with Respect to Vasoregulation was Proposed



Moreover, during pathological conditions such as in subarachnoid hemorrhage red cells release ATP and constrict arterioles directly via muscle P2X and P2Y₂ receptors; see Fiedler (2002), Chatenay-Rivauday et al. (2004), Burnstock (2008), some data were taken from von der Weid et al. (1993), Evans and Kennedy (1994), Hoyer et al. (1997), Hansen et al. (1999)

Example of Current Insight on P2X- and P2Y-Receptor Involvement in Blood Vessels: See Hypothesis

The role of P2X and P2Y1 receptors in the nervous system is particularly well understood



EDDFs have so far not been frequently listed

Adapted from
Ralevic and Dunn, 2015

The Molecular Hypothesis May be of Importance in Lung Physiology: Hormones and Factors That Regulate Blood Flow

- Pulmonary Constrictors

low P_{AO_2}

endothelin

serotonin

prostaglandins

thromboxane A_2

α -adrenergic catecholamines

angiotensin

leukotrienes

neuropeptides

histamine

high CO_2

- Pulmonary Dilators

high P_{AO_2}

prostacyclin

dopamine

nitric oxide

acetylcholine

bradykinin

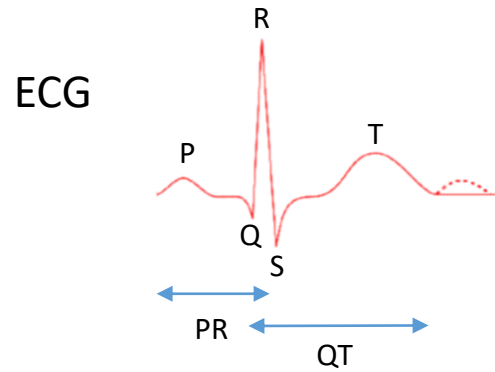
β -adrenergic catecholamines

ATP

ATP is added to treat pulmonary hypertension after cardiac surgery (see Burnstock 2008) and in cardiac resynchronization in sinus arrhythmia or reentrant tachycardia (see Otomo et al. 2008)

The role of caveolae in hypoxia may be seen in the regulation or function of dihydroceramide desaturases in oxygen sensing (DEGS1/2 or DES1/2; see Devlin et al. 2011)

Of Prime Interest: Risk of Atrial Fibrillation - Physiological Function of Caveolin and Indications from Genetics



Long- or short-QT syndromes are often associated with rare mutations in ion channel genes

See MR-Egger regression concerning arrhythmic changes and blood pressure in the “Outlook on Caveolae”

It was found that caveolins are frequently associated with altered PR and QT times and affect atrial fibrillation (cav3, **cav1/2**). Ion channels are also bound by caveolins or are localized to caveolae (TRPV4, TRPC1/4, Na⁺/K⁺-ATPase, f-channels, Ca_v1.2, K_v1.5, kir6.2, Na_v1.5 and NCX), and recently it was found that cav1/2 are associated with heart rate increase and recovery in exercise in the autonomous regulation of the nervous system (this may also relate to the early finding of cav1 in neurons/DRGs).

Vatta et al. 2006

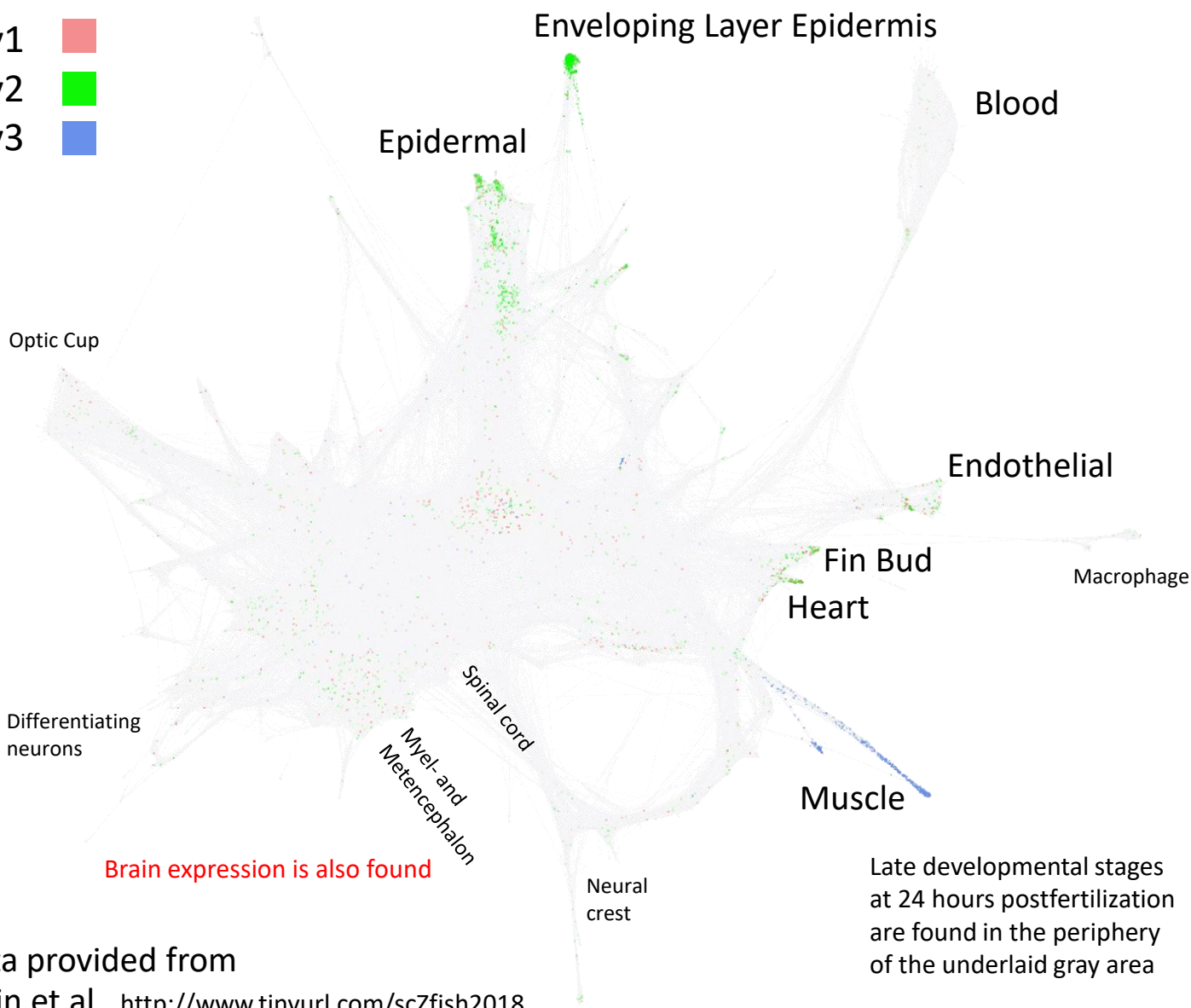
Holm et al. 2010

Ellinor et al. 2012

Verweij et al. 2018

A Study in the Model Organism Zebrafish Confirms the Widespread but Selective Expression of Caveolin Genes

cav1
cav2
cav3



Data provided from
Klein et al. <http://www.tinyurl.com/scZfish2018>

A widespread expression of flotillins/reggies has previously been expected and results in the single-cell graph with peripheral “label”:

flot1a flot1b flot2a flot2b

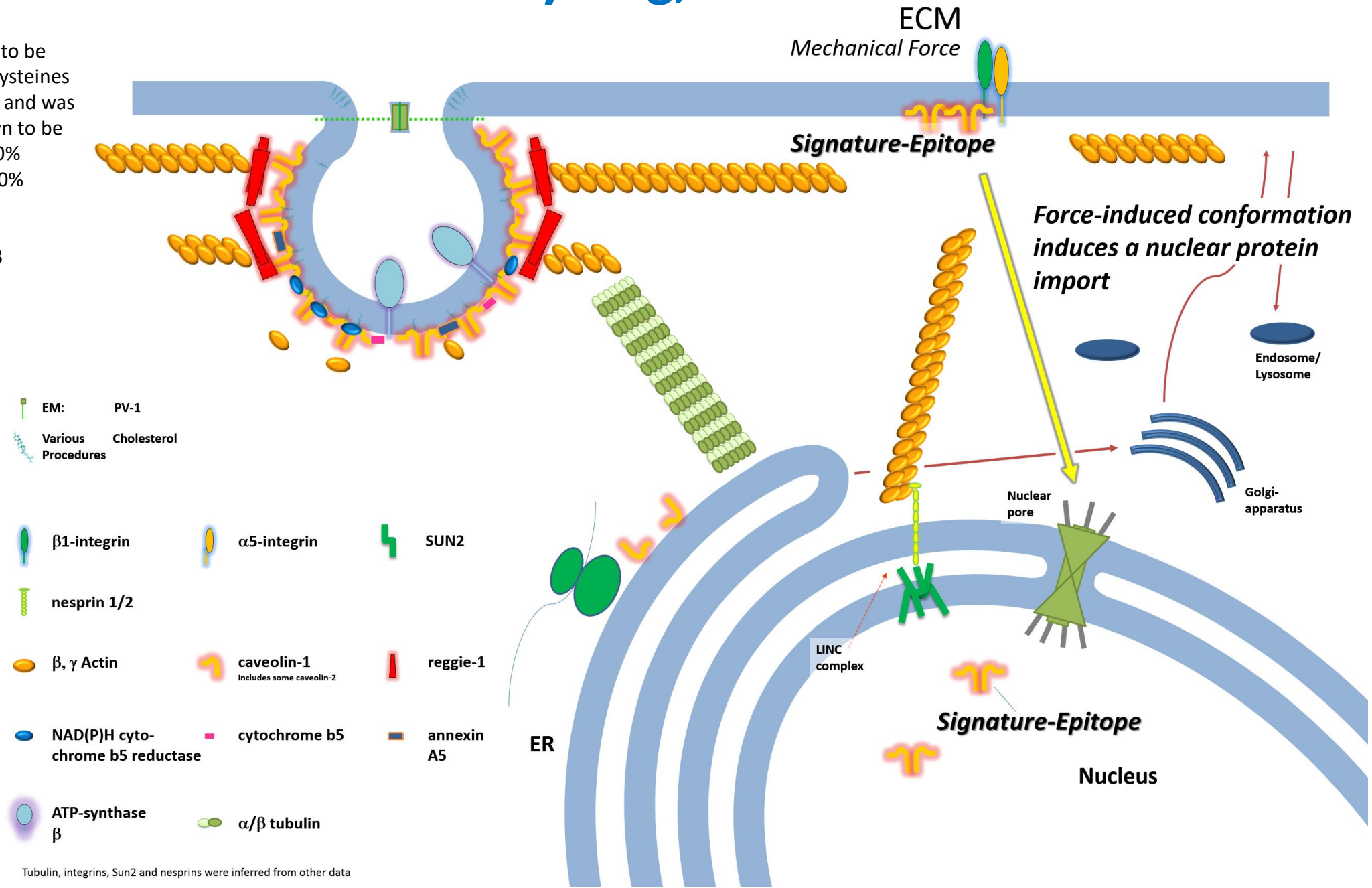


Nkx2.5, a transcription factor/“mechano-repressor”, was recently found to interact with flot1 (Dingal et al. 2015) and in these ways caveolins and reggies could be involved in meso-/ectoderm to heart development

Caveolin-1: Possible Role in Cycling, Adhesion and Cell Growth

Cav1 is found to be modified on cysteines 133, 143, 156 and was recently shown to be acylated by 60% stearic- and 40% palmitic acid

Cai et al. 2013



Data were taken from Chatenay-Rivauday et al. 2004 and Fiedler et al.

Tubulin, integrins, Sun2 and nesprins were inferred from other data

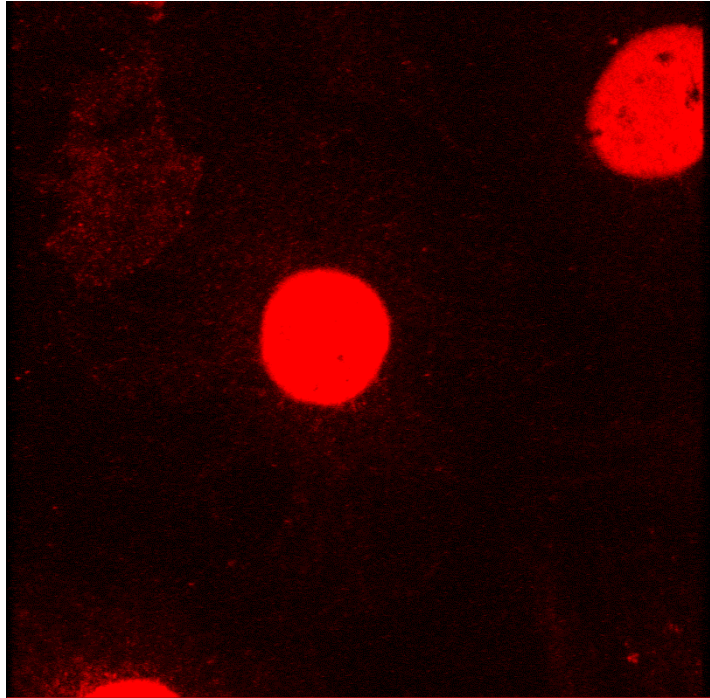
Signature-Antibodies

Cells were plated on collagen I

SVEC4-10 cells

Transformed

Mip



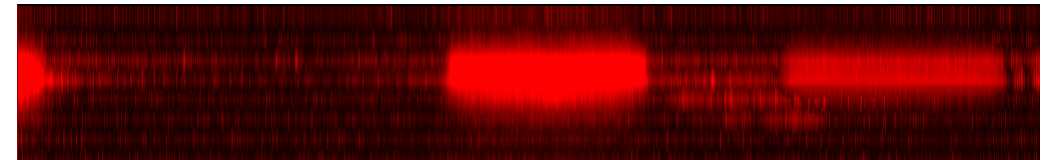
Focal contact-type labeling was not found in all but many cells

■ caveolin-1

The perinuclear extension of cells in the z-direction was only 150 nm as seen in transmission EM

Cell nuclei

Z-projection



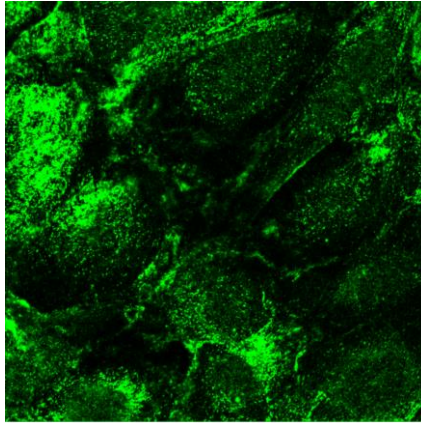
← Approximate size of a single cell →

The signal was confined to optical sections of $\sim 2 \mu\text{m}$ thickness

Would instability of the nuclear envelope allow for an exchange of material with the cytoplasm by non-pore import? Yet, a non-classical nuclear localization sequence has recently been described in caveolin-2

Nuclear Caveolin-1 Likely Shows a Particular Conformer

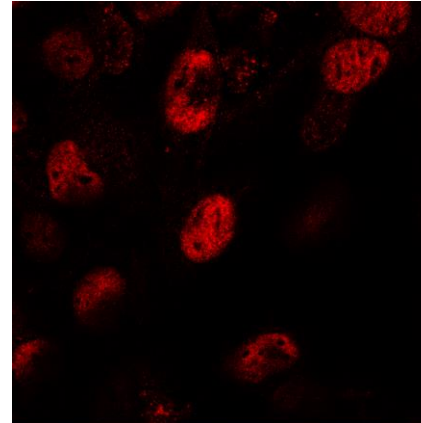
Polyclonal antibodies (C13630)



Cells

SVEC4-10

Polyclonal *Signature*-domain antibodies

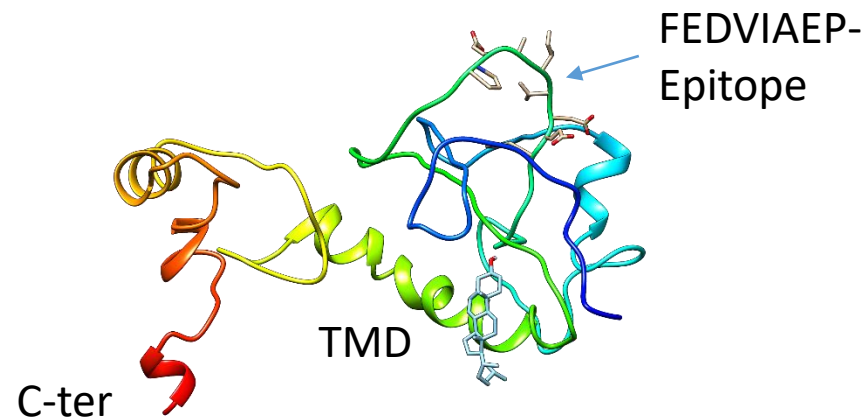


Cells

SVEC4-10

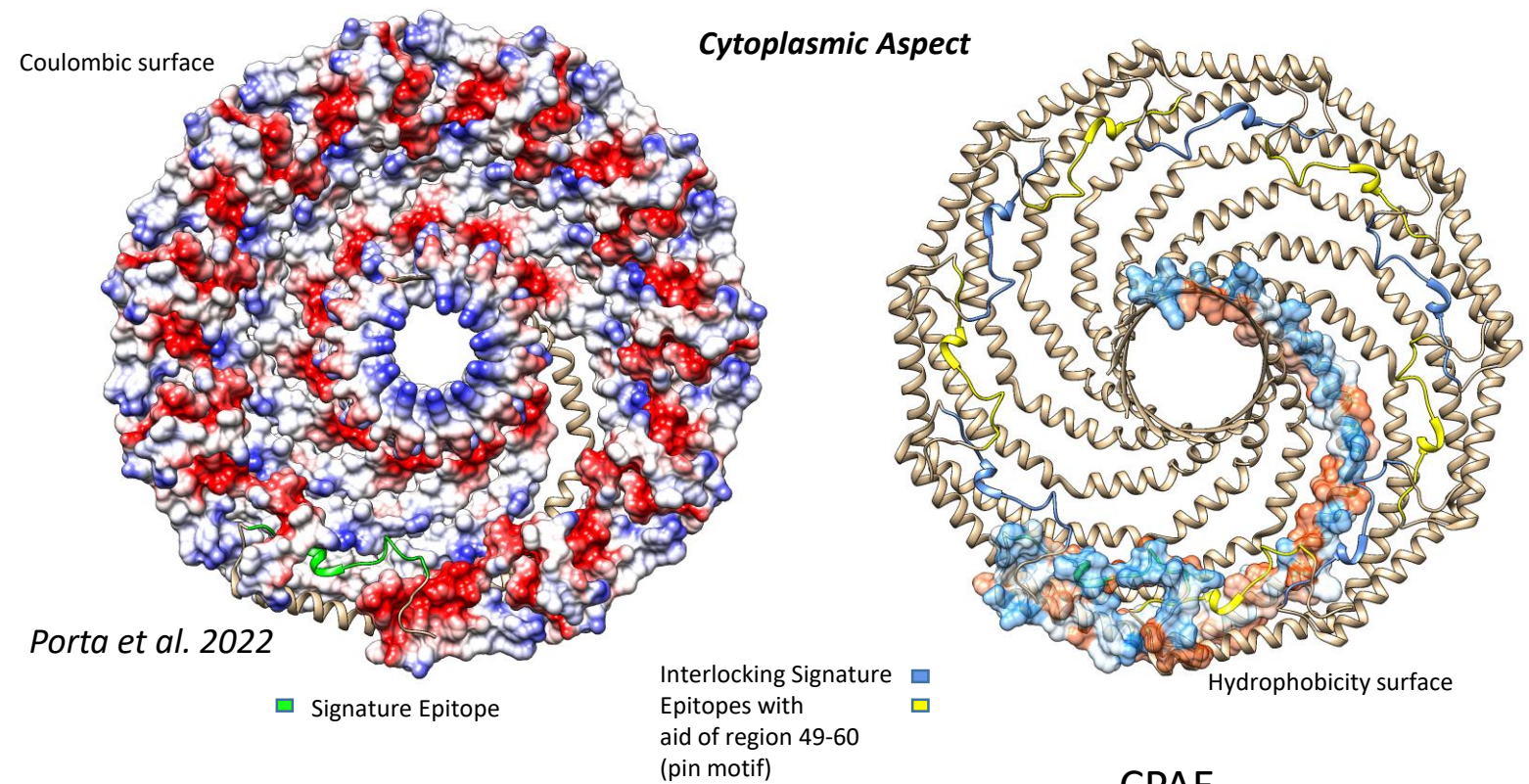
Results confirming a nuclear localization of caveolin:
cav1 - Feng et al. 1999
cav1 - Chatenay-Rivauday et al. 2004
cav1 - Sanna et al. 2007
cav2 - Kwon et al. 2011

this result was not expected



**Nuclear localization
with cav-1 antibodies**

Current Structural Insight: the Cav1-Signature Antibody Recognizes an Epitope that is Likely Shielded in the Caveolin-1 11-mer



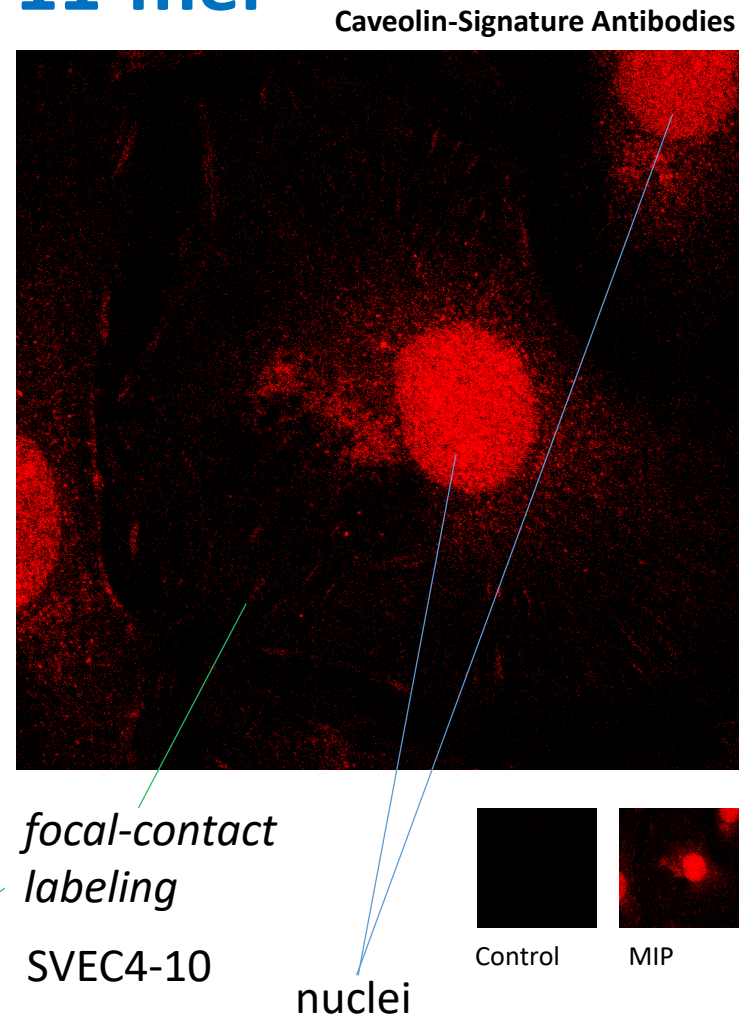
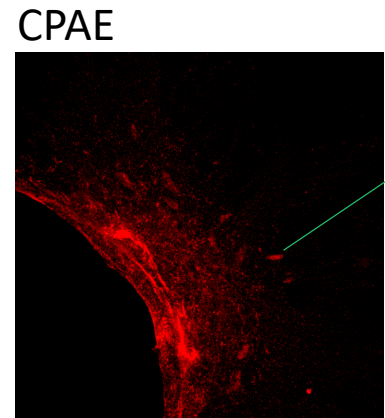
Porta et al. 2022

The (current N-ter.) 3₁₀ helix is part of the KHLNDDVVKIDFEDVIAEPE peptide that was used in antibody production

Chatenay-Rivauday et al. 2004

Rare Labeling in Primary Cultures

other cells were not labeled except few additional cells that showed lysosome-like staining

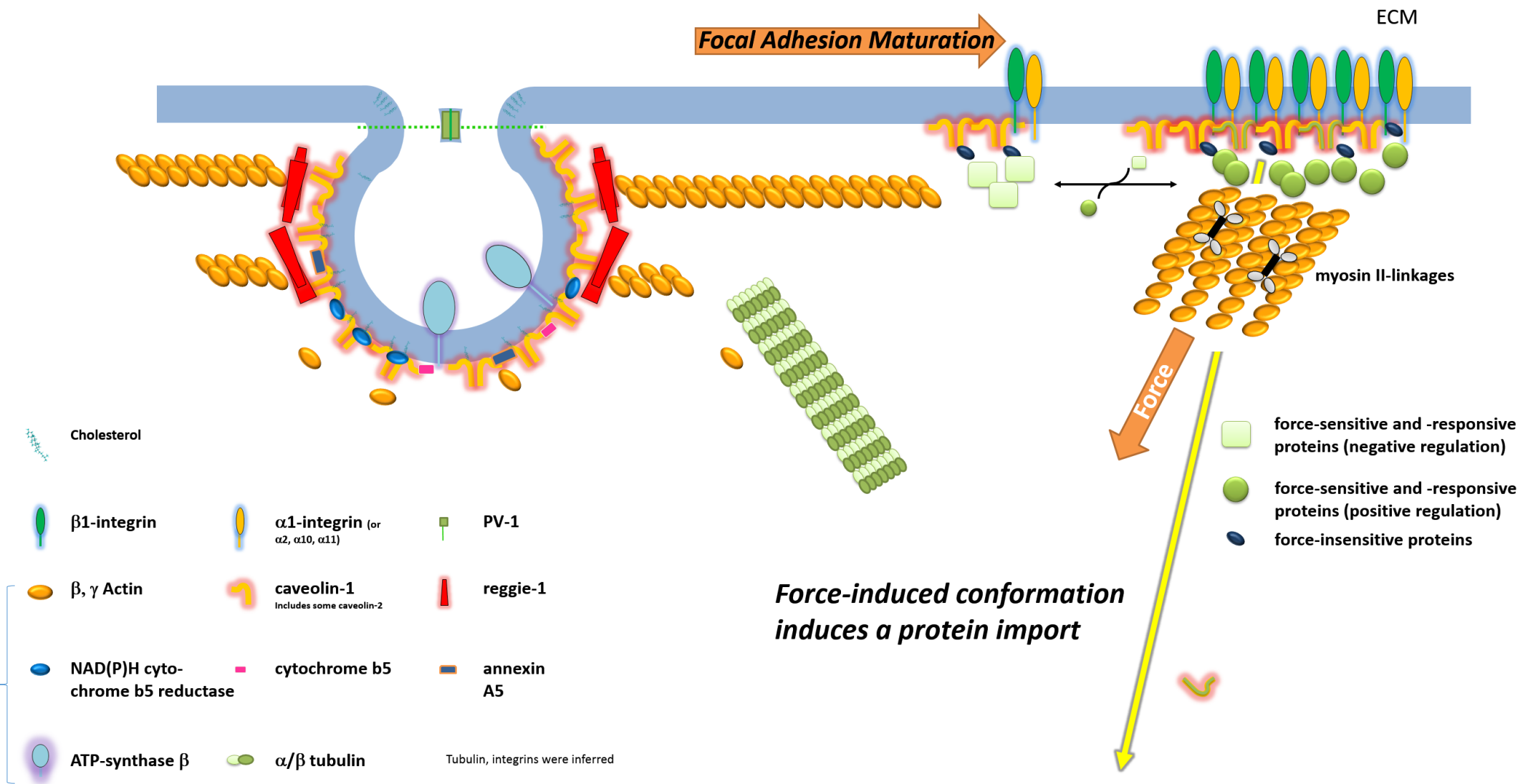


1/10'000 of cells could be labeled and was not found in the "first place"

We conclude that the caveolin-1 11-mer is dissociated or conformationally altered, or both, in focal contacts and in cell nuclei of transformed cells

Adhesions are Reorganized in Maturation

Data were taken from Chatenay-Rivauday et al. 2004 and Fiedler et al.



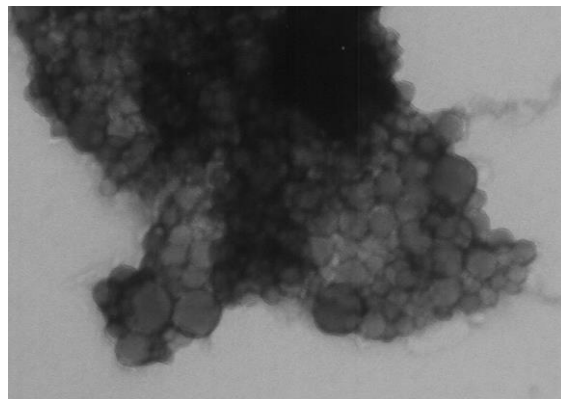
see Wary et al. 1998, Stan et al. 1999 and other sources

Electron Microscopy of Membranes of the Immunoisolation

This experiment involved the release of membranes as described in our 2004 Mol.Biol.Rep. publication and should have appeared in the Supplementary Section (see Fig. 1 g, h)
Chatenay-Rivauday et al. 2004

Silica purification of apical membranes: gentle sonication was used

Residual Pellicle



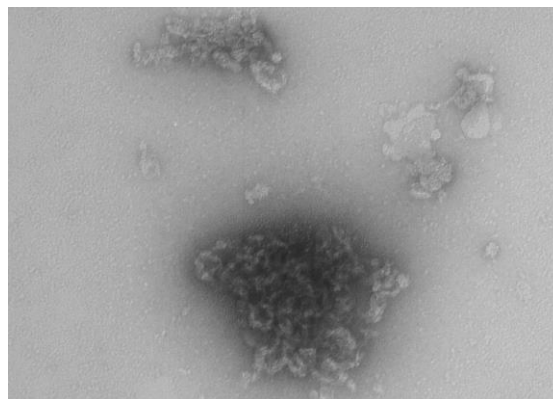
Magnification

55'000

100 nm

approx. size of silica particles
50 nm

«Dense Membranes»

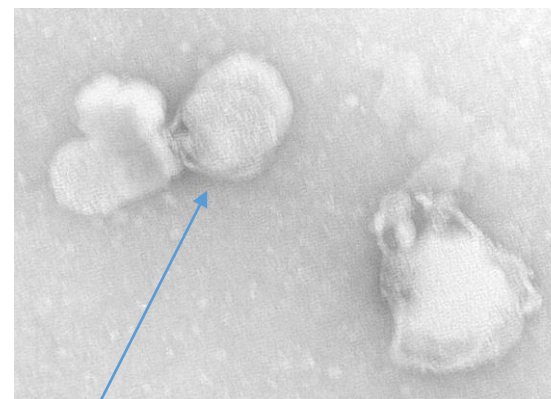


90'000

100 nm

membrane fragments and presumably cytoskeletal elements
were visible

Starting Material (SM)



90'000

100 nm

~ 100 nm vesicles

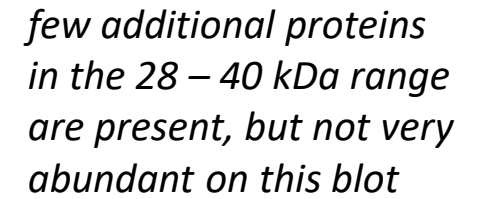
few vesicles > 200 nm
were also visible

→ The immunoisolation efficiency from SM was ~100 %

*The starting material for this EM analysis was
collected from a control reaction incubated overnight
in the absence of antibodies*

Immunoisolations were carried through with a mix of protease inhibitors that were reacting with free thiol-groups, without reducing agents

Immunoisolations were carried through with a mix of protease inhibitors that were reacting with free thiol-groups, without reducing agents



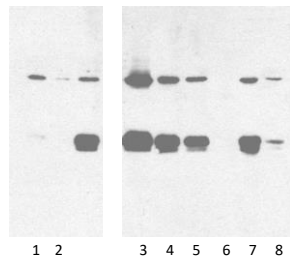
dense and light membranes contain significant amounts of β/γ -actin

Surprisingly only three major proteins were found including caveolin-1

Unrelated reaction shows large amounts of proteins

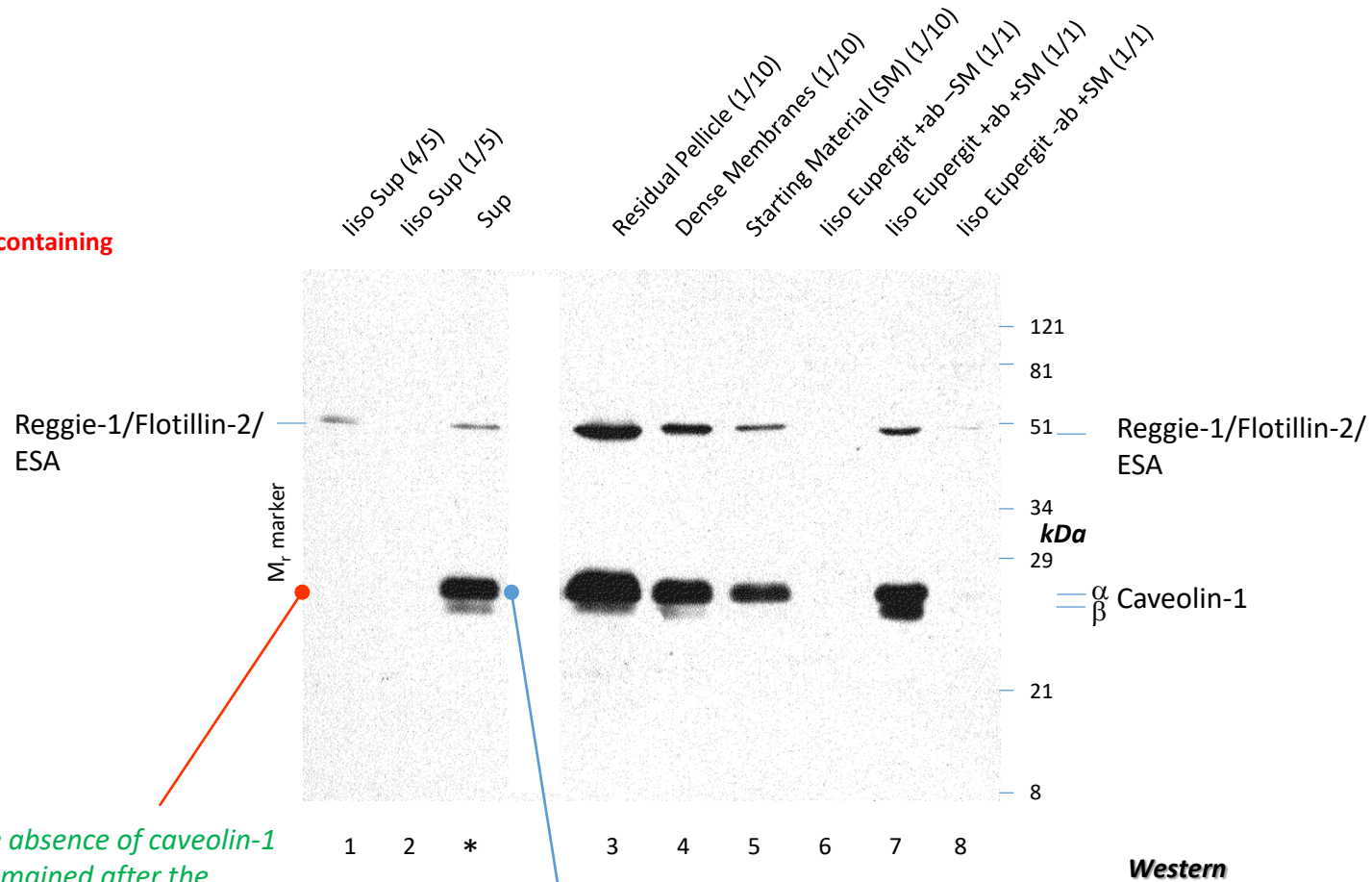
These Early Immunoisolations Suggested the Presence of Two Types of Membrane Domains: Reggie-1 and Caveolin-Reggie-Domains

Not all Reggie-1/Flotillin-2/ESA-containing vesicles could be isolated



ECL: Long Exposure

Note the almost complete absence of caveolin-1 in the supernatant that remained after the reaction and was recentrifuged to pellet membranes

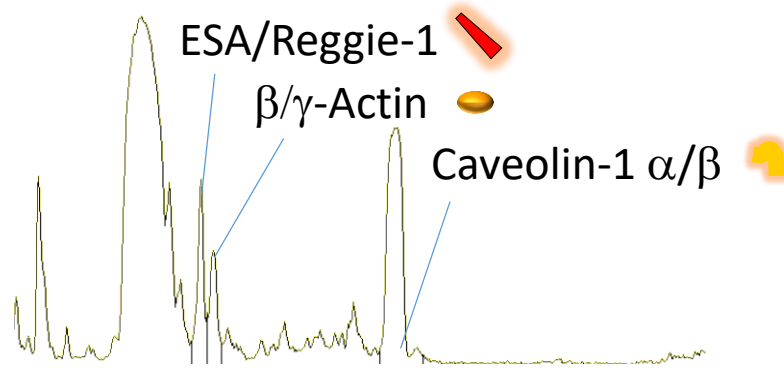


No clathrin could be detected on these blots (ICN pAb clathrin HC)

The immuno-isolation control showed large quantities of caveolin-1 in the supernatant

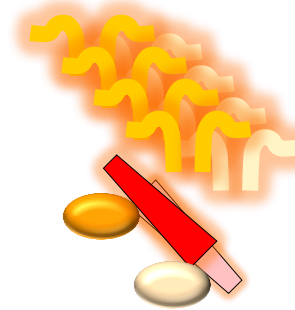
A Molecular Hypothesis with Respect to Vasoregulation was Proposed and Would Entail the Most Abundant Proteins

The Lane Labeled with the Asterisk was Quantified



Similar transfer efficiency and stain with Ponceau was assumed

Stoichiometry of the Protomer



1 : 1 : 8

β,γ -Actin : Reggies : Caveolin-1

In this lane proteins were well resolved

This Quantification was similar to the following determination from silver-stained gradients, some reggies or actin may have dissociated (stoichiometry of the vesicle mixture 1 : 1.2 : 8.5)

A Gaussian Model Quantification Would Suggest the Reduction of Actin in the Eupergit Immunoisolated Vesicles

The stoichiometry in octylglucoside detergent-extracts (sucrose-gradients/high S-value) was **2 : 2 : 8**

ESA/Reggie-1



β -Actin



Caveolin-1 α/β



Grey: inferred subunits

Mixed Vesicles

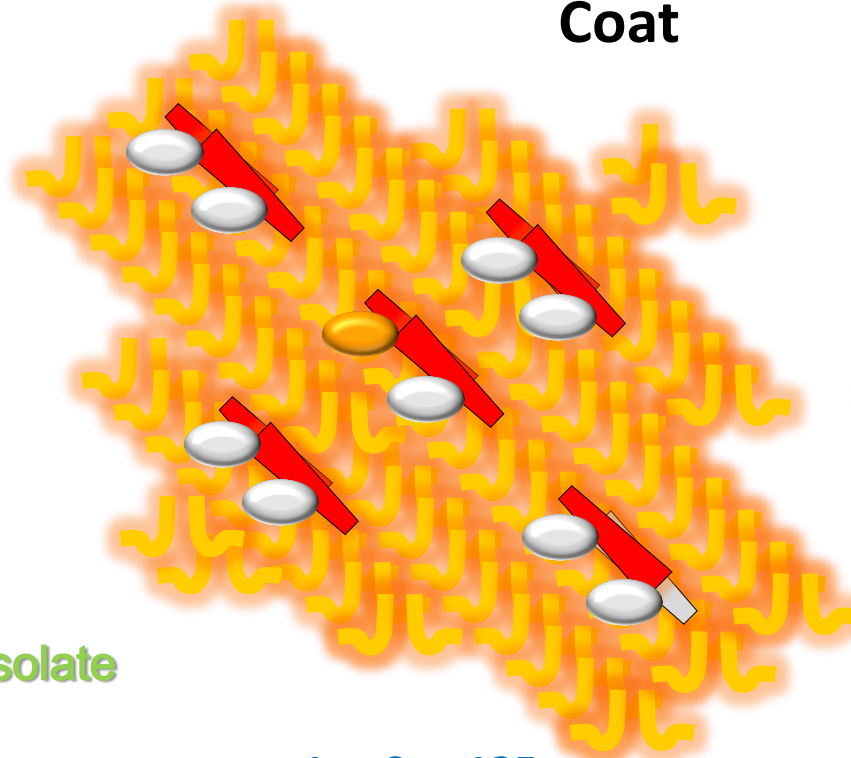


1 : 1 : 8

Gentle immunoisolation with cav1 N1-14



Immunoisolate



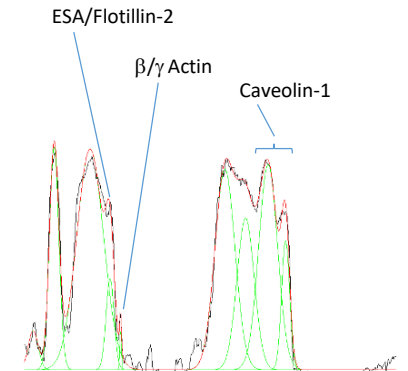
1 : 9 : 135

β, γ -Actin : Reggies : Caveolin-1

β, γ -Actin : Reggies : Caveolin-1

γ -actin could not be determined by immunoblot, but all actin and reggie proteins were quantified by «optical density»

Stoichiometry of the Caveolae Molecular Coat



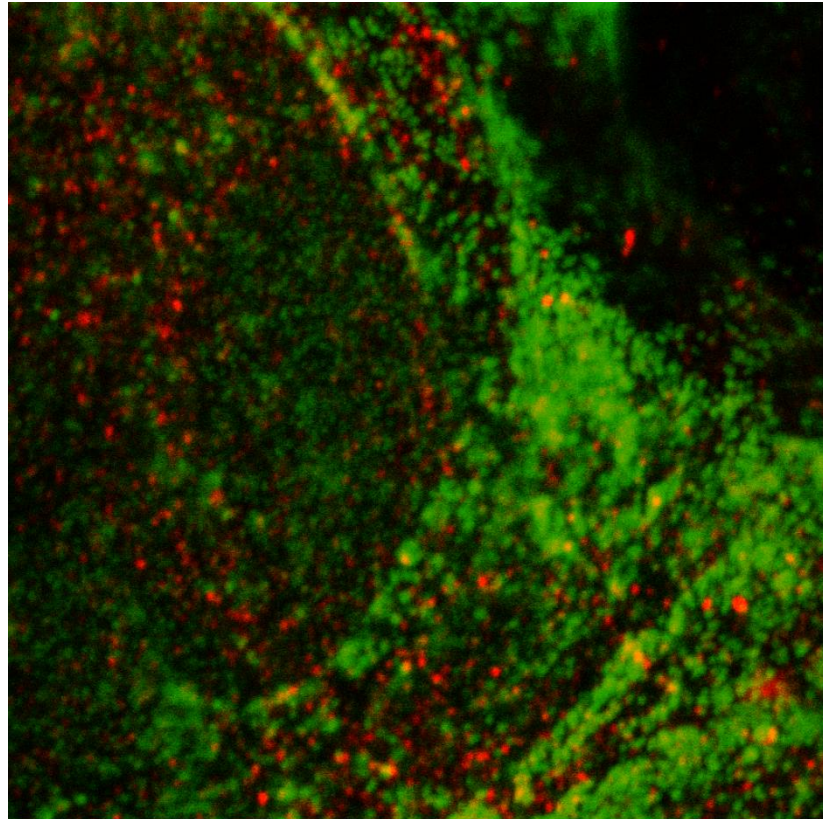
Lane 7 was quantified

The **accessibility** of caveolin-1 in isolated vesicles (cav1 N1-14 antibody) is **not known** if the protein is complexed with reggies and actin (stoichiometry in the immunoisolate $\sim 1 : 9 : 135$ or $1 : 10 : 156$)

Caveolae and the Actin Distribution in Endothelial Cells

See Chatenay-Rivauday et al. 2004

-Gdn

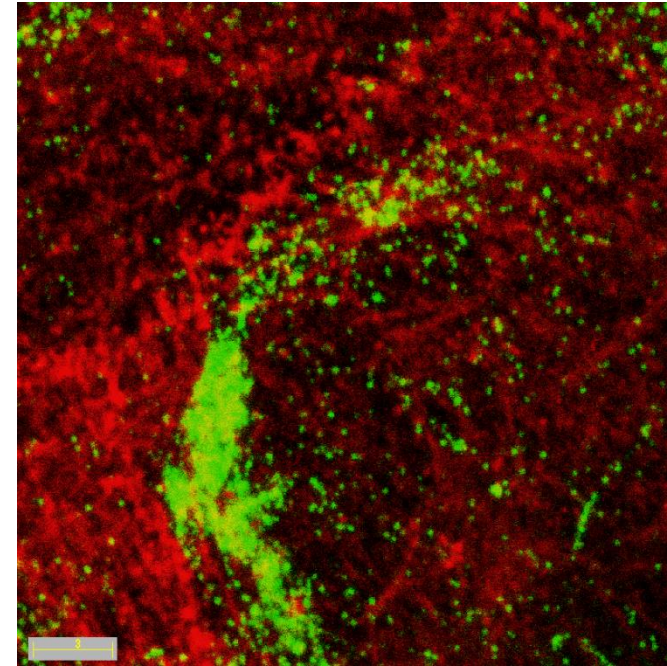


cav-1

β -actin

GdnHCl: Guanidinium-Hydrochloride

+GdnHCl, 3-Dimensional Reconstruction



μm

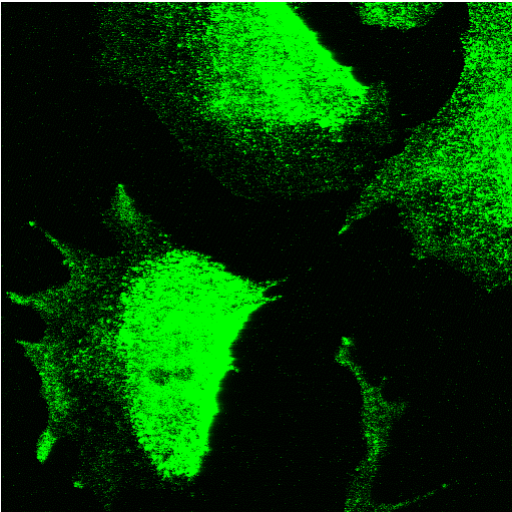
F-actin visibility
was increased in
this way

*In our view, caveolae usually follow the actin-network
in quantity*

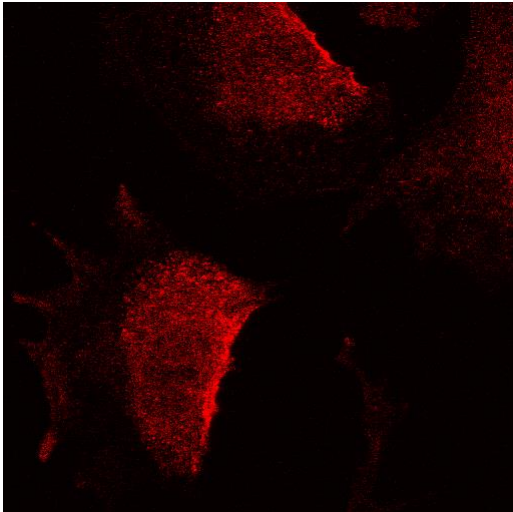
In CPAE Cells Caveolin-1, Actin and ESA/Reggie-1 were Co-Localized

Subconfluent cells without collagen I

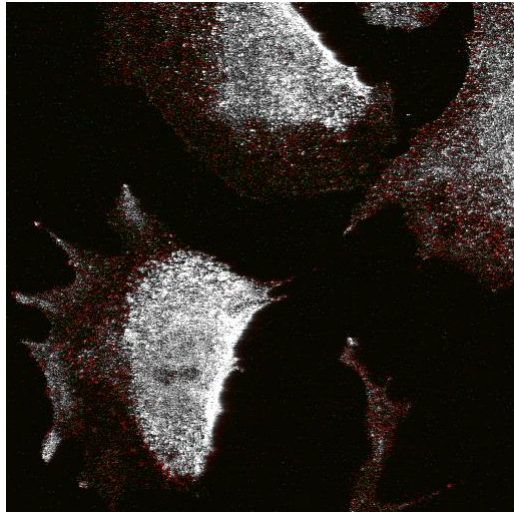
Cells were treated with GdnHCl



■ caveolin-1



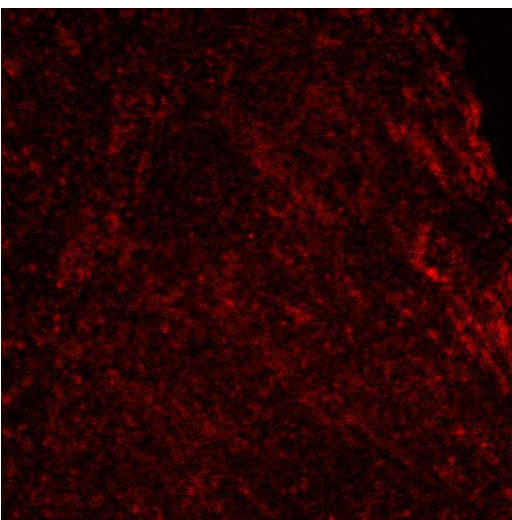
■ ESA



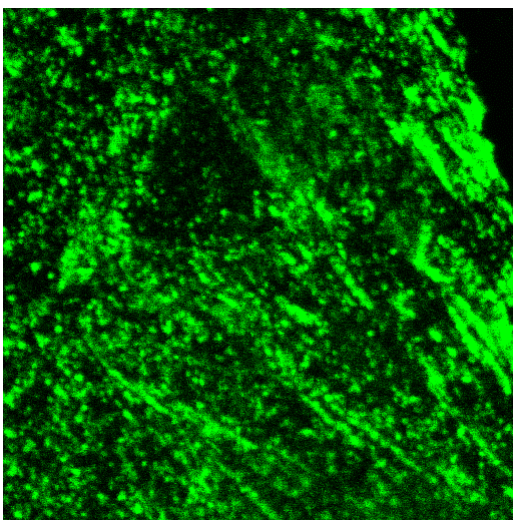
Pearson's R = 0.64 (above threshold)

Note the above threshold labeled ESA-positive structures that represent no caveolae

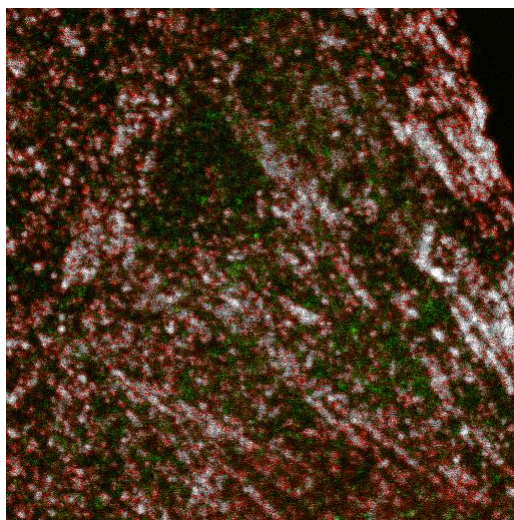
Settings were adjusted to single-labeled coverslips and secondary antibodies



■ caveolin-1



■ Actin



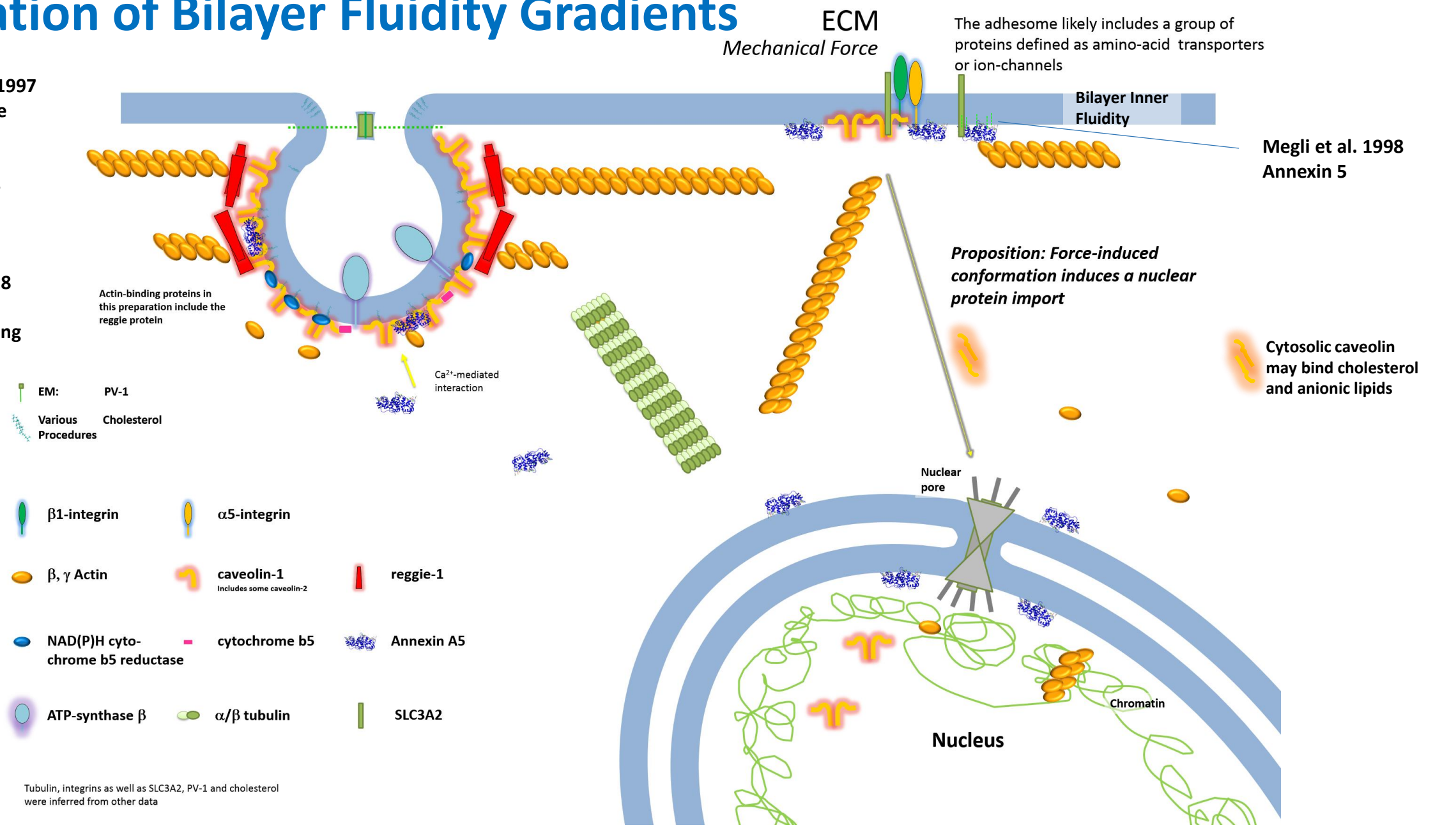
Pearson's R = 0.27 (above threshold)

JAS

New Results Suggest that Mechanotransduction Involves Annexins Via Regulation of Bilayer Fluidity Gradients

Luckcuck et al. 1997
Annexin 5 in the nucleus of developing cardiomyocytes

Raouf et al. 2018
Annexin 6 mechanosignaling



The Preparative Immunoisolation of Caveolae in Conditions Mimicking an Untethering (See Our Later Controls)

Protocol

Cytosol was prepared by bovine lung homogenization in a Waring blender in a buffer containing 25 mM Tris-HCl pH 7.4, 50 mM KCl, 1 mM DTT, 250 mM sucrose, 5 mM EGTA, 1 mM PMSF, 1 mM phenanthroline and PIC (cocktail of 2 µg/ml E64, 10 µg/ml leupeptin, 10 µg/ml pepstatin (1000 x stock in DMSO)). 384 ml of buffer were added to 216 g of tissue. The homogenate was spun for 60 min in a GS3 rotor (Sorvall) at 8500 rpm, 4°C. The supernatant was re-centrifuged in a Ti45 rotor for 90 min at 33000 rpm at 4°C. The supernatant was extensively dialyzed against a buffer containing 25 mM Tris-HCl pH 7.4, 50 mM KCl and 1 mM DTT. The cytosol concentration was determined to be 30 mg/ml with a Bradford assay (BioRad). In test experiments **caveolae** were **released from the silica** particles by cytosol incubations with or without 1 mM GTP, ATP regenerating system (1 mM ATP, 2 mM creatinephosphate, 8 IU/ml creatinephosphokinase; AS), 10 µM palmitoyl-CoA in buffer containing 25 mM HEPES pH 7.4, 50 mM KCl, 2.5 mM Mg-acetate. PIC was added to the solution. Samples were incubated for 1 hour at 37°C, underlaid with 250 µl 1.4 M sucrose in 25 mM Hepes pH 7.2 and separated into supernatant and pellet by spinning in the Eppendorf centrifuge (20 min, 14000 rpm, 4°C). For **preparative caveolae untethering**, 2 mg of a P1 fraction was incubated for 145 min at 37°C in 2.5 ml of a buffer containing 25 mM HEPES pH 7.4, 50 mM KCl, 5 mg/ml lung cytosol with AS, 2.5 mM Mg-acetate, 0.8 mM GTP, PIC and 10 µM palmitoyl-CoA. After the incubation (split in eight Eppendorf tubes), the samples were adjusted to a final concentration of 1.5 M sucrose, 500 mM KCl, 10 mM HEPES pH 7.4 and loaded into the bottom of a SW60 centrifuge tube. It was overlaid with 1.25 ml 1.09 M sucrose in 500 mM KCl, 10 mM HEPES pH 7.4 and 0.4 ml 0.25 M sucrose in 500 mM KCl, 10 mM HEPES pH 7.4 and centrifuged for 210 min, 50000 rpm at 4°C. 3 ml were collected from the top of six gradients and diluted with 4.2 ml of 0.1% BSA, 2 mM EDTA in PBS (IB) to a final volume of 7.2 ml. **Immunoisolation** with Dynabeads M280 coated with sheep anti rabbit IgG: Beads were preincubated with IB, 100 µl beads each were used for the reaction with or without 10 µg caveolin-1 N1-14 antibodies (cav1-N14) in the presence of caveolae (3.6 ml each) and were incubated overnight at 4°C by gentle shaking distributed in six tubes (2 ml) and three tubes (2 ml) with antibodies only. Samples were retrieved with a magnet and sequentially washed with four x 2 ml IB. The polyacrylamide gels were stained with silver to visualize the resolved proteins or prepared for Western blotting carried out with caveolin-1 (C43420, C13620, Cl. Z034, Cl. 2283; ICN, Zymed, Transduction Laboratories) monoclonal antibodies.

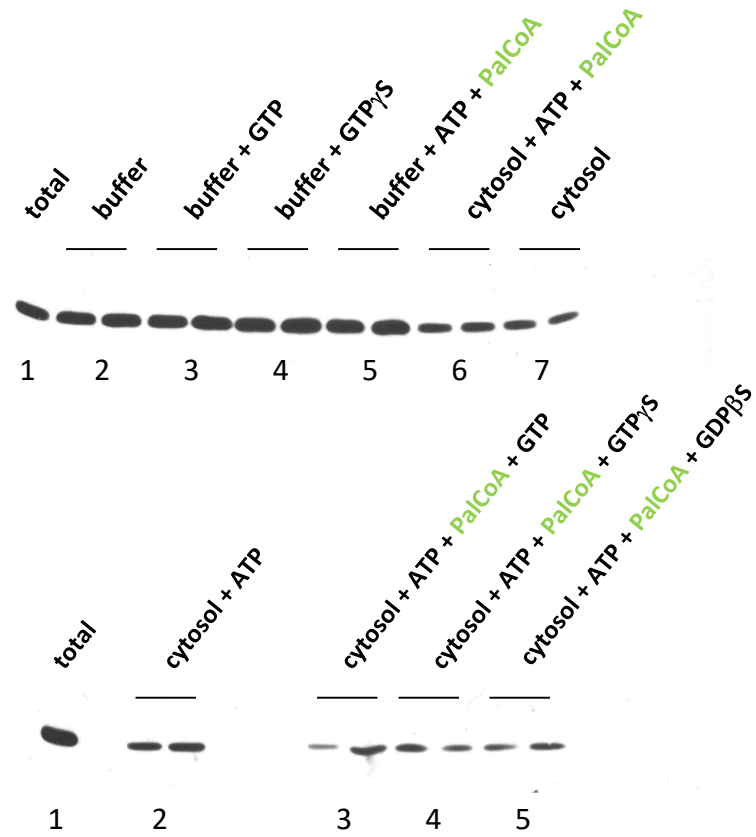
Other reagents can be found in Mol.Biol.Rep. 31, 67-84 (2004)

The Small «Untethering» Incubation Shows the Cytosol-Dependent Release of Caveolae

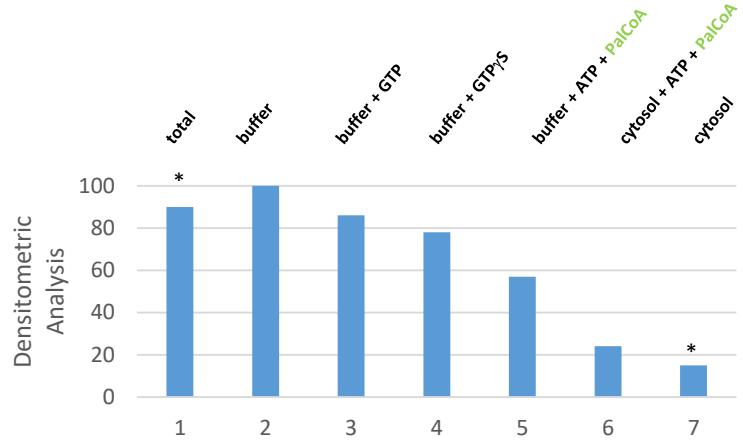
CHO cytosol was used in a concentration of ~3 mg/ml

cytosol was dialyzed against 25 mM Tris-HCl pH 7.4, 50 mM KCl and 0.5 mM DTT

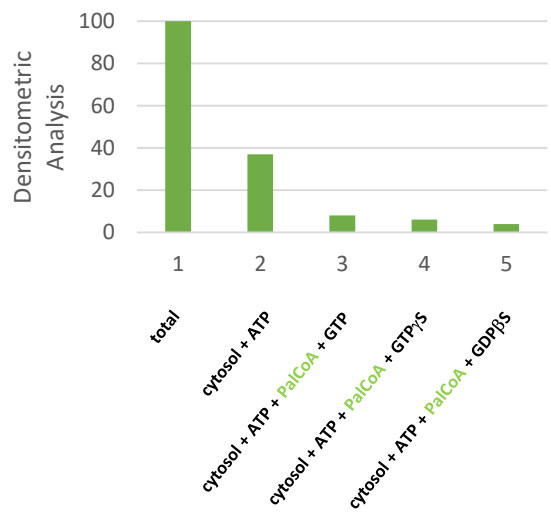
CHO cytosol is a “low salt” preparation in 0.25 M sucrose, 25 mM Tris-HCl pH 7.4, 50 mM KCl



No protein inhibitors were used in this assay



*transfer efficiency at the edge reduced



Cytosol alone and cytosol + ATP stimulate the indicated untethering, unfortunately, here no GTP hydrolysis requirement is visible (3-5)

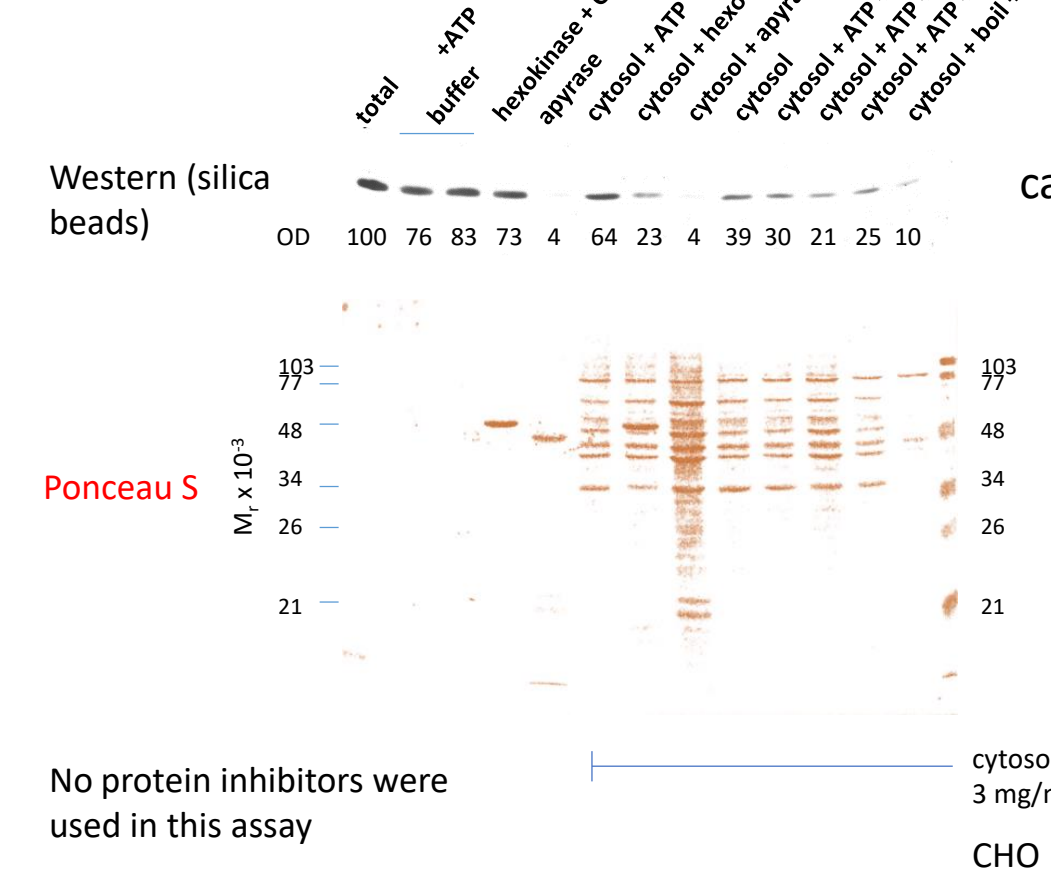
PalCoA was included in *in vitro* assays since the dilute cytosol incubation would drive palmitoylated proteins towards the depalmitoylated side of equilibria

See Aboulaich et al. 2004 who analyzed «caveolae-associated» proteins in adipocytes and found proofs for proteolysis of caveolae components due to PEST-domains (PTRF)

Putative Caveolae Released in the Budding Reaction Could Not be Well Controlled

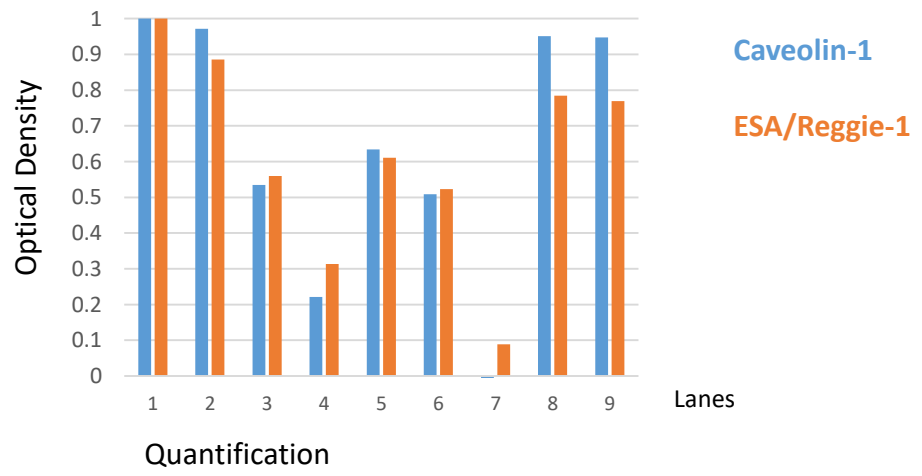
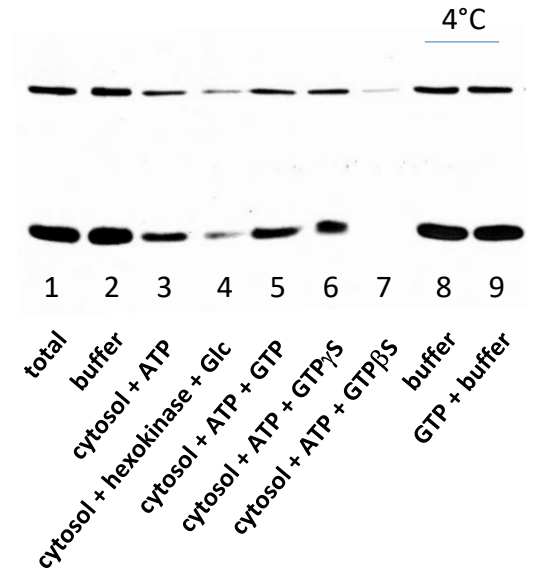
All reactions were at 37°C unless indicated

The Putative Budding Reaction was Similar to an Untethering Reaction, and Both, ESA/Reggie-1 and Caveolin-1 were Released



notice the differential amount of cytosol that binds to the silica beads

Western (silica beads)

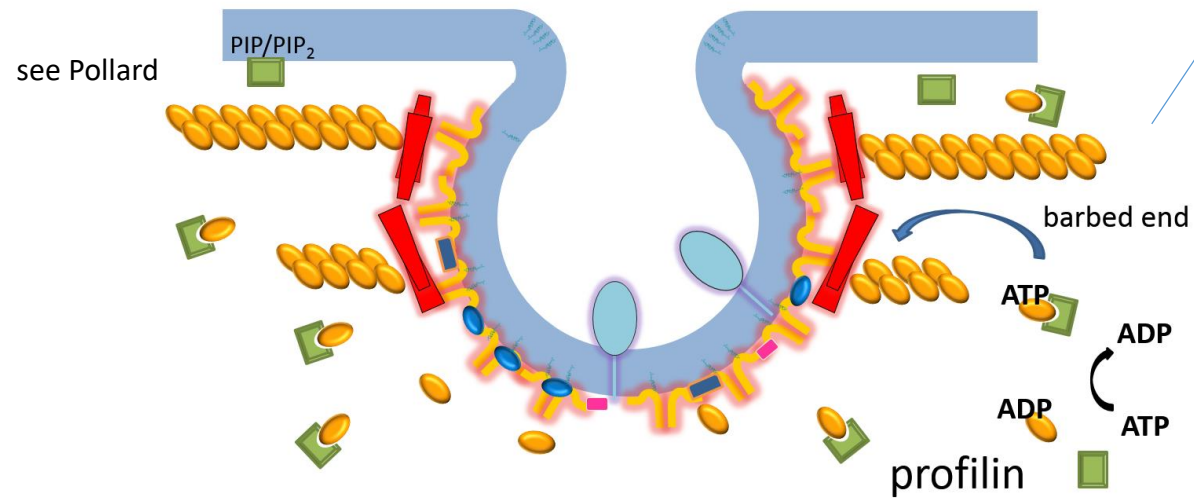


Budding reactions were carried through with membranes from silica coated vascular endothelia from rat lungs prepared similar to Jacobson et al. 1992

In lung and CHO cytosol GTP stimulation and hydrolysis requirement was not evident

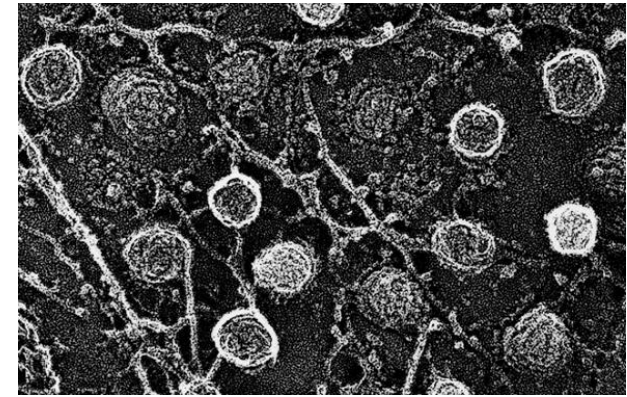
The Cellular Infrastructure Requires Energy

Maintenance of *In Vitro* Tethered Caveolae in the Untethering Requires Energy as Shown by Energy-Deprivation by Apyrase and/or Hexokinase/Glucose



Cortical actin stiffening has also been reported in some low energy conditions which could lead to release of attached membrane vesicles

Caveolae viewed from the cell interior in freeze-etch electron microscopy



With kind permission of John Heuser

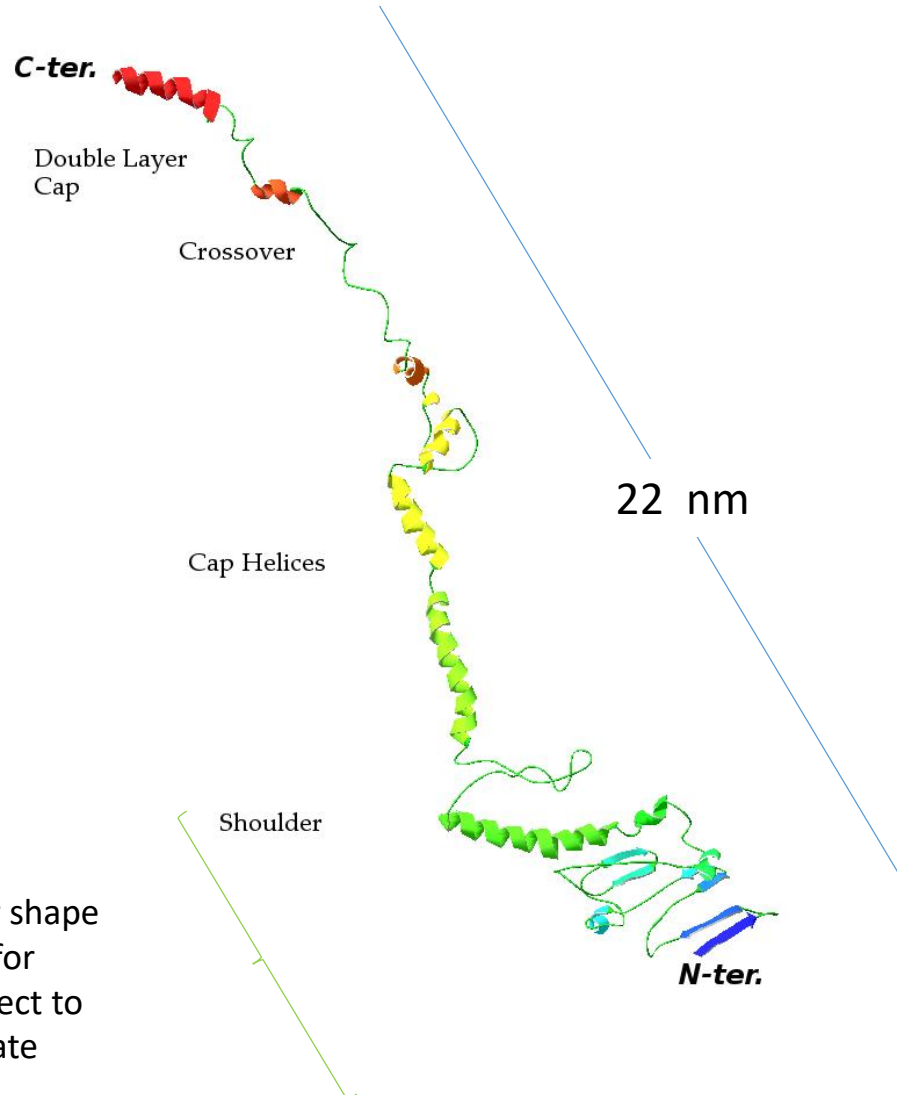
Profilin in the cytosol or other membrane-associated actin-binding proteins including profilin may require the ATP and therefore ATP-actin in the treadmilling and maintenance



The abundance of PEST motif containing proteins has been shown in caveolae, proteolytic degradation could be one pathway of release of caveolae that has not been confirmed (cavs and flots do not themselves contain the PEST motif)

Concerning the Structure of Caveolar Coat Proteins Little was Known: ESA/Reggie-1/Flotillin-2 was Found to be Similar to MVP

The 28-178 solution structures obtained by NMR were not extended to the full length structure model, the **Major Vault Protein (MVP) p100** was used as a template:



Similar modular shape was confirmed for 1WIN with respect to the MVP template

Major Vault Protein (MVP)

- MVP is largely localized to the cytoplasm
- The assembly contains 48 dimeric molecules
- The MVP has a size of 67.5 nm x 41.7 nm
- The ESA/reggie/flotillin proteins are multimers, assemble with actin and bind membrane with palmitoyl/myristoyl residues

A reggie-1 multimer would result in approximate fibrinogen-shape

This was applied to estimate the kD of the complexes (see gradients)

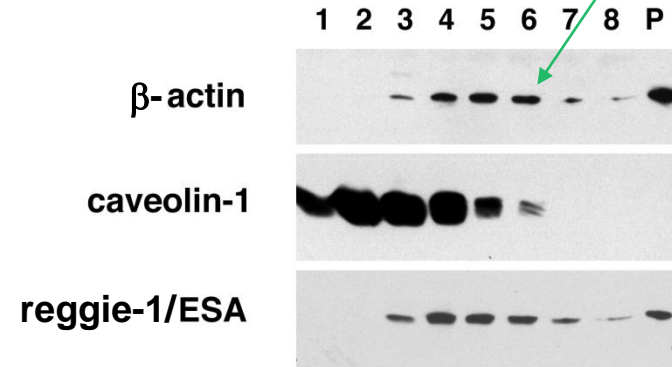
For a report on this similarity see Fiedler 2008

Actin Maintained as F-Actin in 15 h Sedimentation Analysis Demonstrates the Probable Direct Link of Actin and Reggie-1/ESA

EDTA incubation has been shown to lead to aggregates of F-actin that are maintained as semi-denatured proteins. One major drawback of the TNE (Tx)-procedure!

Actin and other proteins were likely lost in the pre-clearing and/or not extracted from the silica beads (e.g. dynamin 1 in OG)

This actin may correspond to F-actin that sediments at a S -value $\leq 42 S$

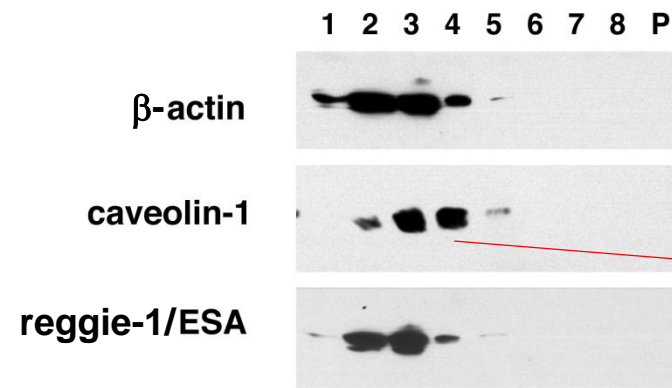


40 mM OG

Estimated $\sim S$ value (12°C) :

Fraction	5	19.3 S
Fraction	8	28.8 S

note that slightly more reggie-1/ESA is found in fraction 3 relative to the pellet (P) compared to this ratio for actin



2% SDS

note that here the ratio of e.g. fractions 3 or 4 to 2 shows the SDS resistant larger caveolin

10% ← sucrose → 30%

P1 membranes (300 μ g)

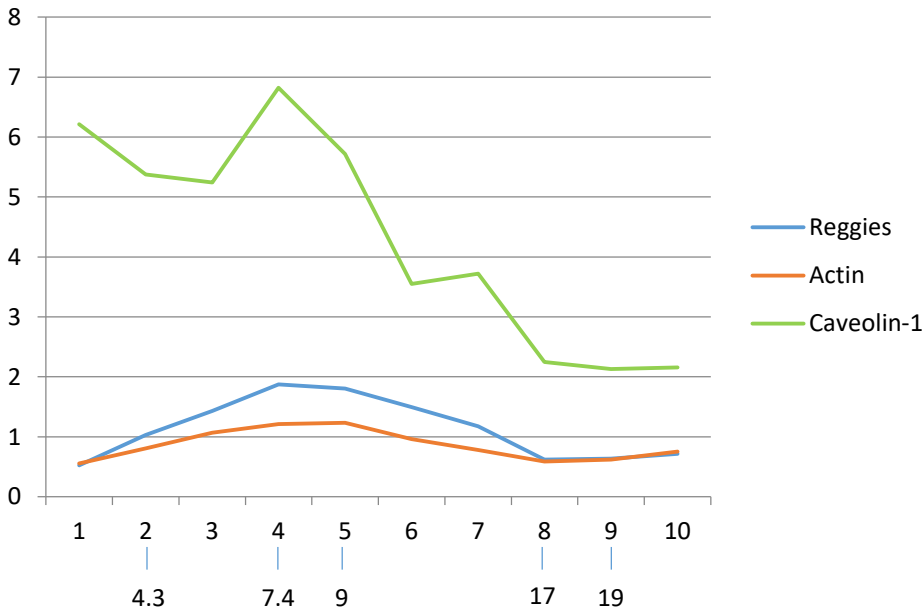
These results from endothelia are consistent with the findings of Langhorst et al. 2007

Sedimentation Analysis in Conditions Including Divalent Cations

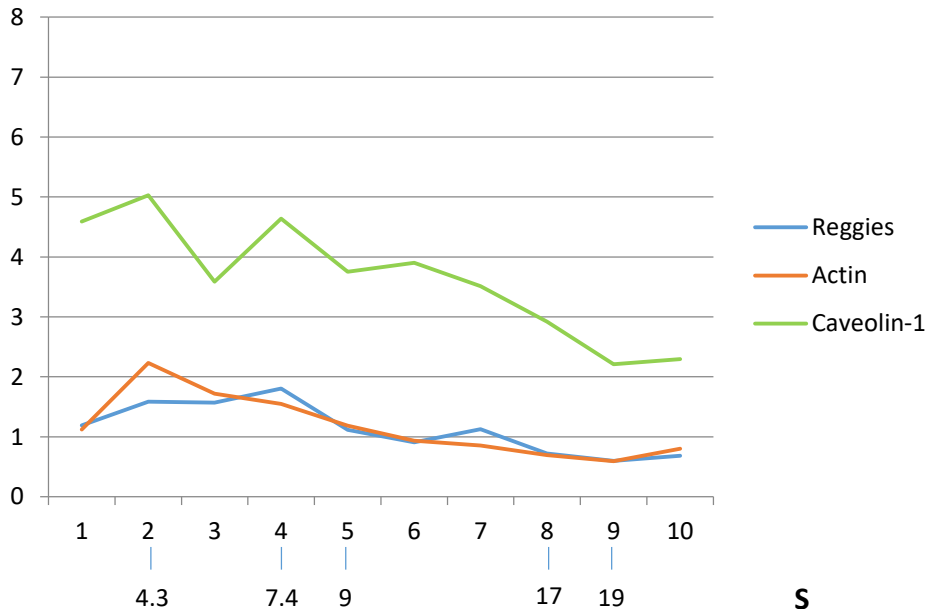
Equal silver stain of proteins by weight was assumed in this calculation

For sucrose gradients see
Chatenay-Rivauday et al.
2004

- ATP + Mg²⁺



+ ATP + Mg²⁺



Caveolin-1 co-immunoprecipitations with actin suggested the preferential interaction with phosphorylated actin

Estimated complex

N=2; Densitometry
Silver-Stain

Fibrinogen-shape was used to estimate the complex molecular weight: Envision dimers of Reggie

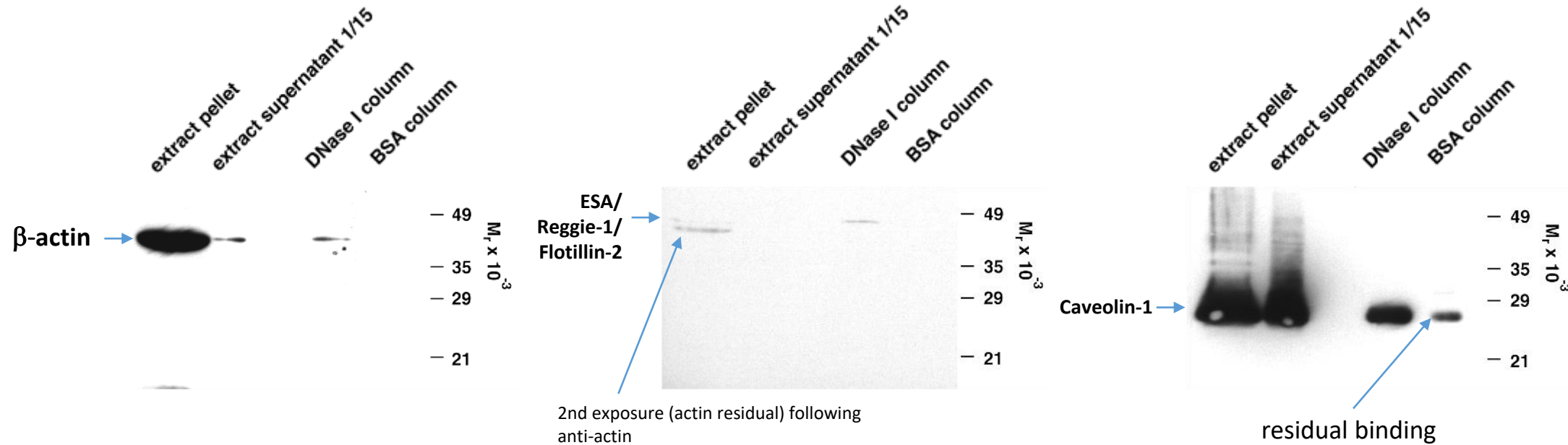
2 : 2 : 8 stoichiometry of Reggies : β,γ -Actin : Caveolin-1 (high S-area)

Gradient with OG (micelle size approx. 25 kDa)

β and γ actin cannot be distinguished

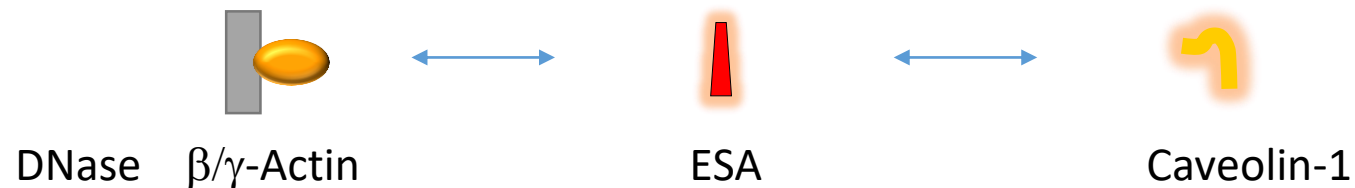
A DNase Affinity-Column Demonstrates Furthermore Caveolin-G-Actin Interaction

F-actin interaction with flotillin has previously been shown



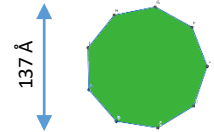
Caveolin-1 interaction with actin may be indirect

40 mM OG, ~0.4 mM free Mg^{2+} , in DBPS, 1 mM EDTA and BSA, protease inhibitors, 1,10-phenanthroline, PMSF was present in the buffer



The majority of caveolin-1 is extracted in these Mg^{2+} -containing conditions

A Geometric Model of a Caveola Including ESA/Reggie/Flotillin and Caveolin



9-mer
cav1

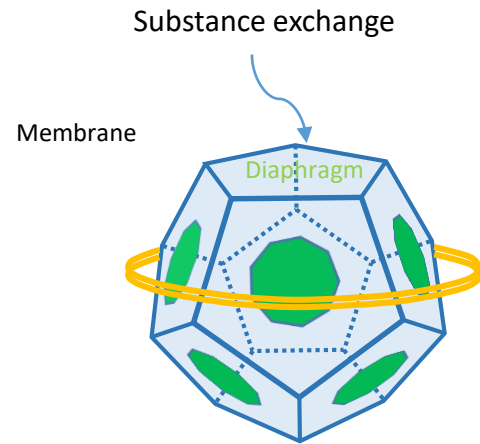
- caveolin
- reggie/flotillin

inner radius 14.45 nm with
edge 21 nm

reggie (at average radius)
cav1 nonamer

See our biochemical data in MBR (2004), reggie is sketched with average diameter and undefined pitch

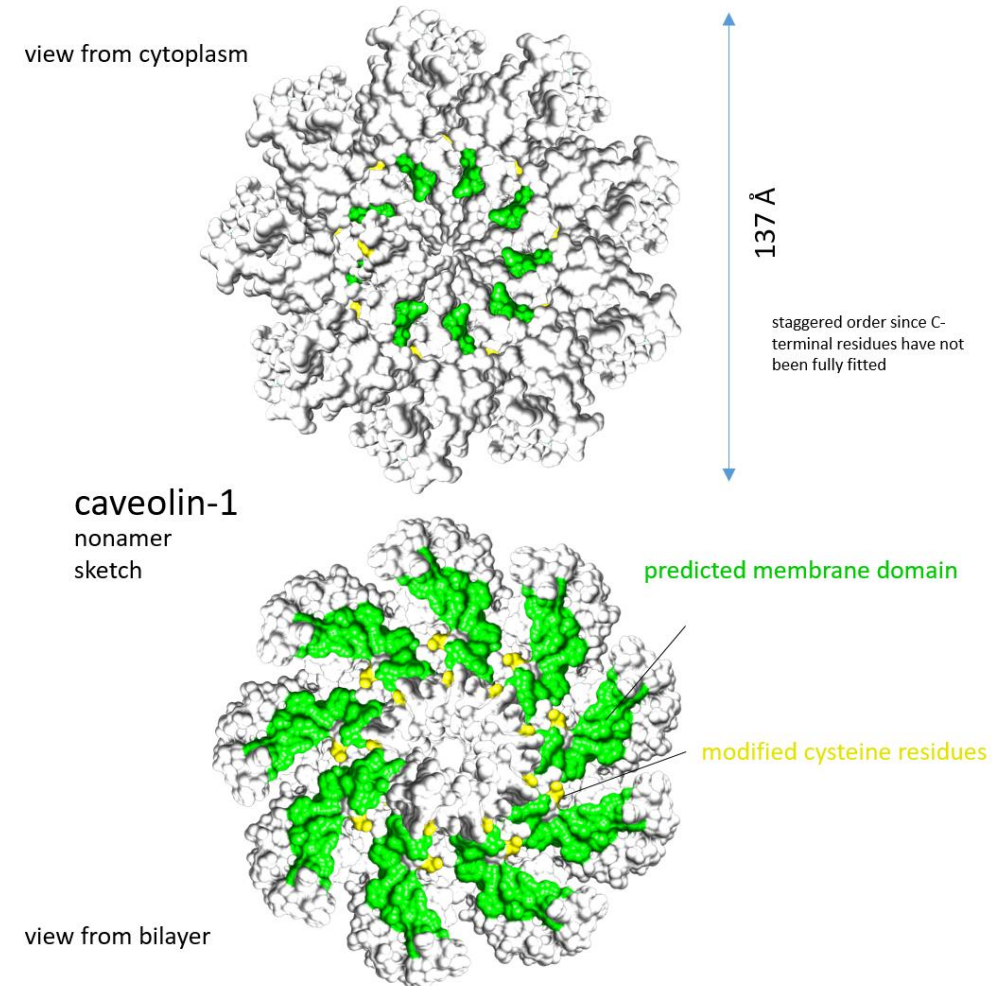
$$V(\text{reggie}) > 42'580 \text{ \AA}^3$$



See „Outlook on
Caveolae“ for the
geometric model with
increased cav1 protein
amount

Whiteley et al. (2012) have described the protein structure
of caveolin-3 by transmission electron microscopy and
found a nonamer of similar dimension than the sketch

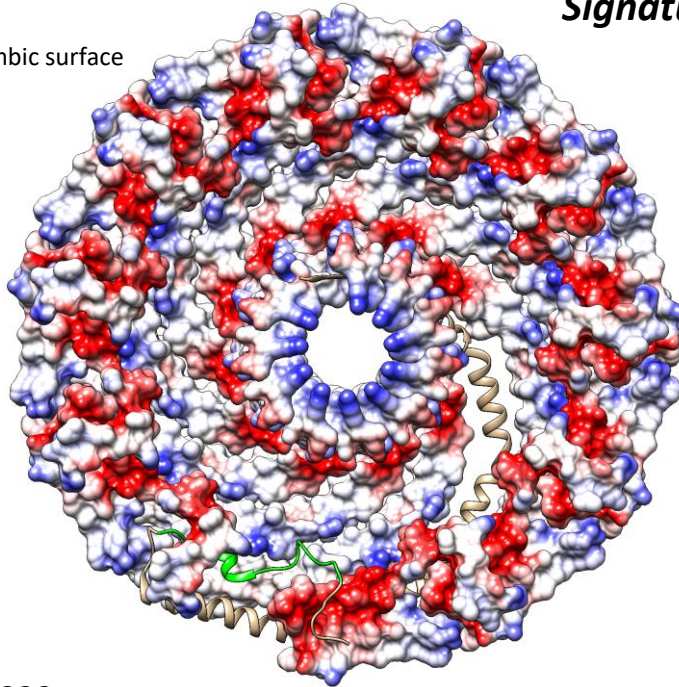
THE JOURNAL OF BIOLOGICAL CHEMISTRY VOL. 287, 40302–40316, 2012



The Proposed 7- to 14-mer of Caveolin-1 was Recently Structurally Determined to be an 11-mer

Cytoplasmic Aspect with Interlocking Signature-Epitopes and Protomers

Coulombic surface

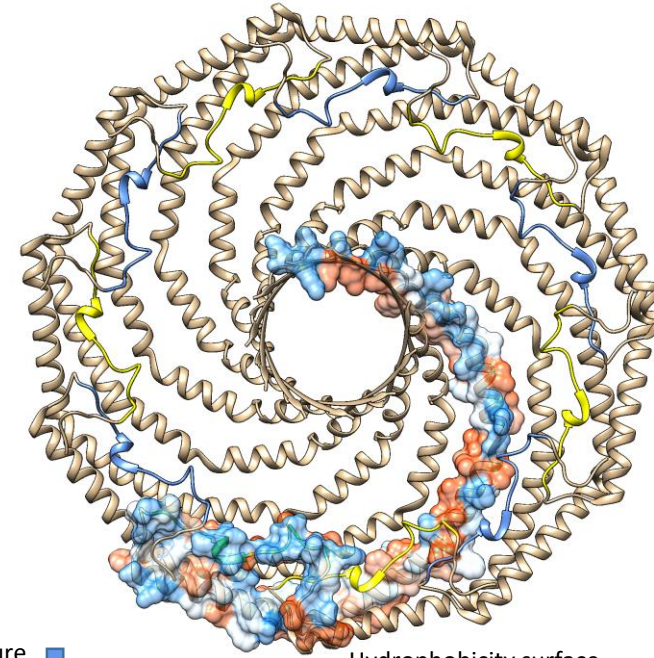


Porta et al. 2022

■ Signature Epitope

The (current N-ter.) 3_{10} helix is part of the KHLNDDVVKIDFEDVIAEPE peptide that was used in antibody production

Chatenay-Rivauday et al. 2004



Interlocking Signature Epitopes with aid of region 49-60 (pin motif)

Hydrophobicity surface

Exciting First Structure Analysis at Higher Resolution (See Stoeber et al. 2016 for the first TEM analysis of 8S-Cav1 complexes)

We had not been able to identify cavin proteins in our preparations, they may have been lost in isolation of plasmalemmal vesicles or they may correspond to coat proteins of other, varying vesicles!

Other Research: Would the Co-Precipitation of Caveolin-1 with Apolipoprotein A4 in Non-Reducing Conditions Suggest the *In Vivo* Interaction?

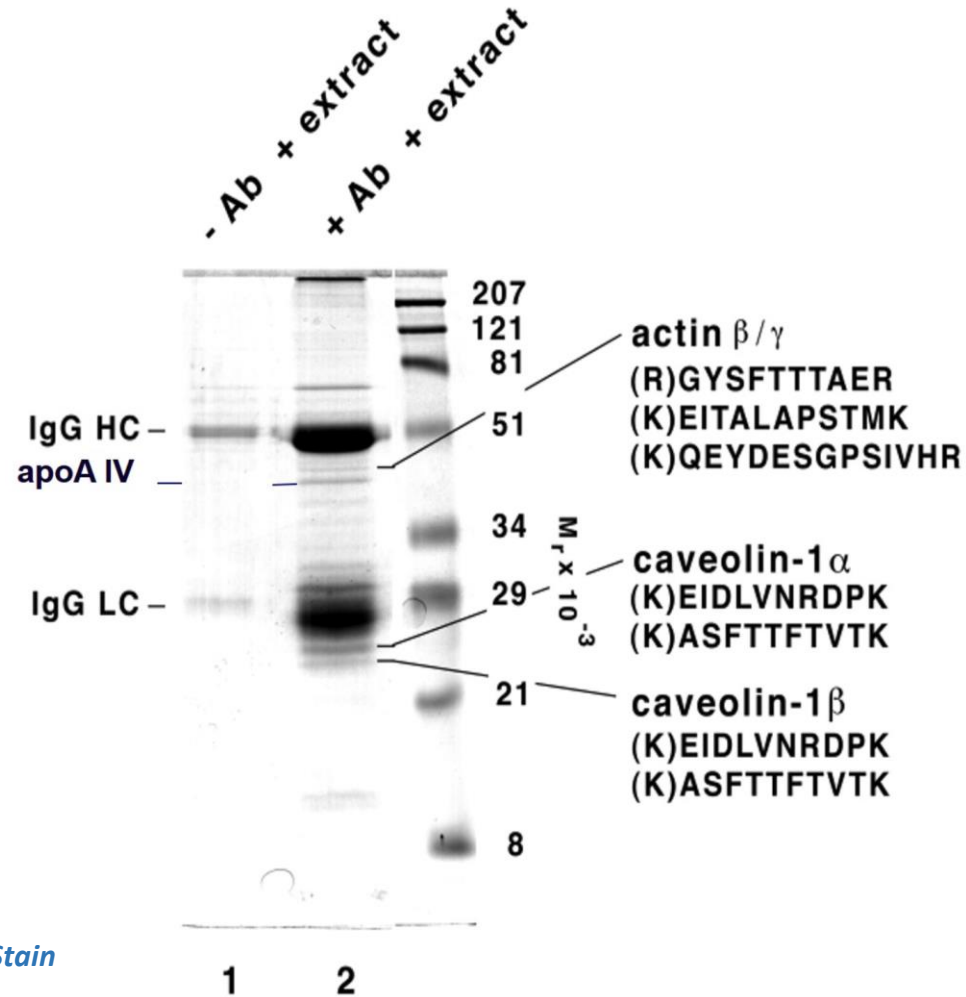
P1 Extraction in

40 mM OG, EDTA, PBS, PMSF
and protease inhibitors

cav1N1-14 antibodies

identified by
microsequencing

Coomassie-Blue Stain



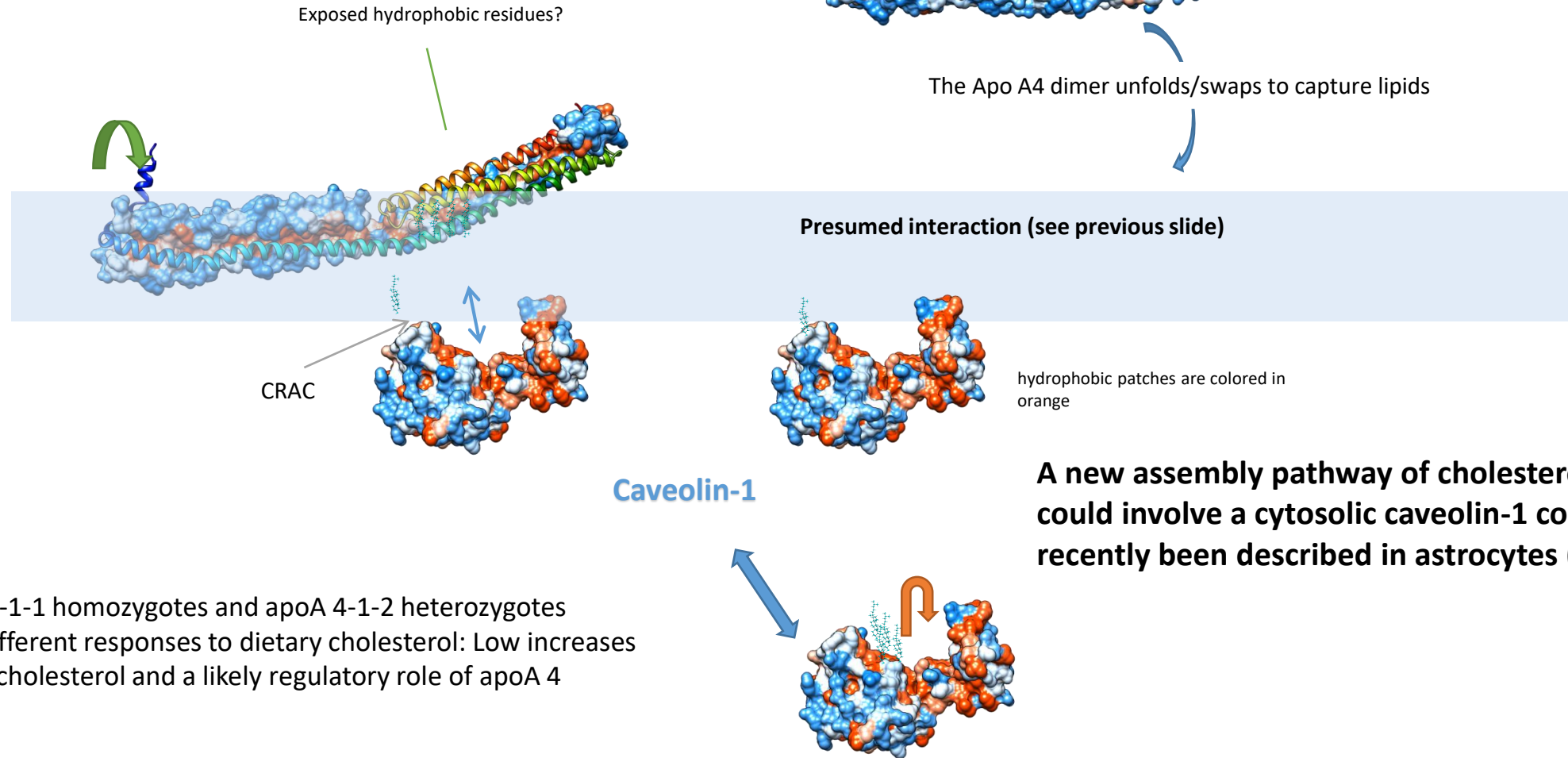
The immuno-precipitation in non-reducing conditions showed the co-precipitation of bound actin and surprisingly apoA IV, an apolipoprotein of particulate, lipoproteinaceous and soluble character which may be bound to caveolin due to hydrophobicity and the presence of caveolin' fatty-acyl chains

Reasons for this experiment

Concerning the structure of the caveolin protein intriguing discoveries have been reported but later on been discounted (plasma membrane surface access)

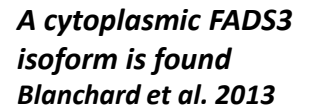
Putative ApoA 4 Interaction with the Bilayer and Caveolin-1

ApolipoproteinA 4



CYB5R3 KO-mice show a reduced level of 1-stearoyl- and 1-palmitoyl-2-linoleoyl-PC and 1-stearoyl- and 1-palmitoyl-2-arachidonoyl-PC in cardiomyocytes (Carew et al. 2022)

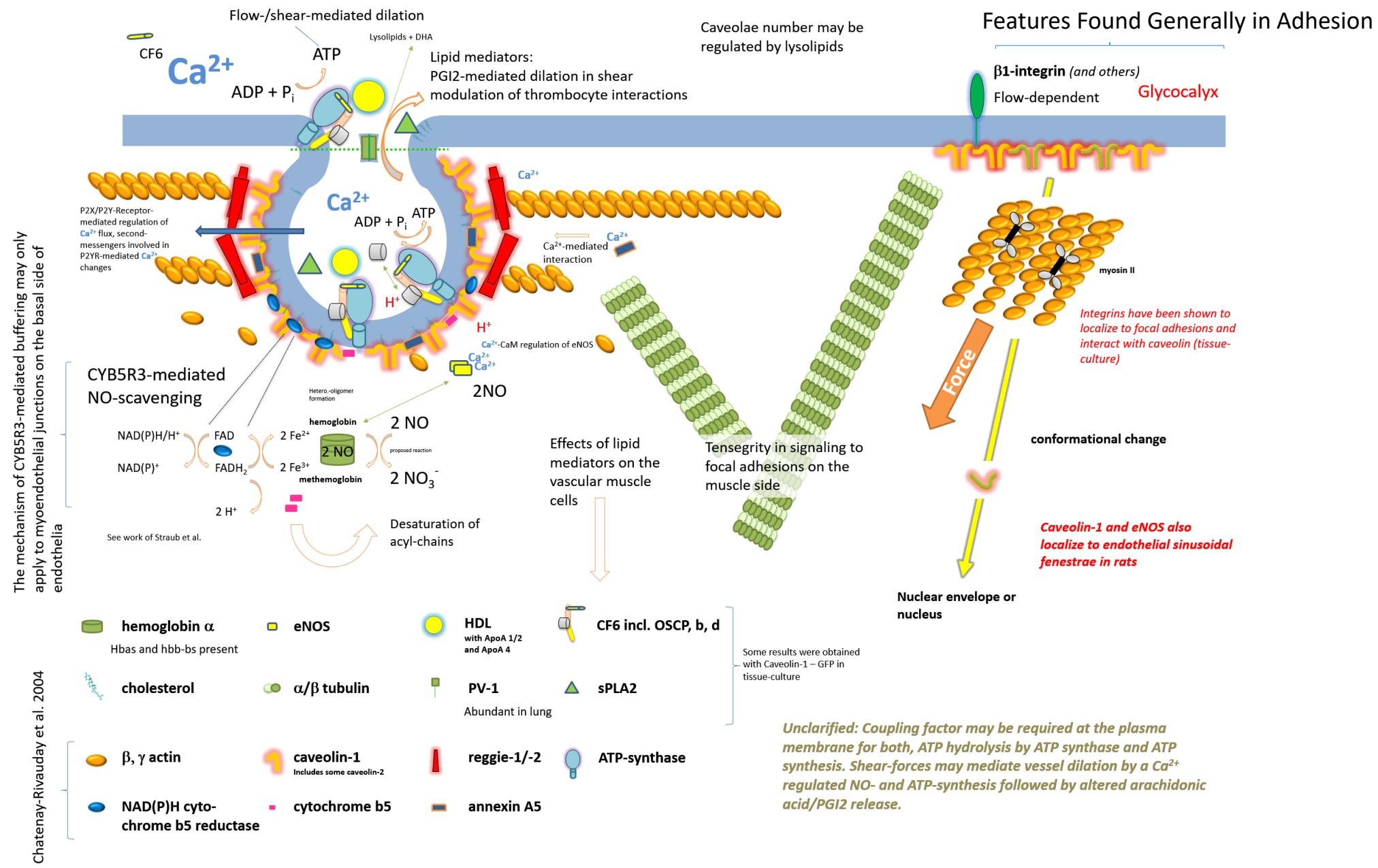
CYB5R3 KO-mice show a reduced level of 1-stearoyl- and 1-palmitoyl-2-linoleoyl-PC and 1-stearoyl- and 1-palmitoyl-2-arachidonoyl-PC in cardiomyocytes (Carew et al. 2022)



A cytoplasmic FADS3 isoform is found
Blanchard et al. 2013

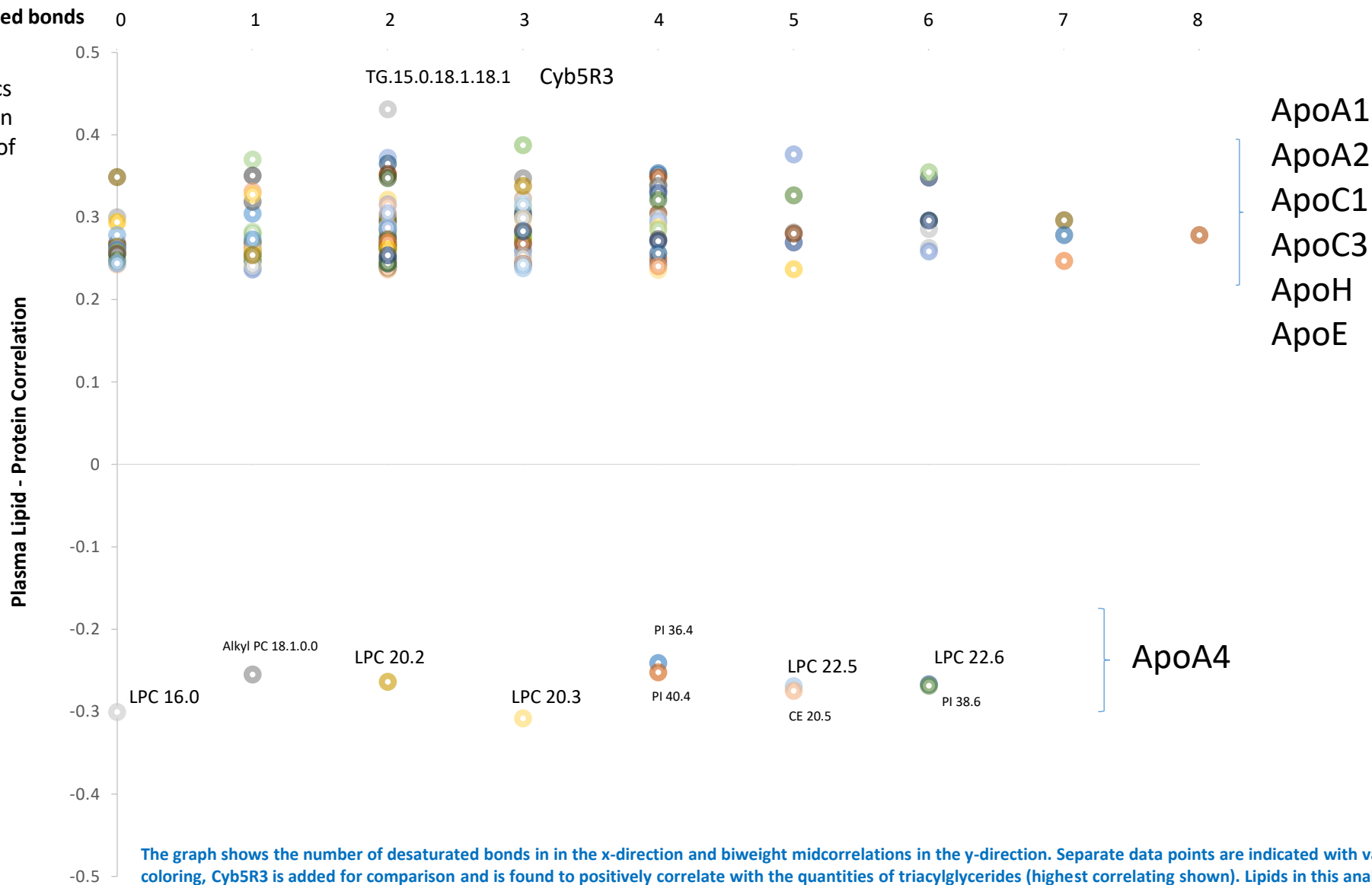
Further Observation: Deficiency of membrane-bound CYB5R3 leads to activation of TGF- β 1 signaling and causes lung fibrosis in mice and likely humans (Bueno et al. 2023)

Shear- and Pressure-Regulated Flow in the Vascular System: Ideas

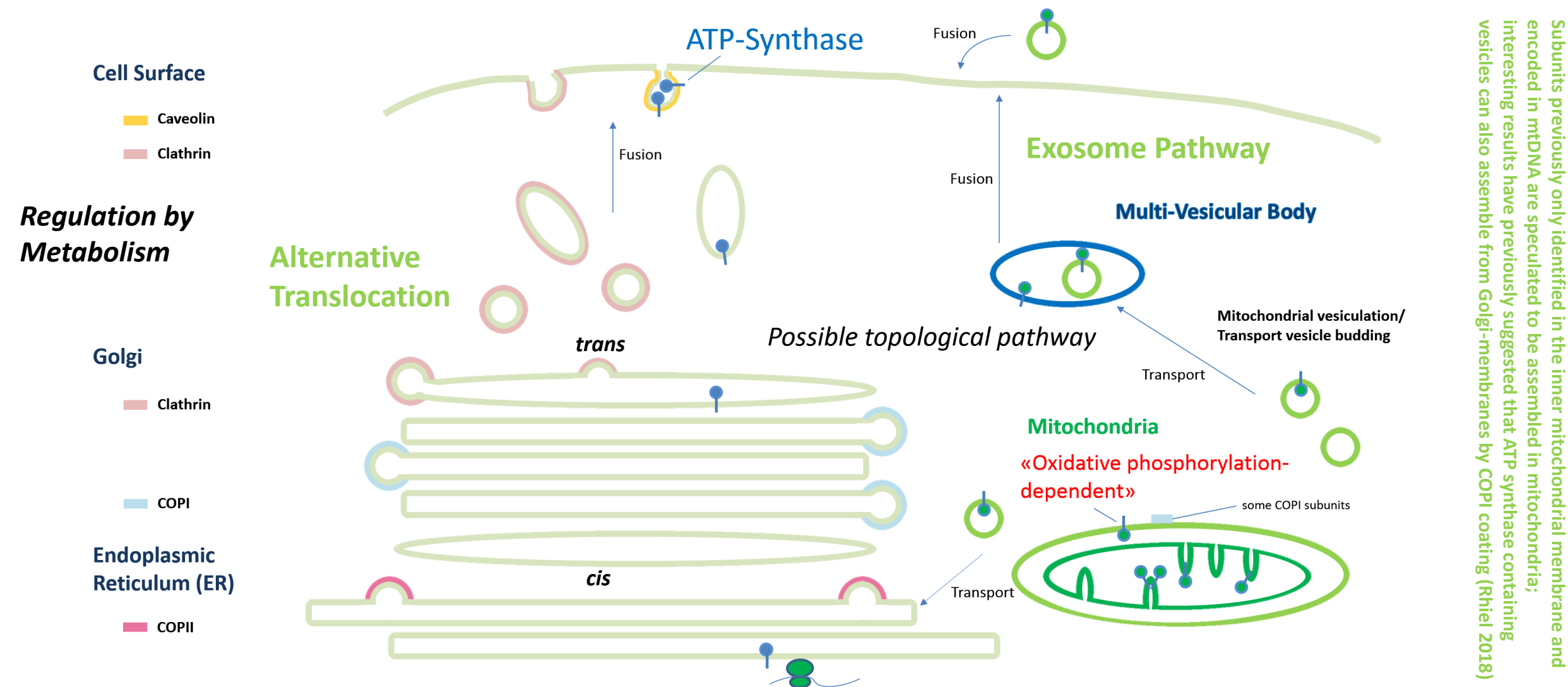


Plasma Lipids: Liver Apolipoproteins Correlate with Lipid Amounts

A recent study in lipidomics demonstrated a connection of liver protein quantities of the apolipoprotein ApoA4 and plasma lysolipids that inversely correlated (Parker et al. 2019).



The Biogenesis of Plasma Membrane ATP Synthase Remains to be Clarified: Exosome (MVB) versus ER Paradigm



Subunits previously only identified in the inner mitochondrial membrane and encoded in mtDNA are speculated to be assembled in mitochondria; interesting results have previously suggested that ATP synthase containing vesicles can also assemble from Golgi-membranes by COPI coating (Rhiel 2018)

The α subunit of F_0F_1 -ATP synthase has been found to be glycosylated in the secretory pathway in neuroblastoma cells by Schmidt et al. (2008); another view (mitochondrial vesicle fusion) concerning the biogenesis of the surface enzyme is held by Rai et al. (2013) and others; unexpected outer mitochondrial membrane proteins imported from the cytoplasm have been shown by Zahedi et al. (2006) in yeast; see results concerning mRNAs of Zabezhinsky et al. (2016)

Conclusions

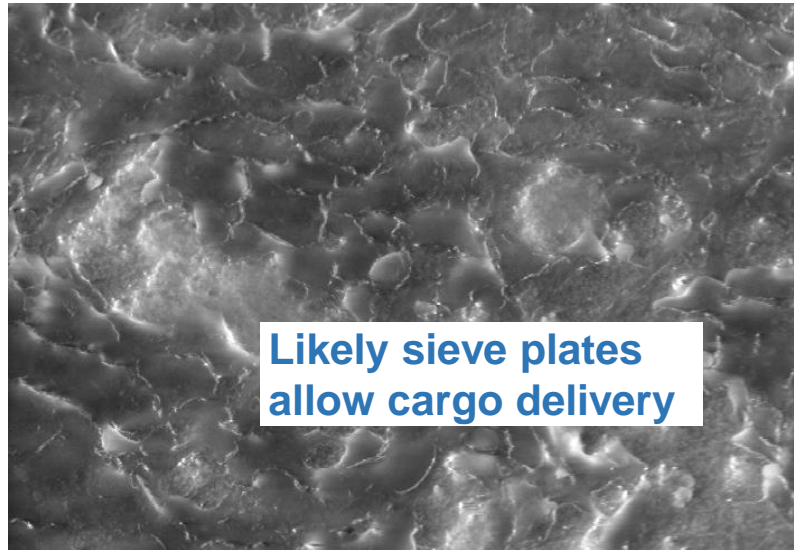
- A recent analysis shows, that pressure overloaded hearts in a mouse model can be normalized and rescued from heart failure with caveolin-1 scaffolding domain (CSD) treatment. This is in line with the proposal on the role of caveolae as a pressure sensor. Pleasant-Jenkins et al. 2017
- In the previous gradient analyses etc. a coat protomer of reggie-caveolin-1- β -actin is suggested as the assembly unit of caveolae in vascular endothelia; some coat proteins or scaffold factors may have dissociated in this analysis. Caveolae purified from an animal source were exposed to little change of shear conditions before isolation. Chatenay-Rivauday et al. 2004
- A role in paracrine signaling is proposed with plasma membrane ATP synthase and ATP in caveolae and their effect on the muscle cell layer in constriction. ATP could enhance signaling from the endothelial cell layer that autonomously regulates blood vessel diameter and has possibly other signalling roles (reset of homeostatic mechanisms). The proteinaceous nature and lipoprotein interaction of caveolin-1 should be elucidated in the future. The ApoA4 role in lipid signalling and lipid homeostasis is currently being researched.
- Cytoskeletal attachment of caveolin-1 is evident when analyzing improved solubilized sub-complexes of caveolin-1 with interacting proteins. Energy-dependent surface attachment of caveolae in isolated plasma membranes (silica procedure) suggests the requirement of cytoskeletal turnover in plasmalemmal stability.

Caveolae: Endothelial model, «budding» assay
and proposed physiological function

Transcytosis in vascular endothelia

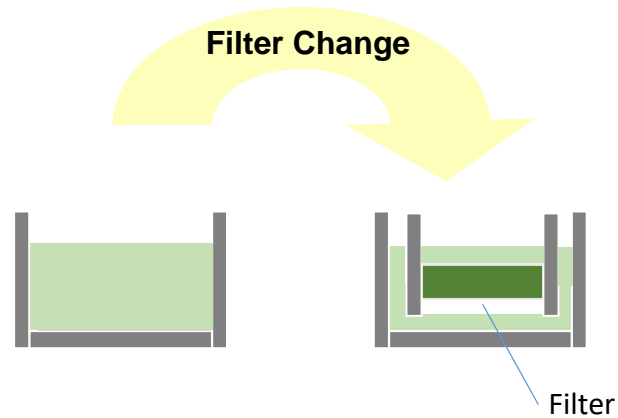
p24–TMED proteins: Are these lectins?

Receptor-Mediated Transcytosis Assay: Lymph Vascular Endothelia



Wisse et al. show geometrically arranged structures to be sieve-plates that could be similar to the structures seen in our work (Kuzmenko et al. 2004)

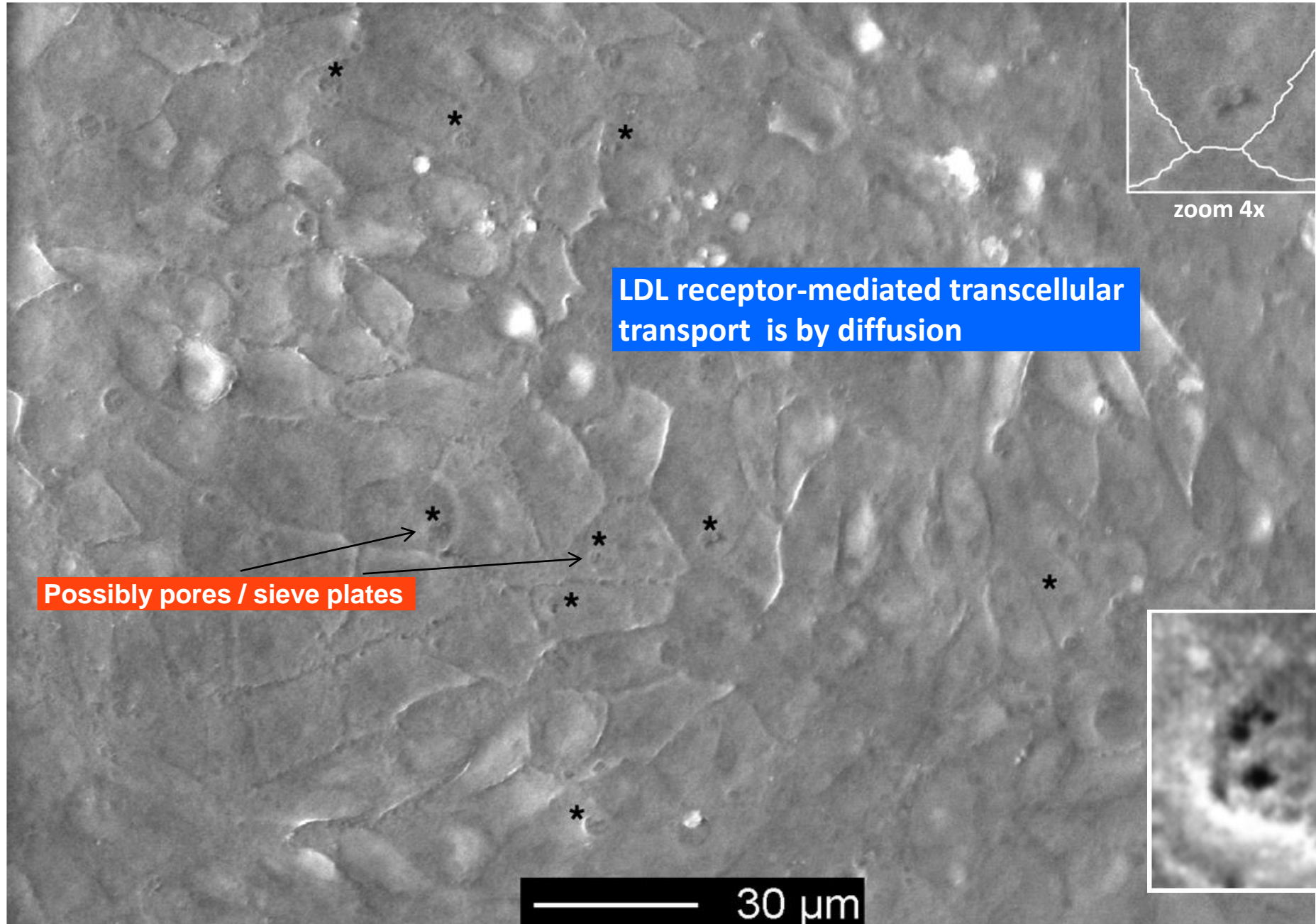
- Addition of ^{125}I -LDL (luminal)
- Abluminal medium sampled
- Transport in the presence of ^{125}I -LDL with or without 25/30-fold excess non-labeled LDL



Transcellular Transfer in Lymphoid Endothelia: ESEM in SVEC4-10

Conclusions were based on the unusual
temperature-dependence and large
residual traffic with Chol-PEG inhibition

Kuzmenko et al.
2004

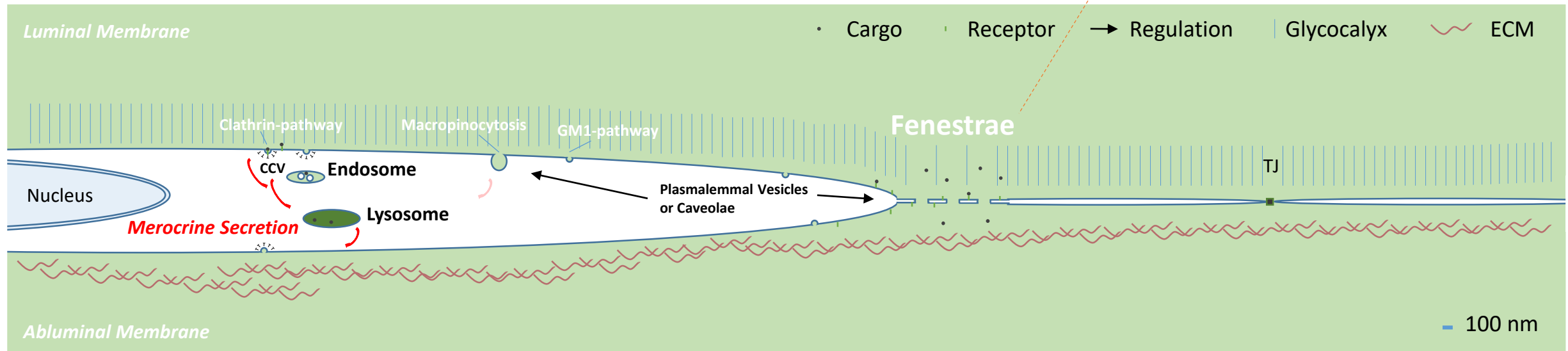


Anti-mouse LDL-receptor antibodies were not available

Transcellular Transfer in Lymphoid Endothelia: ESEM in SVEC4-10

The assumptions that we made on LDL transcytosis including degraded particles and flux of amino acids have been widely confirmed with respect to lysosomal amino acid transfer. We were not able to distinguish the two forms of transfer via membrane or the vesicular pathway (merocrine secretion). Brain transvascular delivery has recently been confirmed with the transferrin-receptor pathway that can be used in drug targeting (Johnsen et al. 2017; Pardridge 2017) for molecules but likely not macromolecules.

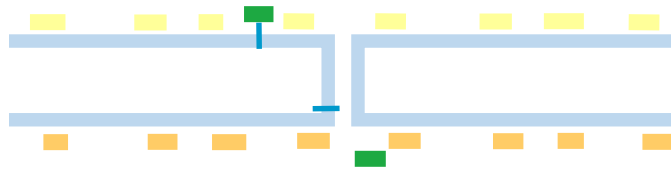
Protein membrane diffusion via channels/'pores'



Large channels at the plasma membrane have also recently been described, P2X receptors may also allow the passage of large molecules that may contribute to measurements in our assay

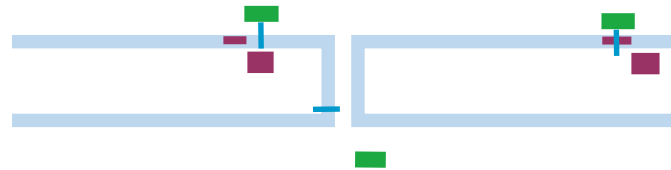
According to some reports, merocrine secretion includes eccrine transport

Current Model on «Intact» LDL Delivery

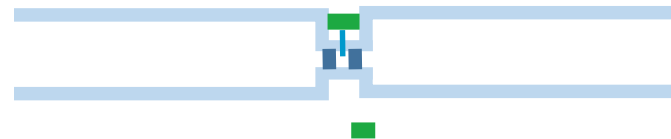


Receptor and ECM charging site of LDL

*The non-equilibrium state of the bilayer
has recently been demonstrated to include
„non-Gaussian statistical“ fluctuations*



Ratcheting: Lipid microdomain and alternative charging site



Receptor and chain of vesicles

see our previous model

■ Ligand | Receptor ■ ■ Charging Site ■ Cytoskeleton

What would energies correspond to that stimulate or activate shuttle mechanisms?
(for «membraneous» see Kuzmenko et al. 2004)

Caveolae: Endothelial model, «budding» assay
and proposed physiological function

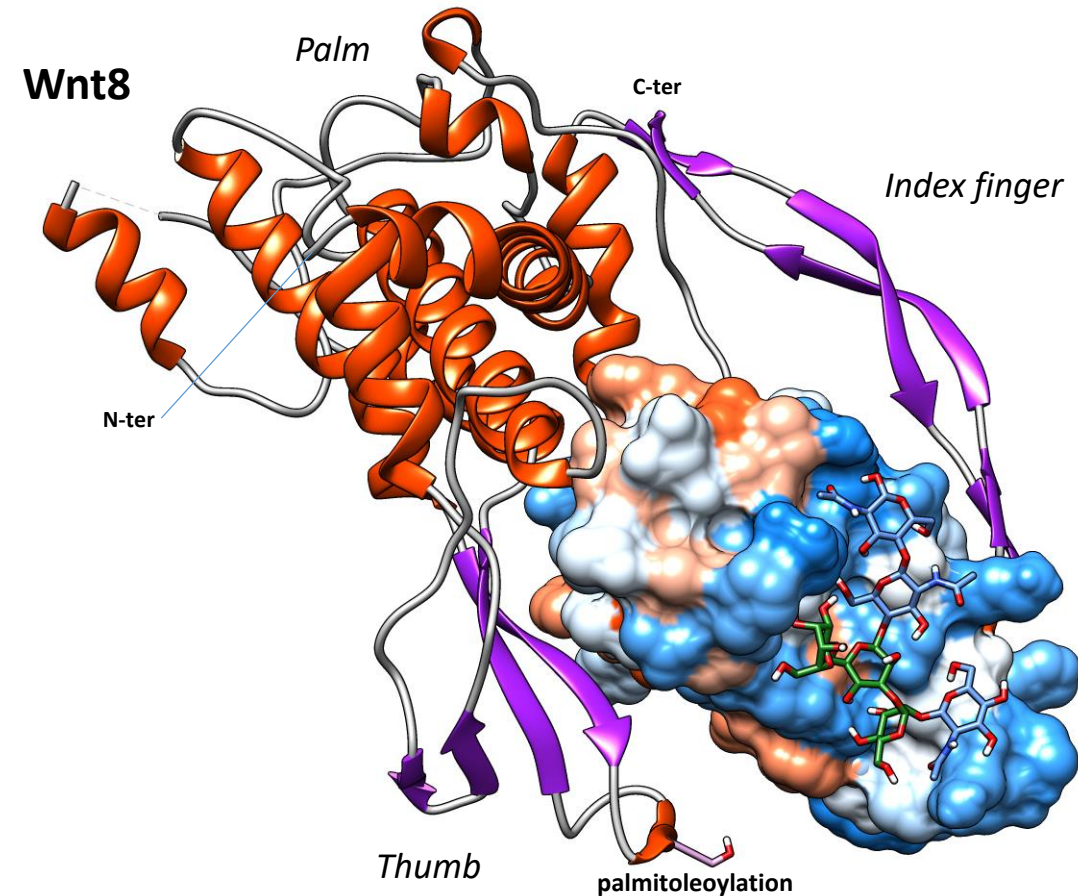
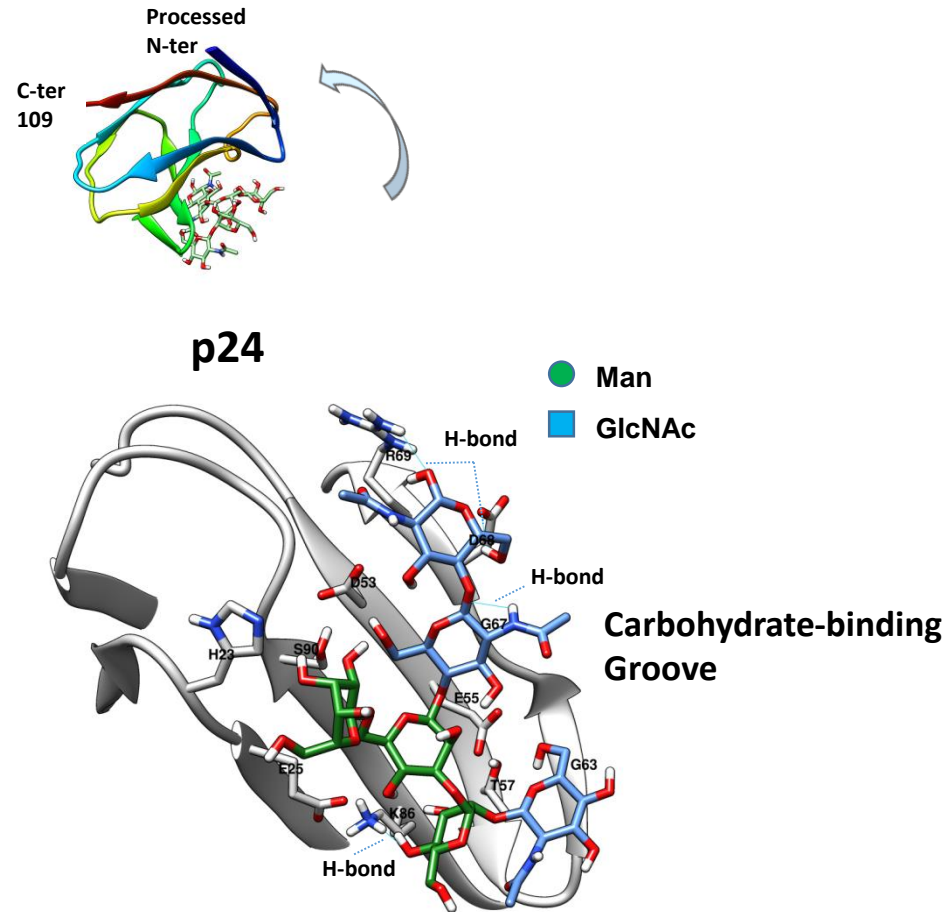
Transcytosis in vascular endothelia

p24–TMED proteins: Are these lectins?

p24-TMED2-Model Cargo-Receptor: *In silico* Wnt8-Interaction

The model was generated with MODELLER (see Sali et al. 2013)

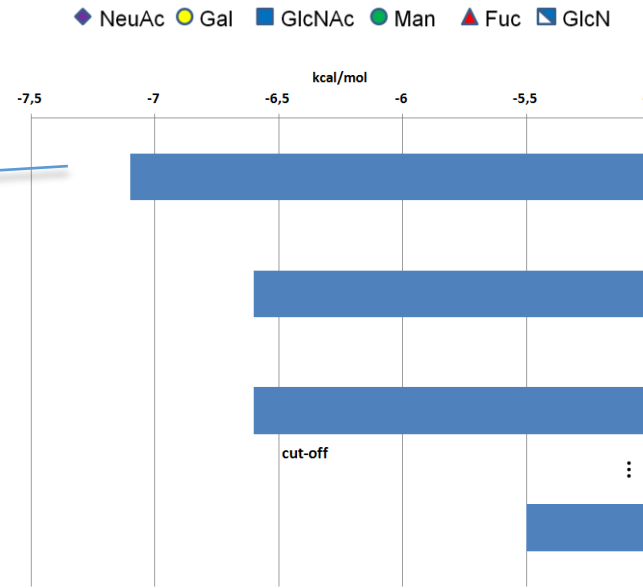
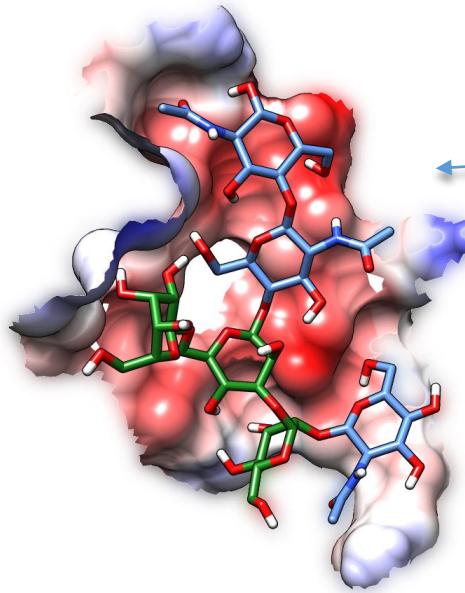
Buechling et al. 2011 had shown, that TMEDs interact with Wnt proteins genetically and TMED5 with Wnt1 biochemically



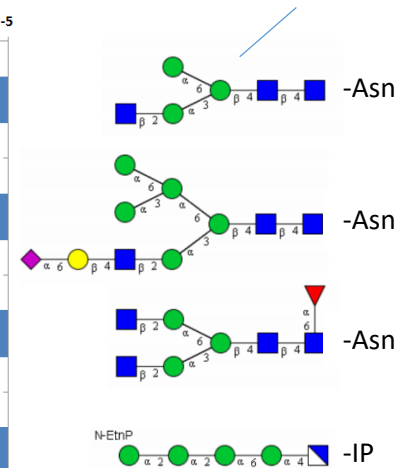
p24-TMED2-Model Cargo-Receptor: Putative Glycan Interactions are Shown in this Study

Contact Area: 314.8 Å²

1.3 – 1.9 H-bonds
per 100 Å²



Hybrid M3-Glycan



The relationship of GPI-anchor biosynthesis to p24-GOLD domains assumed due to a green algae PIG-A fusion of these two domains was found to be based on a probable artefact of DNA shot-gun sequencing and had remained listed in subsidiary databases

with PyRx
Trott and Olson 2010

Collagen Binding to p24-TMED2

with PatchDock

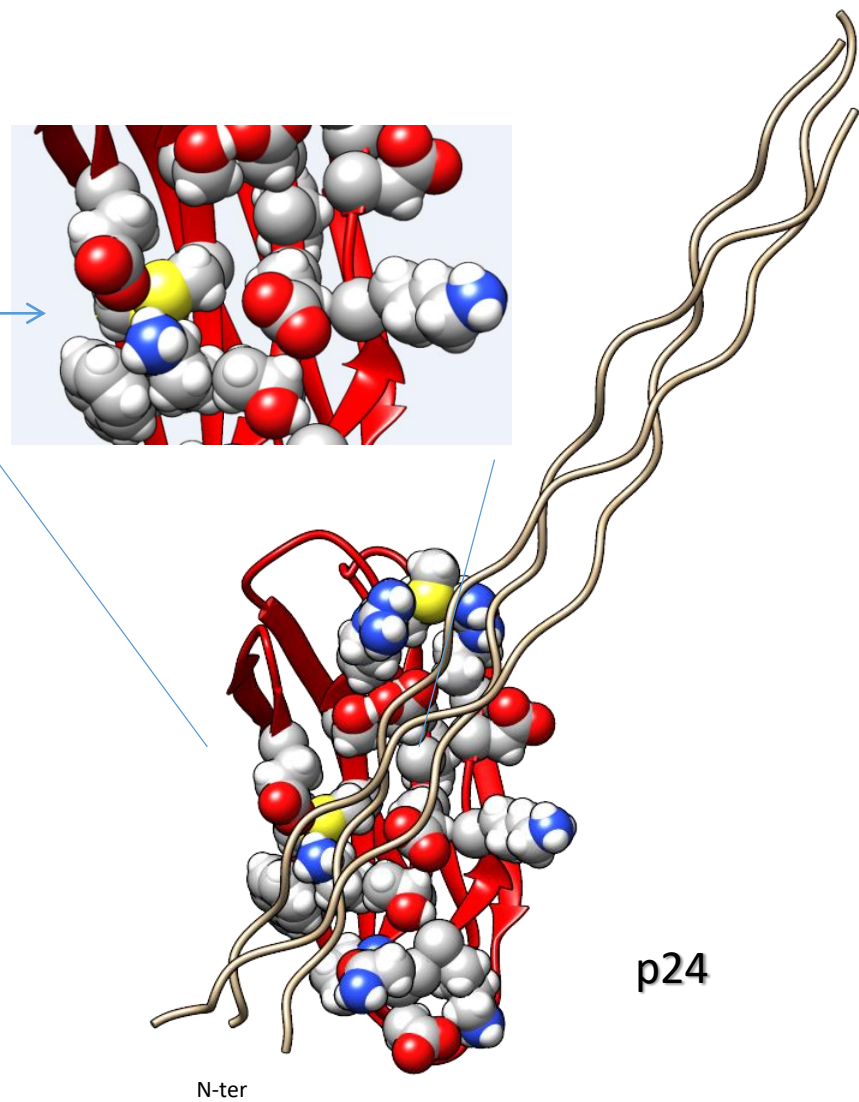
Schneidman-Duhovny et al. 2005

Disulfide

Free-Cys

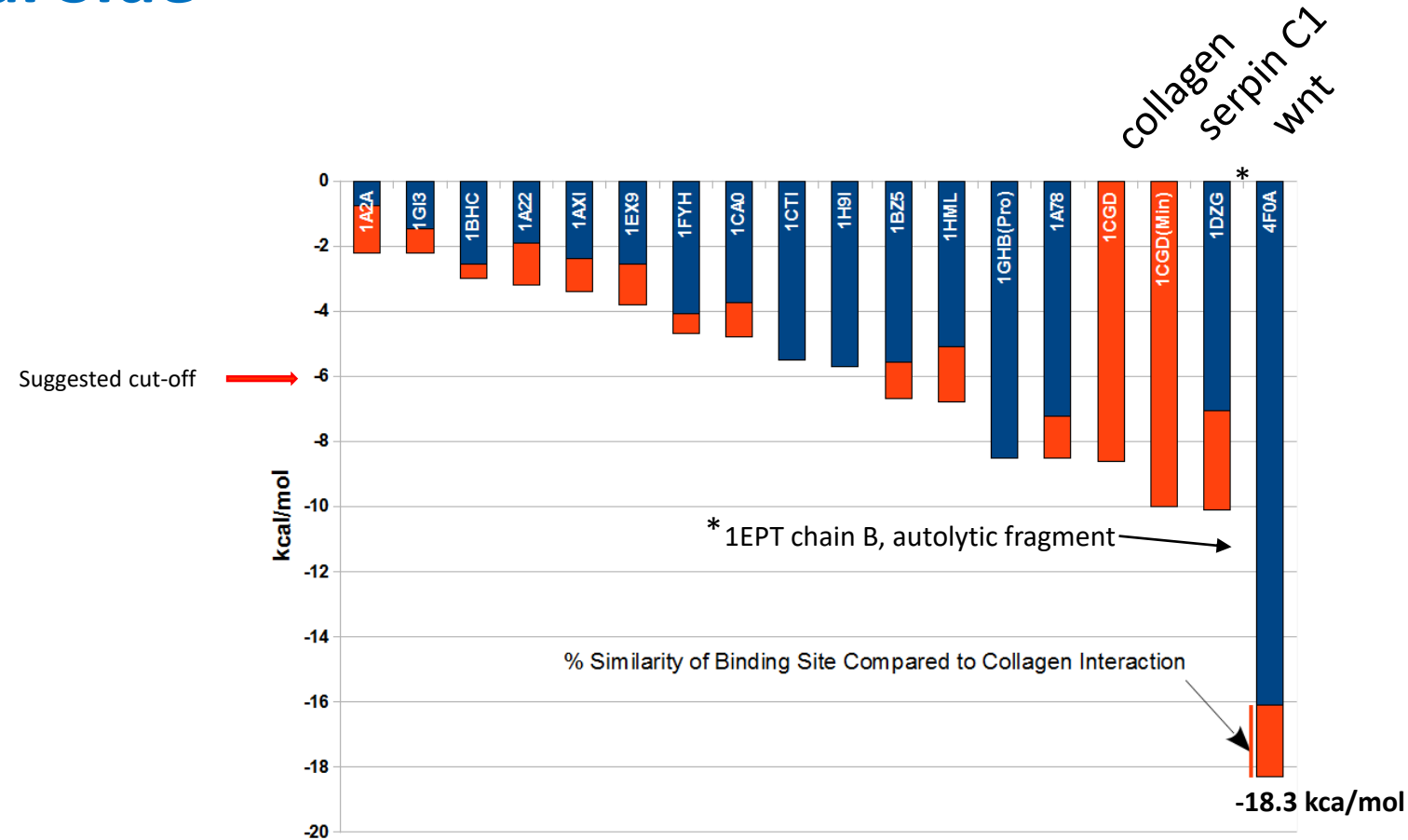
	A	B	C
1	PRO	PRO	PRO
2	HYP	HYP	HYP
3	GLY	GLY	GLY
4	PRO	PRO	PRO
5	HYP	HYP	HYP
6	GLY	GLY	GLY
7	PRO	PRO	PRO
8	HYP	HYP	HYP
9	GLY	GLY	GLY
10	PRO	PRO	PRO
11	HYP	HYP	HYP
12	GLY	GLY	GLY
13	PRO	PRO	PRO
14	HYP	HYP	HYP
15	ALA	ALA	ALA
16	PRO	PRO	PRO
17	HYP	HYP	HYP
18	GLY	GLY	GLY
19	PRO	PRO	PRO
20	HYP	HYP	HYP
21	GLY	GLY	GLY
22	PRO	PRO	PRO
23	HYP	HYP	HYP
24	GLY	GLY	GLY
25	PRO	PRO	PRO
26	HYP	HYP	HYP
27	GLY	GLY	GLY
28	PRO	PRO	PRO
29	HYP	HYP	HYP
30	GLY	GLY	GLY

Cys88
disulfide



In the docking algorithm results varied depending on the Cys rotamer used in the receptor

p24-TMED2 Cargo-Receptor Docking: Proposed Interactions on the Luminal Side



*serpin C1 is also named
antithrombin*

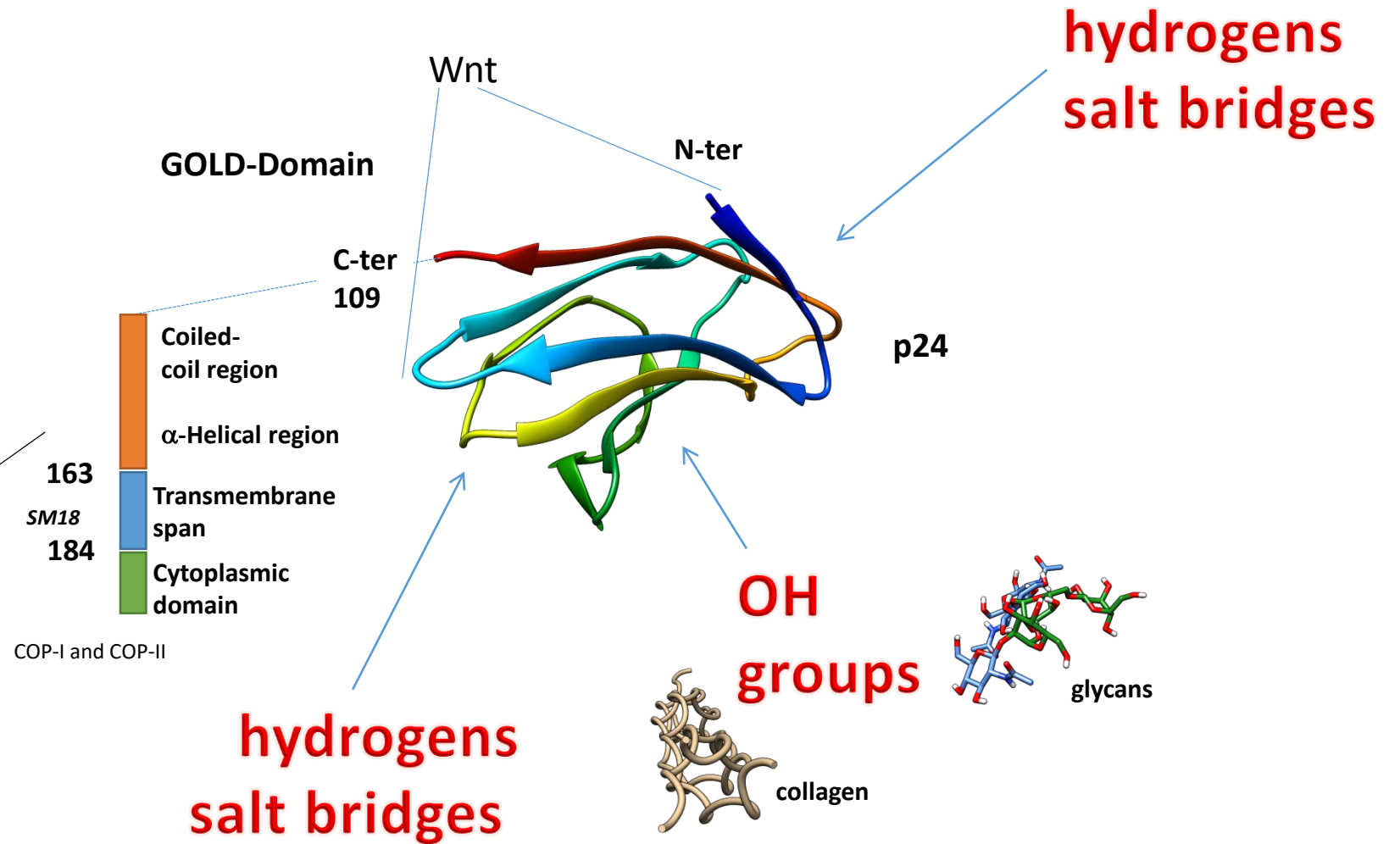
*Interestingly, some legume
lectins had previously been
shown to have a dual
binding interaction, with
carbohydrates and with
proteins*

Collagen and carbohydrates bind to a distinct
surface site which is largely overlapping

The Modeled p24-TMED2 Cargo-Receptor Interactions

The functionally important *transmembrane* Q-residue (Fiedler and Rothman 1997) of p24 binds to sphingomyelin 18 (SM18)

GPI-anchors have recently been proposed to bind to the α -helical region



Previously cysteine residues in the GOLD-domain were thought to mediate dimerization of the p24 proteins, recent evidence points toward a glutamine in the membrane span

Hypothesis: Docking to the X-Ray Structures Would Result in the Same Glycan Hits That were Shown in the BioRxiv Article

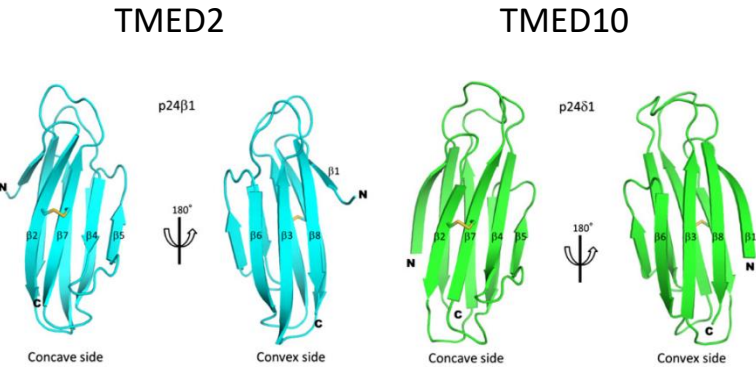
Screen of the following conformers

Library

N-glycan high mannose	19
N-glycan hybrid	17
N-glycan complex	9
Sialoside	27
Fucoside	25
O-glycan core	17
Other glycan	51
Glycosphingolipids	72
Glycosylphosphatidylinositol (GPI)	3

(collected and constructed
from database sources GLYCAM
and glycoSCIENCES.DE)

5AZW	A and B	TMED2
5AZX	A and B	TMED10



Nagae et al. (2016)

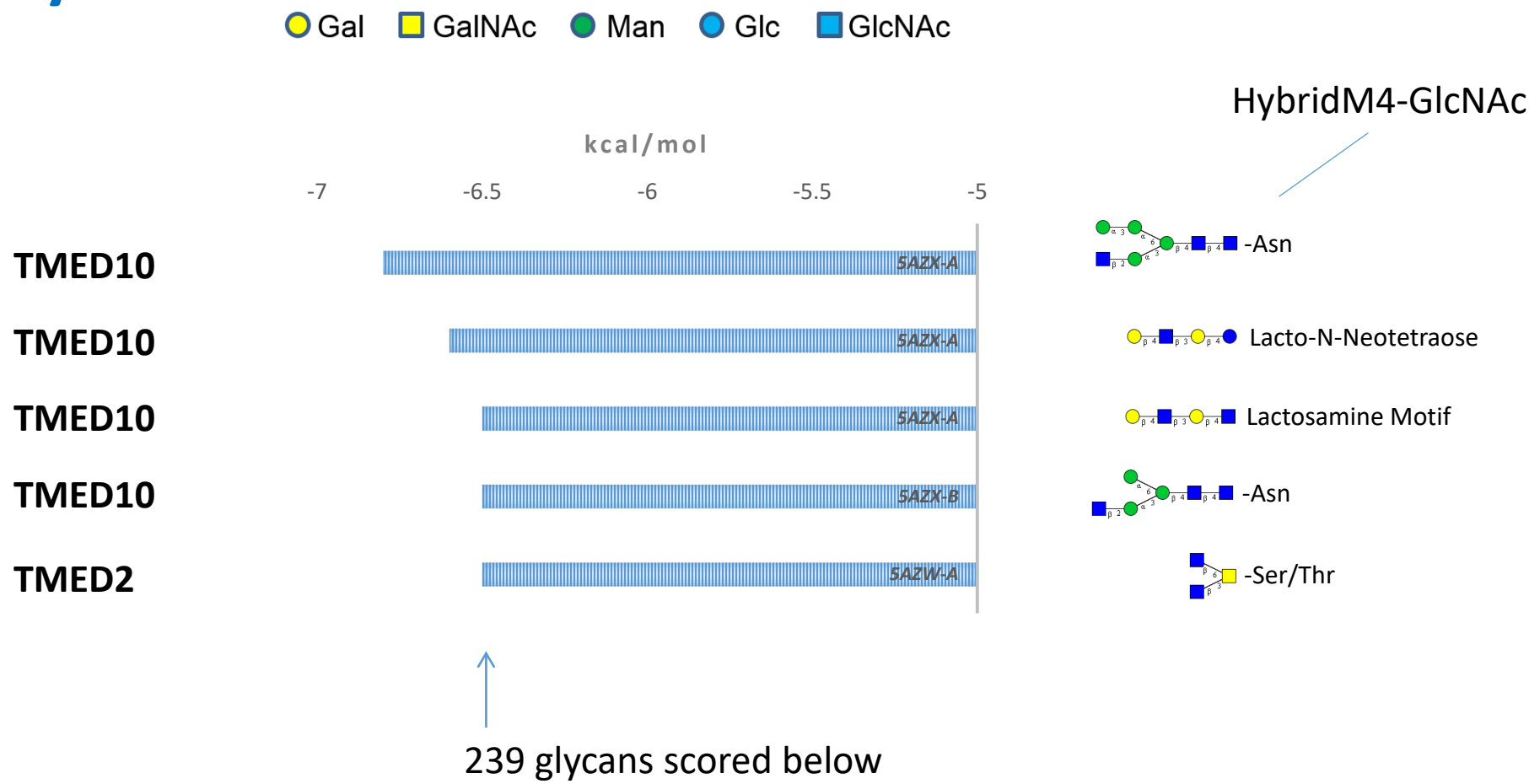
An Extended Library Including the Glycosphingolipid-Headgroups was Generated

Some GSL (glycosphingolipid)-headgroups were found with «other» glycans

2'-Fucosyllactose	Isoglobotriglycosylceramide	type III A antigen
3-Fucosyllactose	IV 3-nLcOse4	type III H antigen
Asialo_GM1	KDN-GM1	type IV A antigen
Asialo_GM2	Lacto-N-fucopentaose_I	type IV B antigen
Difucosyllactose	Lacto-N-fucopentaose_V	type IV H
Forssman antigen	Lacto-N-neohexaose	VI 3GalNAca-IV 6kladoLcOse8
Forssman Branched	Lacto-N-neotetraose	VI3(Galb 1-4GlcNAcb)-Lc4Cer
Forssman-like iGb4	Lacto-N-tetraose	X-hapten, SSEA-1, Lex-5
Gal_Gb4	LeC	
GalNAc-GD1a(Neu5Ac/Neu5Gc)	Lex-7	
GalNAc-GD1a(Neu5Gc/Neu5Ac)	Lex-9	
GalNAc-GM1	Ley-6	
Gb3	Ley-8	
GD1a (NeuAc/NeuGc)	Ley-A-9	
GD1a (NeuGc/NeuGc)	LM1, iso-LM1	
GD2	Neu5Gc_aD_OH1	
Globo_H	P antigen	
Globo-Lex-9	Para-Forssman x3b	
Globoside I/Cytolipin K	paragloboside, nLc4Cer	
GM2-extended	para-Lacto-N-neohexaose	
GP1c	trimeric Lex	
GQ1aa	type I A antigen	
GQ1c	type I B antigen	
GT1b Ac	type I H antigen	
GT1ba	type II A antigen	
GT1c	type II B antigen	
GT2	type II H antigen	

Details can also be found in MCS Search (some further GSL headgroups were not named and listed separately if only differing by isomer and so far not designated uniquely)

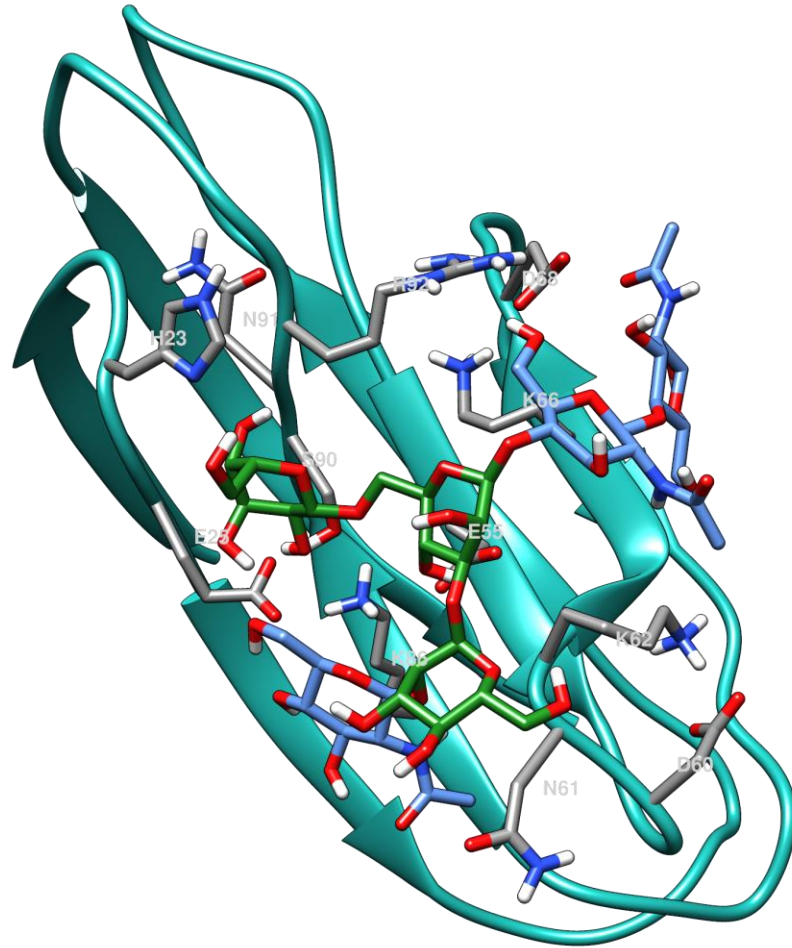
X-Ray Structures: The M4 Glycan was Found as the Top-Interacting Carbohydrate



A lysine clash at the crystal interface / binding site is here detected for TMED2 (see docking in next slide for a CPU-«short-cut»)(Single-CPU or thread ~2.6 GHz with or without shared memory with above data: Run ~16 months)

The Molecular Dynamics «Fortuitous Approach» Shows Previously Modeled Hybrid M3 N-Glycan Binding

A similar approach had been coined “maximum-entropy”

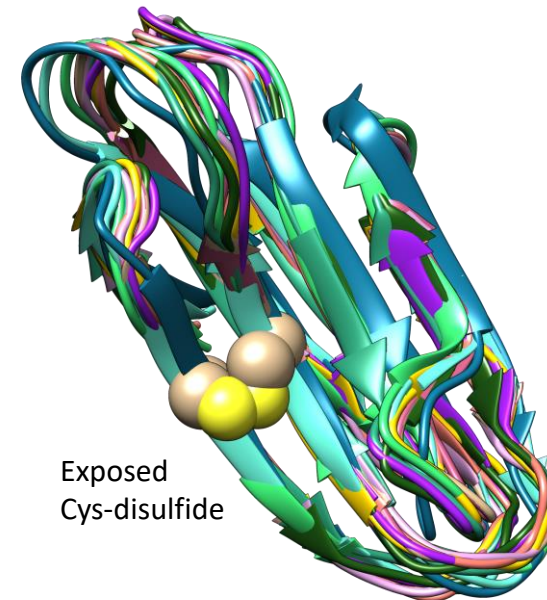
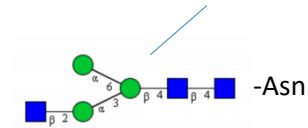


highest binding -6.5 kcal/mol

1 of 10 conformers from a short MDS production run shows binding above cut-off

● Gal ■ GalNAc ● Man ● Glc ■ GlcNAc

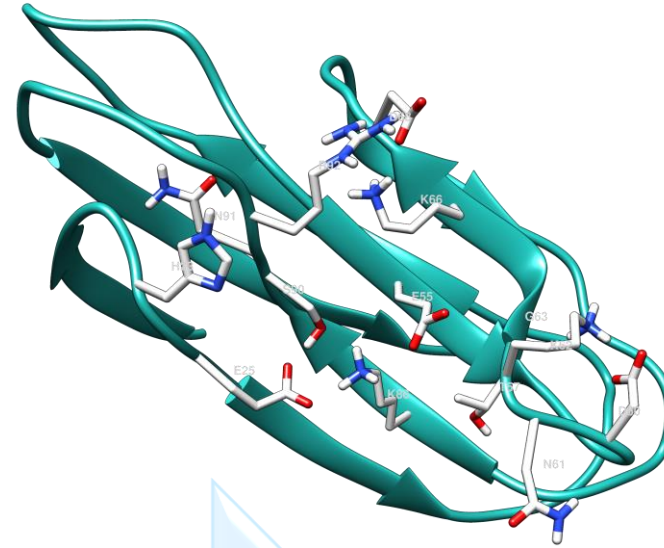
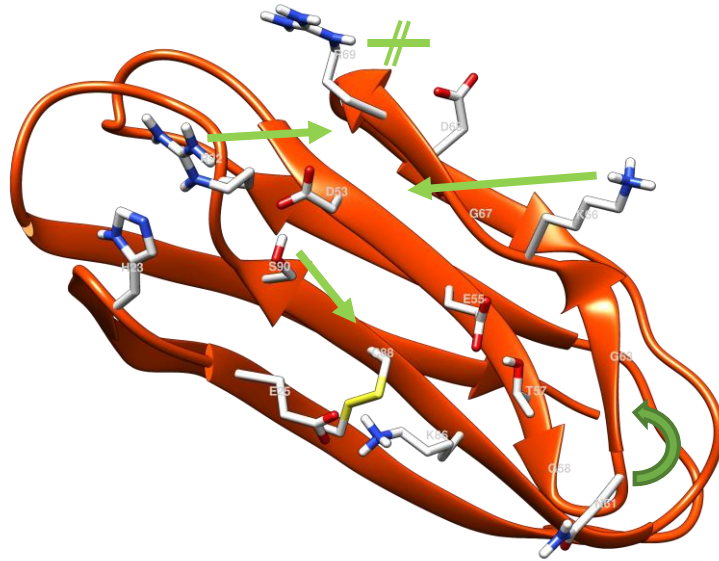
Hybrid M3-Glycan



Exposed
Cys-disulfide

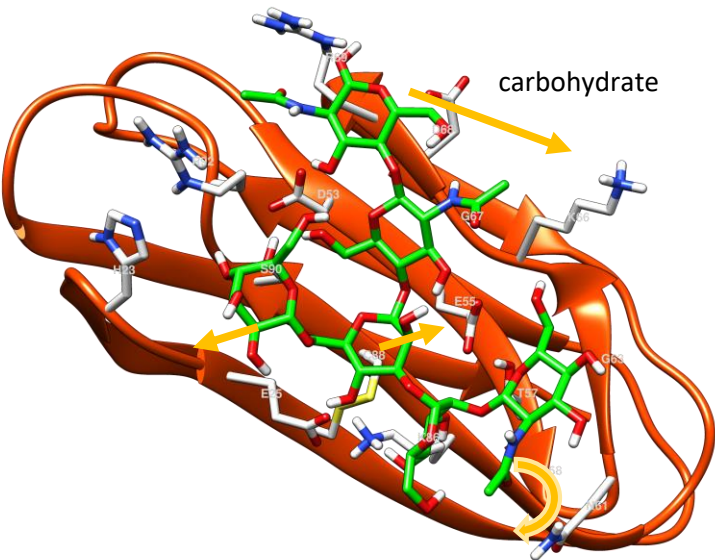
The Morphing of Model to Structure 5AZW with Hybrid N-Glycan Overlaid

Model



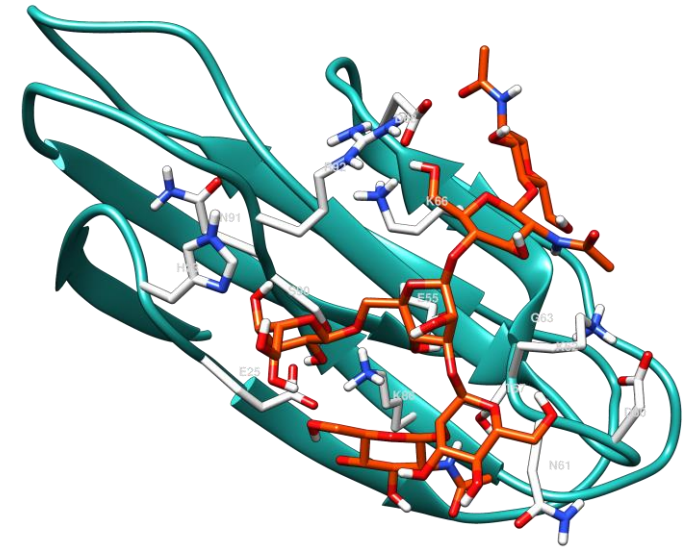
MDS was used to generate 1000 conformers, 10 were tested in PyRx docking without freely rotating protein side-chains, the top-score is shown

RMSDs relative to 5AZW_A: 2.59, 1.23, 1.87, 2.78, 3.84, 4.15, 3.61, **3.13**, 2.80, 2.77, 2.57



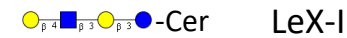
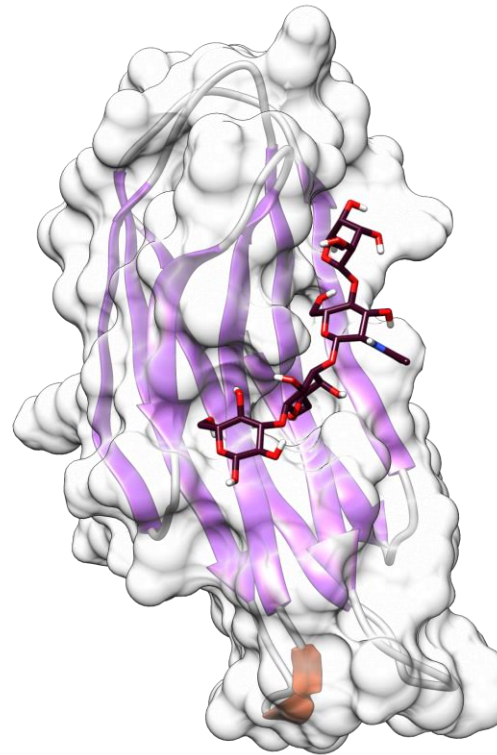
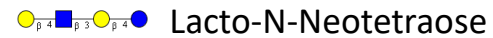
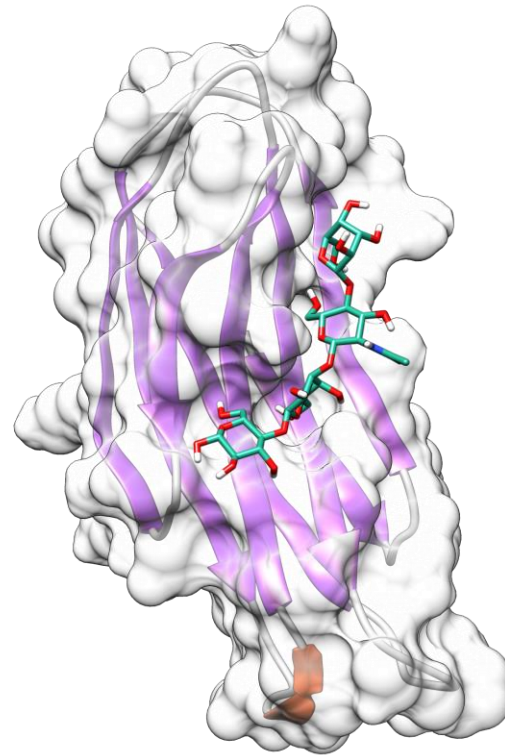
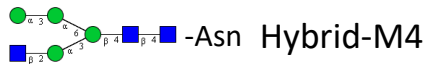
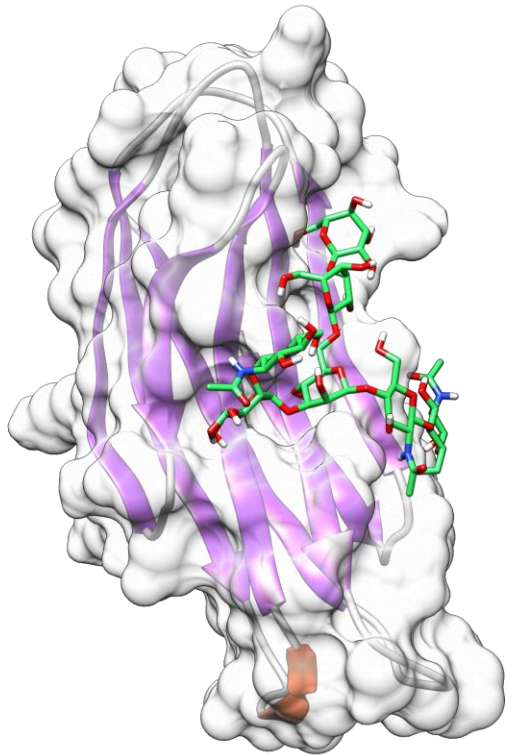
Q-score: 0.565
RMSD (overall) 1.9
in alignment

residues labeled 3.5 Å



A Hybrid N-Glycan was Found as the Top-Interacting Carbohydrate With TMED10

● Gal ■ GalNAc ● Man ● Glc ■ GlcNAc

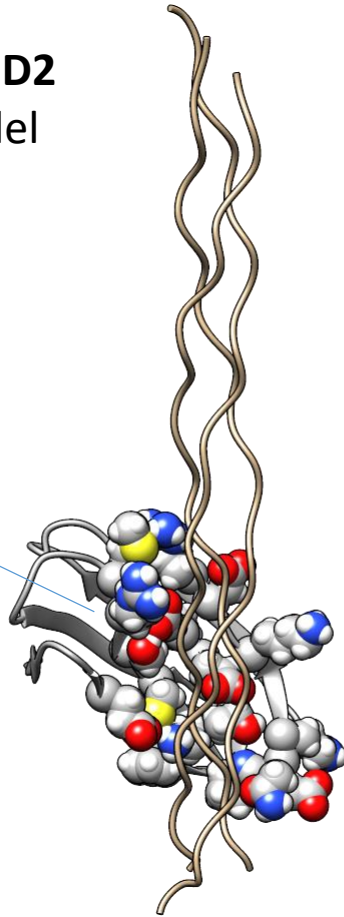


The equal binding to LeX-I and Lacto-N-tetraose may suggest, that the binding site is indifferent with respect to the Galactose -Glucose linkage

The binding groove of carbohydrates is similar to the collagen binding site

The Collagen Interaction is also Confirmed with p23-TMED10

TMED2
Model

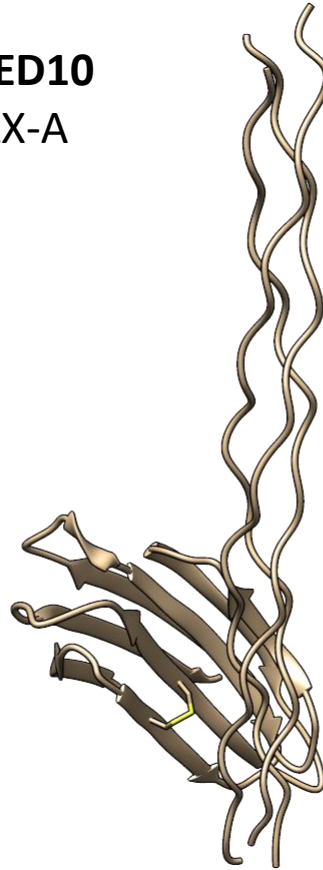


concave binding
site

ΔG Pisa -10.6 kcal/mol

collagen model peptide 1cgd

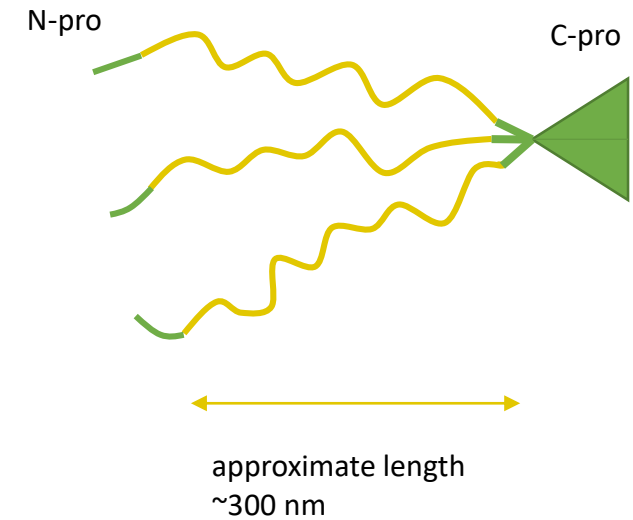
TMED10
5AZX-A



ΔG Pisa -9.6 kcal/mol

collagen model peptide 1cgd

Collagen assembly from
procollagen with N- and
C-propeptides



Collagen «folds» into triple
helical molecules

Collagens: The Most Abundant Proteins in Humans

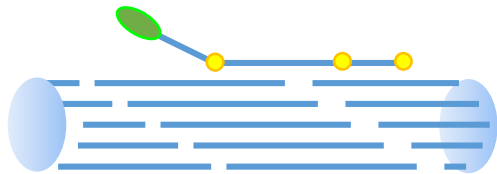
Some examples

Collagen I



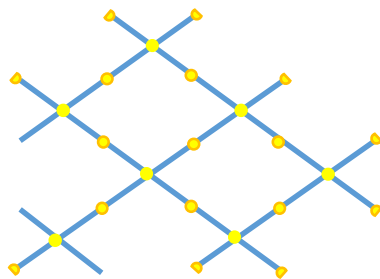
Fibril (I, II, III, V, XI, XXIV, XXVII)

Collagen IX



Fibril-associated (IX, XII, XIV, XVI, IXX, XX, XXI)

Collagen IV



Network (IV, VIII, X)

see Ricard-Blum, 2010

- Triple-helical domain (Gly-X-Y)
- Non-collagenous domain
- Thrombospondin domain

The Results Found for the X-Ray Structures

Similarity given by PDBeFold

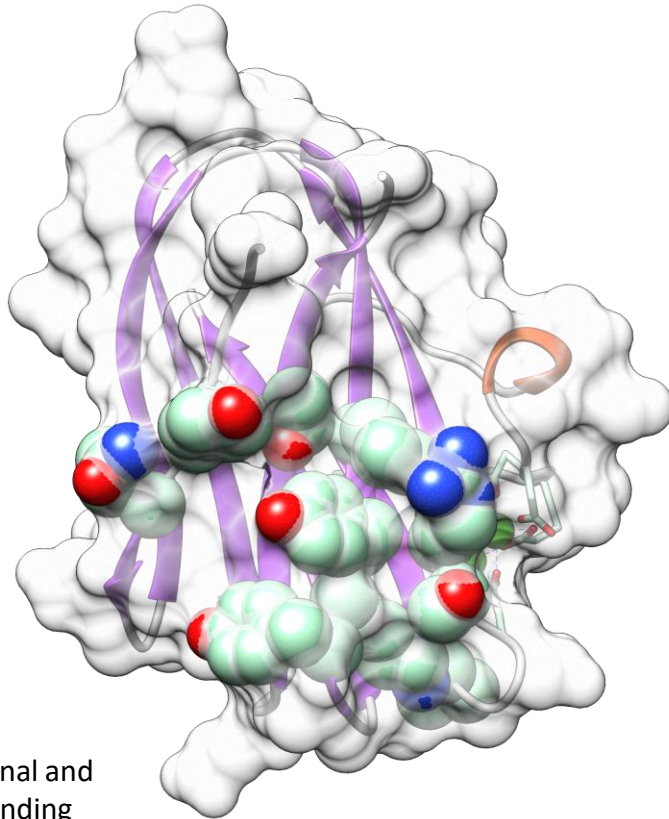
The lectin Q scores with the X-ray TMED-p24 structures are distinctly lower than the collagen binding domain values and thus collagen may be a preferred interactor

		Q-Score						
Collagenase collagen binding domain	5AZ	WA	WB	XA	XB	YA	YB	
	1nqj	0.45	0.47	-	-	-	-	Without Calcium
	3jqx	0.44	0.46	0.42	0.44	0.43	0.43	
	3jqw	0.44	-	0.44	0.44	0.42	0.43	
	Best lectin score	0.28	0.29			0.28		These lectins should be compared with a more sensitive, dynamic procedure
		Chitin	Melbiose	Galactose				
- Lower scores not listed								

TMED2 TMED10

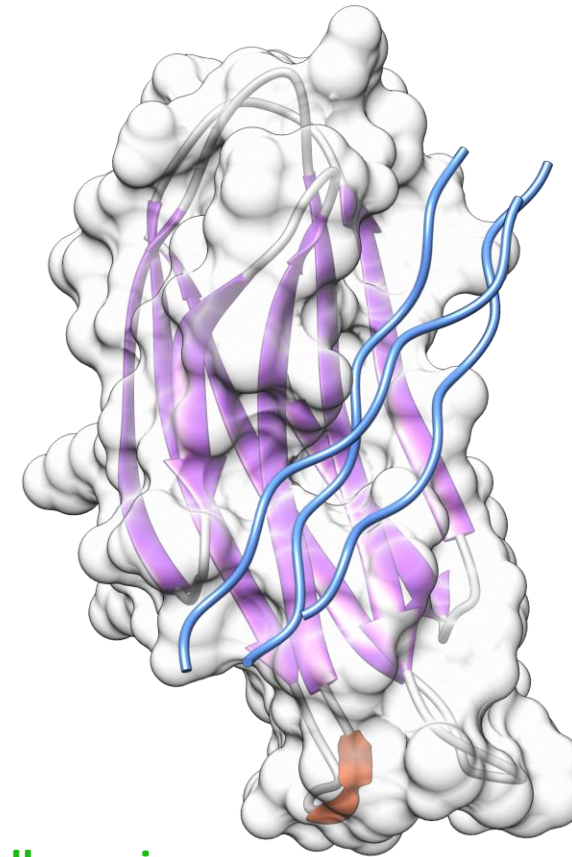
The Current Test Approximately Confirms the Collagen Interaction of Bacterial CBD as Well

1NQD – Collagen-binding domain (“1NQJ” with Ca^{2+})



Spheres – Mutational and NMR analysis of binding

5AZX – TMED10



5cvb

Wilson et al. 2003
Philominathan et al. 2009

The Best Interacting Collagen is
Collagen 1 Alpha Type I
(structural alignment with 1NQD)

Best Results on Collagen Docking in Molecular Dynamics and in PatchDock

		PISA kcal/mol		Filament collagen	
Bound to		5AZ	WA		
model synthetic chaperone/ integrin antibody					
	1cgd			-9.6	
	4au3			-7.4	«1-1-1»
	1dzi		-4.4	-5.9	«1-1-1»
	4bkl		-5.4	-7.4	«1-1-1»
Results not improved with MDS					
Native Collagens					
	5cti I		-8.8	-6.8	2-1-1
	5cva I		-9.2	-4.8	1-2-1
	5cvb I		*	-8.1	1-1-1
	5ctd I		-9.1	-7.7	2-1-1
			TMED2	TMED10	

* Possible collision of termini

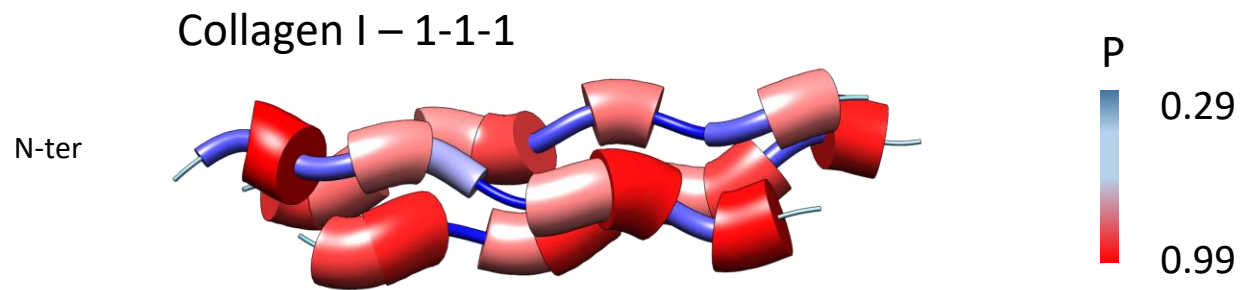
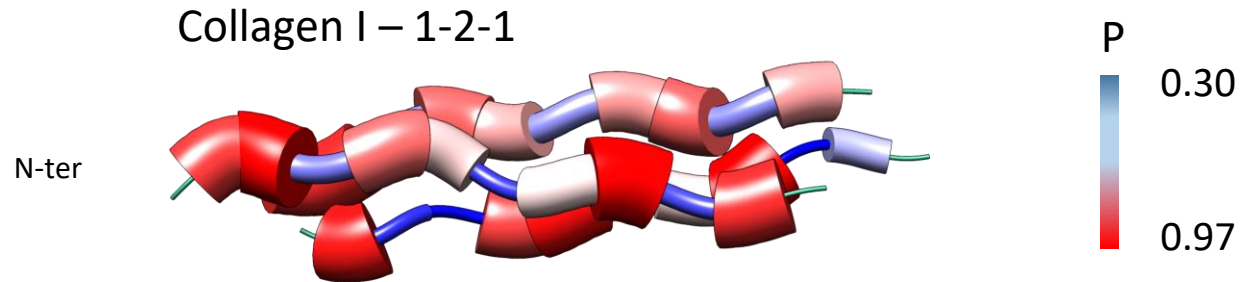
It seems, that preferentially collagen found in cancer cells interacts with the TMED10-p23-p24 δ 1-TMP21 structure, on the other hand, different collagens may preferentially interact with the TMED2 p24 protein

Would a «conformational disease» include collagen in 1-1-1 oligomeric form?

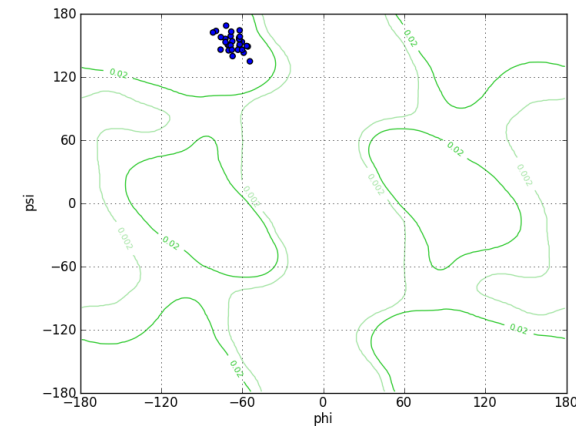
PatchDock: Schneidman-Duhovny et al. 2005
PISA: Krissinel 2010
AMBER: Pearlman et al. 1995

Different Collagens Have Different Probabilities in Chain Geometry

Ramachandran probabilities



Approximate location of the collagen peptides in the phi-psi plots



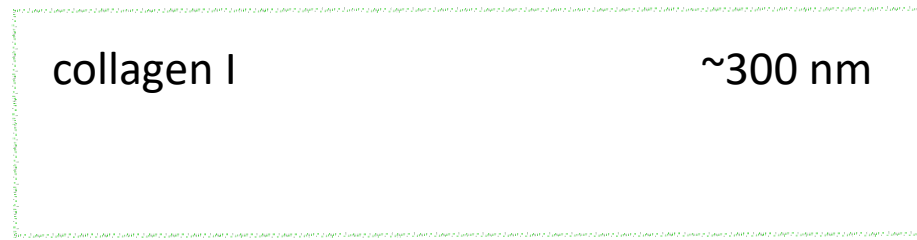
Here it is not obvious, how many examples in chain geometry were included for early/representative determinations, since structural examples in full length without cross-links were lacking...

Dunbrack and Karplus, 1993

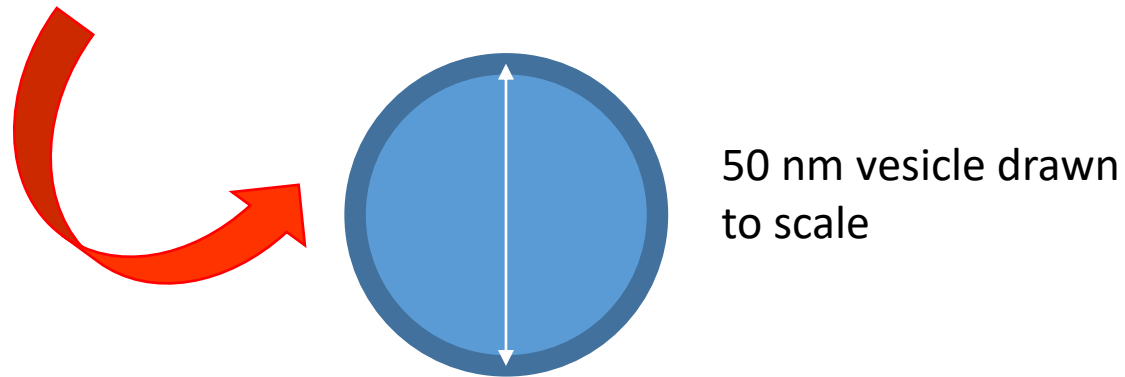
...physical potentials have not yet lead to collagen predictions

The Problem of Collagen Traffic and Assembly Has Recently Been Described And Required Knowledge on Collagen Structure

Annu. Rev. Cell Dev. Biol. 2015. 31:109-24



CED: Collagen-enriched domains were described in the ER that may form vesicular structures or tubules that merge with the CGN



Suggestions include the continuous connection of ER and Golgi or of individual Golgi cisternae

Budding of COPII-coated ER vesicular / tubular structures

Minimal Packing in Unperturbed Random Chains: Ideal Case

Porod-Kratky

To estimate the structure of intracellular collagen a model of Porod-Kratky was used

The assumption: bond-angle randomly chosen after 12 amino acids curved translation

Persistence length a was for $x \rightarrow \infty$; L_c (contour) chosen for collagen

$$a = \frac{l_b}{1 - \cos \gamma} \quad l_b \text{ bond/molecule length}$$

$$\langle r^2 \rangle_0 = 2aL_c \left[1 - \frac{a}{L_c} \left(1 - e^{-\frac{L_c}{a}} \right) \right]$$

$\langle r^2 \rangle_0$ dimensions of chain

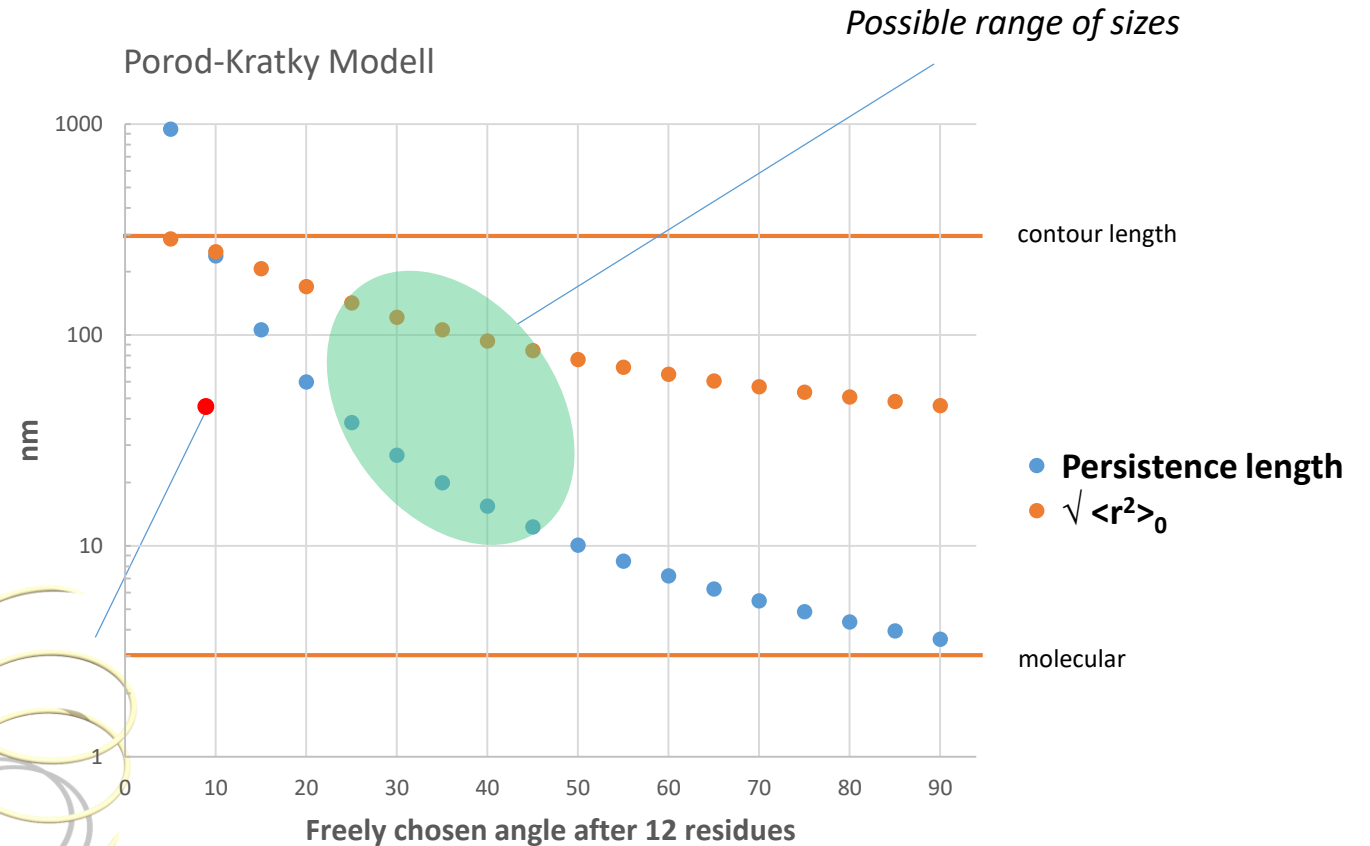
The curvature of the 12 amino acid segment was determined to be 9.2° without further structural data for the complete triple-helical collagen Walker et al. 2017

Actually the persistence length of collagen was found to be relatively short (60 nm) Hofmann et al. 1984

Tropocollagen has an even shorter persistence length Sun et al. 2002

angle chosen ignoring torsions

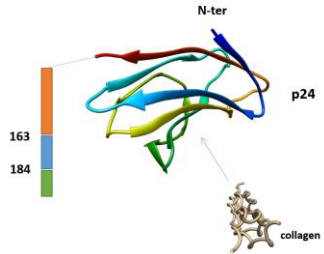
Here strictly chosen angle after 12 residues



Formulas adapted from Kratky and Porod 1949

A Protein Assembly Would Mechanochemically Require Only ½ to 20 ATPs to Bend Collagen to a 46 nm Diameter Helix

The efficiency of an ATP-consuming mechanical reaction was assumed to be 50 %



ΔG for the cellular hydrolysis of ATP is approximately -50 kJ/mol

The Young's modulus Y of tropocollagen is assumed to be 0.3 – 12 GPa (Sun et al. 2004; Vesentini et al. 2005; Buehler 2008)

It is assumed that the energy E_{arc} (Landau and Lifshitz, 1986) is found with $E_{\text{arc}} / L_c = Y I / 2 R_c^2$

L_c rod length, I moment of inertia, R_c radius of arc; see Boal, 2002

The collagen triple-helical length is found to be 300 nm, the proposed diameter of 1.5 nm (hydration) is assumed

The energy required would correspond to 12.7 – 505.3 kJ/mol. This would amount to hydrolysis of 0.5 – 20.2 mol ATP per mol assembled triple-helical collagen neglecting energy released during polypeptide translocation and C- and N-terminal interactions of pro-peptides and domains etc.

Non-covalent enzyme-substrate complexes have energies between -13 and -50 kJ/mol

p24 proteins could also be dimeric or hetero-oligomeric

For comparison: The calculations based on persistence length (see previous graph) would result in a coiled structure of ~90 nm end-to-end distances

Alternatively, the energy of a single or multiple interactions of TMED2/TMED10 would suffice to hypothetically structure collagen to form a super-helix given the interaction energies shown by MD simulation/PISA

University of Basel, Basel, Switzerland

Fribourg